

Effects of changes in external conditions on smoldering in biomass pellets

Dissertation for
for the award of the degree of

Doktoringenieurin
(Dr.-Ing)

By M.Sc. Ingunn Haraldseid

Date of birth: 11.10.1988 in Haugesund (Norway)

Accepted by the Faculty of Process and Systems Engineering of the Otto-von-Guericke-University Magdeburg

Reviewer:

JProf. Dr.-Ing Alba Diéguez Alonso (Chairman)

Prof. Dr.-Ing. habil. Ulrich Krause (Reviewer)

Prof. Dr. scient Vidar Frette (Reviewer)

Dr.-Ing. Martin Schmidt (Reviewer)

Submitted on: 25.01.2023

Graduation Colloquium on: 09.06.2023

Abstract

Smoldering fire is a hazard present during storage, handling, and transport of biomass materials. One such biomass material is wood pellets, where several storage incidents with such pellets have been reported. Onset of smoldering combustion has been investigated using a top-ventilated system with wood pellet samples with heights of 6, 8, 10 and 12 cm. Smoldering combustion is a complex event, where several factors affect the onset. The main factor impacting the possibility of smoldering combustion was the duration of heating. As the sample was heated was prolonged, the likelihood of smoldering increased.

The temperature for smoldering in wood pellets sample was erratic, however, the mass loss seemed to be systematic. The mass loss was divided into three phases: before, during and after an intense combustion period. The findings showed an unexpected trend, were independent of sample height, 45 % of the mass was lost during external heating and low intensity smoldering, 15 % of the mass was lost during the intense combustion period, and 40 % was left afterwards.

Two different biomass materials, wood pellets and oily pellets were tested in the top ventilated system. The natural oil content of the oily pellets impacted the smoldering combustion. Temperature development during external heating was similar for both pellet types, however, the self-sustained smoldering was different. Oily pellets endured a lower thermal runaway temperature, and a lower temperature of the intense combustion, however, the duration of the intense period was longer for the oily pellets.

Reversed smoldering combustion resulted in an inhomogeneous smoldering front. Temperature measurements of the air flow above the wood pellets showed a surprising distribution of the air flow to and from the sample. Results showed surrounding air entering the sample in the middle, associated with the warmest area of the smoldering combustion, while the warm smoke exited along the pipe wall, above the cooler areas of the sample.

Transition from smoldering to flaming fire occurred in long-run experiments, where the sample was refilled to initial sample mass in 8 h intervals. The transition to flaming fire was determined by high temperatures above the sample, and high mass-loss rate. Refill of sample caused an increased char layer in the lower parts of the sample, leading to a warmer hot spot, which resulted in conditions prone for transition to flaming fire.

The impact of the external conditions such as air supply on the different materials, and the conditions inside the pipe (air flow and hot spots) is a step closer to understanding safe storage and handling of biomass materials, in order to reduce the hazards biomass materials present. The understanding of smoldering behavior is important to develop an extinguishment system for such a hazard.

Zusammenfassung

Schwelbrände können bei der Lagerung, Handhabung und Beförderung von Biomasse entstehen und stellen damit eine große Gefahr dar. Beim Biomassematerial Holzpellets wurde über mehrere Zwischenfälle bei der Lagerung berichtet. Der Beginn des Schwelbrandes wurde in einem von oben belüftetem System mit Holzpellet-Proben einer Höhe von 6, 8, 10 und 12 cm untersucht. Ein Schwelbrand ist ein komplexer Prozess dessen Beginn von mehreren Faktoren beeinflusst wird. Der wichtigste Faktor, der sich auf die Möglichkeit einer schwelenden Verbrennung auswirkt, ist die Dauer der Erhitzung. Je länger die Probe erhitzt wurde, desto größer war die Wahrscheinlichkeit eines Schwelbrandes.

Die Schwelbrandtemperatur in der Holzpellet-Probe war unregelmäßig, der Massenverlust schien jedoch systematisch zu sein. Der Massenverlust wurde in drei Phasen unterteilt: vor, während und nach einer intensiven Verbrennungsphase. Die Ergebnisse zeigten einen unerwarteten Trend: Unabhängig von der Probenhöhe gingen 45 % der Masse während der externen Erwärmung und des Schwelens mit geringer Intensität verloren, 15 % der Masse gingen während der intensiven Verbrennungsphase verloren, und 40 % blieben danach übrig.

Zwei verschiedene Biomassematerialien, Holzpellets und ölhaltige Pellets, wurden in dem von oben belüftetem System getestet. Wobei der natürliche Ölgehalt der ölhaltigen Pellets die schwelende Verbrennung beeinflusste. Die Temperaturentwicklung während der externen Erhitzung war bei beiden Pellets Arten ähnlich, der selbstständig ablaufende Schwelbrand in sich jedoch unterschiedlich. Die ölhaltigen Pellets gingen bei niedrigen Temperaturen durch, hatten geringere maximale Verbrennungstemperaturen während der Phase der intensiven Verbrennung. Des Weiteren war die Phase der intensiven Periode bei ölhaltigen Pellets länger.

Die rückwärtsgerichtete Verbrennung (reverse smoldering) führte zu einer inhomogenen Schwelbrandfront. Temperaturmessungen des Luftstroms über den Holzpellets zeigten eine überraschende Verteilung des Luftstroms zur und von der Probe. Die Ergebnisse zeigten, dass die Umgebungsluft in der Mitte in die Probe eintrat und mit dem wärmsten Bereich der schwelenden Verbrennung verbunden war, während der warme Rauch entlang der Rohrwand über den kühleren Bereichen der Probe austrat.

Der Übergang von Schwelbrand zu Flammenbrand trat in Langzeitexperimenten auf, bei denen die Probe in 8-Stunden-Intervallen immer wieder auf die Ausgangsmasse aufgefüllt wurde. Der Übergang zum Flammenbrand wurde durch hohe Temperaturen über der Probe und hohe Massenverluste bestimmt. Das Nachfüllen der Probe führte zu einer höheren Holzkohleschicht in den unteren Teilen

der Probe, dies führte zu einem wärmeren Hot Spot der wiederum die Voraussetzungen für den Übergang zu Flammenbrand schuf.

Die Erkenntnisse über die Auswirkungen der externen Konditionen wie der Luftzufuhr auf die verschiedenen Materialien und die Konditionen im Inneren des Rohrs (Luftstrom und heiße Stellen) können zu einer sichereren Lagerung und Handhabung von Biomassematerialien beitragen und die Gefahren, die davon ausgehen verringern. Das Wissen über Schwelverhalten ist wichtig, um Löschsysteme für solche Herausforderungen zu entwickeln.

List of symbols

\varnothing	Diameter
p90	Probability of smoldering 90 %
p50	Probability of smoldering 50 %
p10	Probability of smoldering 10 %
m_1	Mass at start of intense combustion period
Δm	Mass loss during intense combustion
m_2	Mass at the end of the intense combustion period
m_0	Start mass / initial mass
t_1	Start time intense combustion period
t_2	End time intense combustion period
m	Mass
t	Time
Δm_s	Mass loss first phase of the experiment (external heating)
t_{tot}	Total time of experiment
T_{cut}	Temperature when hotplate was switched off
t_{cut}	Time when hotplate was switched off

List of abbreviations and definitions

EMRIS	Emerging Risks from Smoldering Fires
Oily pellets	Pellets from shell casing of sunflower seeds
HVL	Western Norway University of Applied Sciences
Pellet A	Wood pellets from Norwegian producer
Pellet B	Wood pellets from Swedish producer
et. al	And others
NS	Norwegian Standard
SS	Swedish Standard
TGA	Thermogravimetric Analyzer
TRA	Thermal runaway
Hot spot	Four warmest thermocouples above 300 °C
STA	Simultaneous Thermal Analysis
W	Wood pellets (Type A)
O	Oily pellets

Table of content

Abstract	II
Zusammenfassung	III
List of symbols	V
List of abbreviations and definitions	V
Table of content.....	VII
1. Introduction	1
1.1 Background	1
1.2 Research goals	2
1.3 Structure of thesis	3
1.4 Limitations.....	3
1.5 Joint experimental work	4
2. Smoldering in biomass	5
2.1 Smoldering	5
2.2 Handling, transport, and storage of biomass materials.....	9
3. Experimental method	12
3.1 Materials.....	12
3.1.1 Wood pellets type A and type B.....	12
3.1.2 Oily pellets	13
3.2 Top-ventilated system: onset of smoldering.....	14
3.2.1 Top-ventilated system: Experimental setup	15
3.2.2 Top-ventilated system: Experimental procedure.....	16
3.3 Top-ventilated system: Air flow in at height 20 cm / 33 cm.....	17
3.4 Restricted air supply to sample.....	19
3.5 Long-run experiments with refill of pellets.....	21
4. Onset of self-sustained smoldering and intense combustion period.....	24
4.1 Typical smoldering and non-smoldering behavior in the top-ventilated system.....	24
4.2 Residue after non-smoldering experiments with wood pellets.....	27
4.3 Onset of self-sustained smoldering	29
4.4 Rapid increase in mass-loss rate during intense combustion	34
4.4.1 Determining the mass loss during the intense combustion period	35
4.4.2 Mass loss during the intense combustion period.....	38
4.4.3 Conditions needed for the intense combustion period to occur.....	43
4.5 Mass-loss rate during external heating as an indicator of non-smoldering or smoldering	51
4.5.1 Method for finding the duration of the first mass-loss phase of the smoldering and non-smoldering experiments.....	51

4.5.2	Results from the mass loss in the initial phase	53
5.	Oily pellets from sunflower seeds	55
5.1	Smoldering behavior of oily pellets	56
5.2	Comparison of wood pellets and oily pellets	57
5.2.1	Temperature distribution inside sample	58
5.2.2	Mass loss during smoldering combustion	63
6.	Air flow above the sample and effect of coverage of pipe	65
6.1	Temperature of sample and air flow in at the height 20 cm	65
6.1.1	Warm and cold air flow in the pipe	68
6.1.2	Temperature in and above sample	70
6.1.3	Temperature in sample and air flow at peak temperatures	73
6.1.4	Temperature of steel pipe	76
6.1.5	Air flow on top of the pipe (33 cm).....	77
6.2	Impact of top coverage on smoldering combustion in pellets	80
6.2.1	Effects of coverage of opening for a sample height of 10 cm	81
6.2.2	Effects of coverage of the opening for a sample height of 12 cm	82
6.2.3	Air supply at the height 20 cm with coverage of pipe opening	83
6.2.4	Mass-loss rate during intense combustion: effect of coverage	84
7.	Long-run smoldering experiments with transition to flaming	86
7.1	Typical smoldering behavior in the long-run experiments.....	86
7.2	Transition from smoldering to flaming fire	89
7.3	Hot spots in sample before transition to flaming.....	91
7.4	Mass-loss rate during transition to flaming combustion	94
8.	Discussion	96
8.1	Onset of smoldering	96
8.1.1	Cut-off temperature vs duration of heating	96
8.1.2	Effect of prolonged external heating	97
8.1.3	Minimum sample height.....	97
8.2	Mass loss during smoldering in a top-ventilated system	98
8.3	Air flow above sample and reduced opening of pipe	101
8.3.1	Air flow in the cross-section.....	101
8.3.2	Reduced pipe opening to pellets sample.....	102
8.4	Transition from smoldering to flaming fire	103
8.5	Wood pellets and oily pellets	106
9.	Conclusion.....	109
10.	Further work	110

11. Bibliography	111
Attachments.....	i
I. Technical drawings.....	ii

1. Introduction

1.1 Background

New greener energy sources are being developed to replace fossil fuels and reduce pollution [1-3]. A well-established energy source is wood pellets, commonly used for heating of public and domestic buildings [4, 5]. Because demand for wood pellets is increasing, other biomass pellets from for example agriculture residue and other biomass waste products, are also being produced [6, 7]. Biomass materials consist of plants or residue of organic materials [8, 9]. Examples are residue from the production of sunflower oil, or wood boards, while in other cases the production is based on whole wood logs. The residue is (most commonly) pressed into a cylindrical biomass pellet using heat.

The main motivation for the use of the biomass fuel, is to replace high-pollution products, by products from renewable green energy sources. Renewable energy sources are important, however, there have been incidents where these materials have started to self-ignite, and a smoldering fire has been the result [1, 10].

In recent years, biomass has been used in thermal power plants in Denmark, and as a substitute to coal in other European countries [2, 11]. Hedlund et. al [1] argues that there are certain risks in the usage of biomass materials that are under communicated. Large amounts of pellets are needed to create energy in the power plants. The most common bioenergy material is wood pellets, in 2016, over 16,5 million tons were traded internationally. To meet the demand for renewable bioenergy, non-wood materials have also been pelletized, such as rice straw, wheat straw and hay [6]. The increased demand means more transportation and storage needs, as pellets are imported from all over the world [1]. Stelte [11] argues that these types of materials are considered harmless and therefore the risks involved in the transport and handling of these materials are underestimated. These new types of biomass materials have a bulk density and moisture content, which makes them prone to smolder [12]. Typical for materials prone to smolder, is the combination oxygen attacking the surface of the fuel and the slow burning [13, 14]. Smoldering fires can burn for a long time, even decades, and are difficult to extinguish [12, 15]. Biomass is a material prone to smoldering, and to be able to determine the risks involved in the handling of biomass materials, one needs to understand the basic behavior of the pellets during a smoldering combustion.

Biomass materials should be handled with care, as they are prone to self-heating leading to smoldering fires [12, 16]. Fires in silos have been an issue for several years. By storing biomass materials in silos or storage halls it causes the smoldering to be situated deep inside the storage unit. Silo fires often starts as a smoldering fire, which can then transition to flaming fire and in some cases a gas explosion, which may cause severe accidents [13]. A smoldering fire will ruin the material in the silo. In addition, attempts to extinguish the fire will normally destroy the silo. Water is not a good extinguishing agent

when it comes to wood pellets in silos. Water causes the wood pellets to expand and harden, causing difficulties in emptying a silo. To be able to extinguish the fire, and empty the silo, the pellets need to be removed by cutting large openings in the silo walls. Such accidents are costly due to the large impact on the units and restoring costs [12, 17].

Over the years, smoldering fires have been an important research topic, where more research is needed for different materials and products. As the biomass industry increases, producing new non-wood materials, it is important to understand not only the fundamentals of combustion in these materials, but also how different external surroundings can affect materials differently. The concept of smoldering combustion gives rise to several questions in terms of what effects the ignition, whether the smoldering is of high or low intensity and conditions for a transition from smoldering to flaming combustion. Increased understanding of the smoldering phenomena is important to ensure safe storage of biomass materials such as wood pellets.

1.2 Research goals

In this thesis the understanding of the phenomenology of smoldering behavior in biomass pellets using small-scale laboratory experiments. The research goals are divided into two main categories:

Effect of air flow

In this category the research aims to gain a fundamental understanding of the onset of smoldering combustion in wood pellets in a top-ventilated system. Here, an important factor is the air flow from the surroundings to the pipe and sample. A reasonable assumption is that the cold air will enter the sample along the side walls, with warm smoke exiting from the middle of the sample. Furthermore, the effects of reducing the opening of the top ventilated system could be important. Smoldering combustion also continues at low oxygen concentrations, so one may ask if it will extinguish when the air supply to the sample is reduced?

Behavior of biomass materials

Two different types of biomass material are used in the experiments in order to compare smoldering behavior with the same experimental setup and external conditions. The types of materials used are wood pellets and sunflower seed shell pellets (denoted as oily pellets in this thesis) as these are stored, transported, and handled in the same manner.

During storage, silos are refilled with pellets, and an undetected fire could be located inside the storage unit. How does the supply of fresh fuel affect the smoldering combustion deeper inside the unit?

Would a refill of the sample simply quench the smoldering combustion, or would fresh fuel increase the smoldering combustion? To extend the duration of the smoldering combustion and simulate the

refilling of a silo, the sample was therefore refilled to its initial mass in intervals to replace the combusted material. Refilling of material could affect the temperature development in the sample.

During experiments with refilling and a long duration, transition from smoldering to flaming combustion was observed. It is important to understand the conditions in the sample needed for a transition from smoldering combustion to flaming to occur.

1.3 Structure of thesis

The structure of this thesis is as follows: Section 2 describes smoldering in biomass, previous research and challenges. The materials, and experimental equipment and method used are described in section 3. Results on the behavior of smoldering in wood pellets in terms of onset of smoldering and the behavior of mass loss during smoldering combustion are described in section 4. Analysis of a biomass material consisting of sunflower shell, denoted as oily pellets are found in section 5. The results from the analysis of the air flow can be found in section 6. Section 7 describe the long-run experiment results, and the transition from smoldering to flaming behavior, followed by the discussion (section 8) and conclusion (section 9). Further work within smoldering in biomass pellets can be found in section 10.

1.4 Limitations

The experimental setup is small-scale, and an upscaling of the experimental results could in some cases be difficult. The experimental setup consisted of a steel-pipe, surrounded by insulation, there is no other visible observations of the pellets other than from the top of the pipe. Only temperature measurements can display the movement of the combustion front. The aluminum plate has sides exposed to the surroundings, even with insulation of the aluminum plate, there would be some heat loss to the surroundings, however, temperature measures of the aluminum plate show a sufficiently high temperature.

The temperatures were only measured in the centerline of the steel pipe. There could be movement of heat fronts in other locations of the pipe that are missed due to the thermocouple placement. However, more thermocouples, would require a larger steel construction and have a larger impact on the combustion of the sample in this small experimental setup.

Air flow measurements were conducted by measuring the temperature of the air flow above the sample. Velocity and direction of air flow was discussed, however, more than one bi-directional probe was needed, and in a pipe with a diameter of 15 cm, the bi-directional probes would have too large of an impact on the natural movement of the air flow to and from the sample. In addition, there are large

amounts of tar in the smoke from the smoldering combustion in wood pellets, and this could affect the equipment negatively.

There has also been an issue getting a hold of oily pellets. Therefore, there has not been as many experiments as wanted for the two types of biomasses.

1.5 Joint experimental work

The initial experiments with the limitations for the onset of the smoldering behavior was a collaboration between three PhD candidates, Edmundo Villacorta, Ragni Fjellgaard Mikalsen and me, where all has contributed equally to the work and resulted in a joint article [18]. Experiments were conducted at HVL premises in Haugesund, Norway and at SP Fire Research, Trondheim, Norway. This part is described in section 4.2 and 4.3 and are previously presented in the PhD thesis of Mikalsen [19].

The long-run experiments were conducted by Anita Meyer, were I contributed with refilling of the sample and data analysis.

2. Smoldering in biomass

2.1 Smoldering

Smoldering combustion is a challenging hazard worldwide [20], and poses risks in natural habitats, such as in soil during and after forest fires [15], but also increasingly in industrial settings [1, 21]. Spontaneous combustion in storage, production and handling units, causes damage to equipment and structures, in addition to the loss of inventory [12].

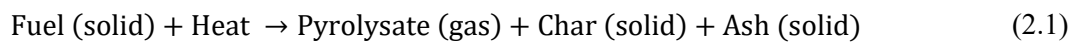
Smoldering combustion is distinct different from flaming fires in that there are no visible flames and that it burns at lower temperatures. These characteristics make smoldering fires difficult to detect [22]. A smoldering fire is slow, with an average spread rate of 1 mm/min, while a flaming fire is fast, with a spread rate between one and two orders of magnitude larger than smoldering fire. The difference in spread rate is caused by the heat transfer mechanisms, flaming fire has radiant heat transfer, while for smoldering combustion the heat is conducted. The spread rate in smoldering combustion is in many cases controlled by the oxygen supply to the areas within the fuel. The oxygen supply and the low temperatures cause this to be a slow process [20, 23-25]. A characteristic feature of smoldering is how the oxygen reacts directly with solid fuel surface [20, 23, 25]. Materials that are prone to smoldering are porous, and char is formed during heating, examples of such materials are wood pellets (and other biomass pellets), waste and cotton [14, 20, 23].

The basic behavior for smoldering and flaming fires are similar, when heat is released the combustion spreads through the sample. To be able to obtain fires of all sorts, heat generated must exceed heat loss. However, there are differences in behavior, while flaming fires have temperatures between 1500 – 1800 °C, smoldering fires have a temperature range from 500 – 700 °C. In addition, it is more difficult to extinguish smoldering fires than flaming fires [13, 14, 20, 23]. Suppression of a smoldering fire by reduction of oxygen is demanding, when compared with flaming fires, suppression of smoldering fires can last for months compared to minutes or hours for flaming fires [20]. A smoldering fire in a storage silo will typically be located deep inside the silo and extinguishing these types of fires is difficult. Depending on the material stored, water as an extinguishing agent could be unsuitable. Water added at the top of the silo would have difficulties in penetrating to all the material in the silo and reach the deeply situated fires [17, 26]. To extinguish a smoldering fire in a biomass material such as wood pellets, water is not recommended due to the pellets tendency to swell in contact with water, followed by hardening of the material. This could prevent the flow of water and also destroy the storage unit [27].

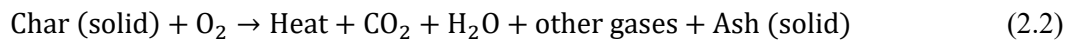
Smoldering combustion spreads through materials with different reactions in each zone of the smoldering combustion. The smoldering front has three zones: pyrolysis zone (zone 1), charred zone (zone 2) and residual zone (zone 3). The pyrolysis zone results in visible smoke, and a rapid increase

in temperature. In the charred zone there could be glowing, and the fuel reaches a maximum temperature due to heat release during oxidation of the char. In the third zone, behind the smoldering front, the residue left consists of ash and porous char, in this zone the temperatures decrease [14, 28, 29]. The chemical process during smoldering follows the zones, beginning with a pyrolysis of the material, followed by oxidation of fuel. In some cases, secondary oxidation may also occur [20, 23]. Secondary char oxidation can take place in both the char from oxidation of the solid and in the pyrolyze during gas oxidation [20]. Smoldering is a phenomena that occurs in the solid phase of the fuel, the chemical process is schematically shown in equations 2.1, 2.2 and 2.3 [15, 20].

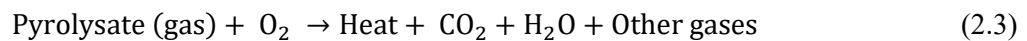
Pyrolysis:



Solid oxidation:



Gas oxidation:



One-dimensional smoldering fires can be categorized into two types determined by how oxygen enters the combustion zone: forward smoldering and reversed smoldering. When oxygen enters through the ash to the smoldering front, the smoldering is defined as forward smoldering since the air and smoldering front moves in the same direction. If oxygen enters the smoldering front through the unaffected fuel, the combustion is defined as reversed smoldering, see Figure 2.1 [13, 20].

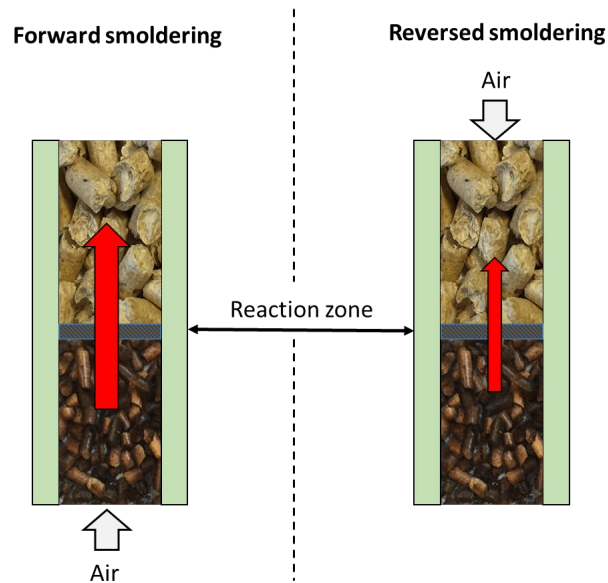


Figure 2.1: Forward and reverse smoldering propagation [20, 30], where the lower layer consists of material affected by heating, while the top layer contains pristine fuel. The reaction zone is in the middle. In forward smoldering, the air enters through the affected material, while in reverse smoldering the air enters the sample through the pristine fuel. The red arrows indicate a slight difference in the front velocity for the two types of smoldering combustions.

A self-sustained smoldering combustion is obtained when the heat release is large enough to balance the energy needed to dry the material, drive the pyrolysis, pre-heat the unburnt fuel and compensate for heat loss to the surroundings. Once a self-sustained process is initiated, the oxygen supply to the sample influences the combustion. Oxygen supply and heat loss will determine the rate of spread of the combustion front. More oxygen at the combustion front, increased the front velocity [20, 23, 25, 31]. Conditions needed for self-sustained smoldering can be represented by a smoldering square [32], see Figure 2.2. A porous media, oxygen supply, ignition source and the layer of thickness need to co-exist for a smoldering combustion.

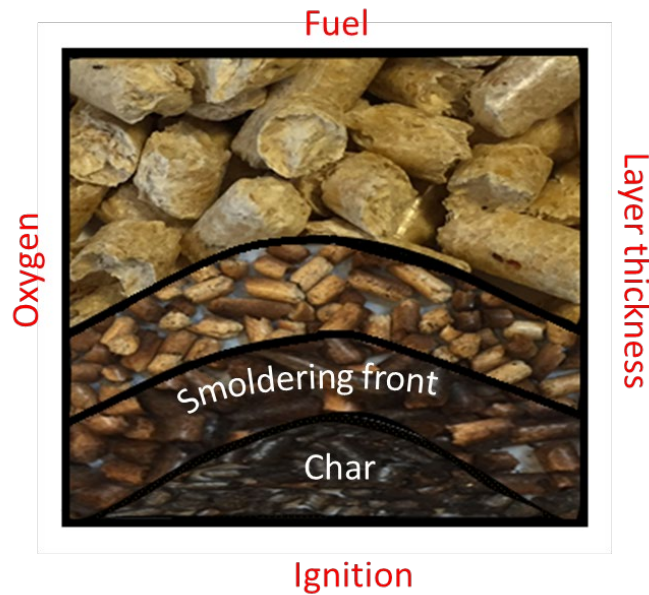


Figure 2.2: Smoldering square [32]. The four conditions needed to obtain a smoldering process. An ignition source, sufficient oxygen supply, porous fuel, and a minimum layer thickness.

A smoldering fire behaves differently in different types of materials, depending on the physical properties and shape of the material. Self-sustained smoldering is possible in porous materials, which when heated form char [14]. A smoldering combustion can be ignited from a weak ignition source, such as a hot surface, or by self-heating due to decomposing of the material. The four ignition methods: radiant, conductive, ember and self-ignition are applicable for smoldering combustion, and each of them show a lower critical energy needed to obtain a fire, compared with flaming fires [20].

Transition from smoldering fire to flaming fire is a problem in both residential and wildland fires. A transition from smoldering to flaming combustion is possible when enough heat and pyrolysis gases are produced and there is sufficient oxygen supply. The three conditions could lead to a spontaneous gas-phase ignition [13, 20]. A transition from smoldering to flaming fire occur under certain conditions. An increase in velocity and higher temperature combined with an increasing oxygen supply could accelerate a transition to flaming combustion [20]. The transition from smoldering to flaming is spontaneous, and it is difficult to determine when the transition will occur [13, 14]. Hagen et.al [33] studied smoldering in cotton and found a correlation between the boundary conditions and the density of the cotton sample for transition to flaming. Putzeys et al. [34] studied piloted transition to flaming in non-fire retarded polyurethane foam, and found that the smoldering front's velocity and temperature impacts the transition from smoldering to flaming. A transition to flaming fire could be difficult to obtain since surrounding conditions could impact the transition itself [30]. Previous research indicates that there are several conditions, connected to both external and internal processes,

such as oxygen supply, hot spots inside the sample, charring of the material, with enough cavities in the char, that are necessary for a transition from smoldering to flaming [25, 35, 36].

2.2 Handling, transport, and storage of biomass materials

Biomass materials is one type of material that is prone to smolder. Due to an increase in the usage of biomass materials as an energy source, the demand is increasing worldwide. This results in transport of these materials over long distances [37]. Wood pellets needs to be handled gently during transport, as such pre-processed materials are fragile and break apart easily during transportation and handling. The dust created from wood pellets is highly explosive and is harmful to inhale [11, 12, 27]. With an increase in transport of these materials in large container vessels, the risks associated with off-gassing and explosion needs to be addressed [11]. Furthermore, knowledge on smoldering behavior is needed to ensure safe transport, handling, and storage. The production and distribution process for biomass pellets is shown schematically in Figure 2.3. During production, the material is grounded to smaller particles, before extruded into a pellet shape, often using heat. The materials are transported all over the world by ships, trucks, and trains. A common storage unit for pellets is silos, however, indoor flat storage is also used [11, 27].

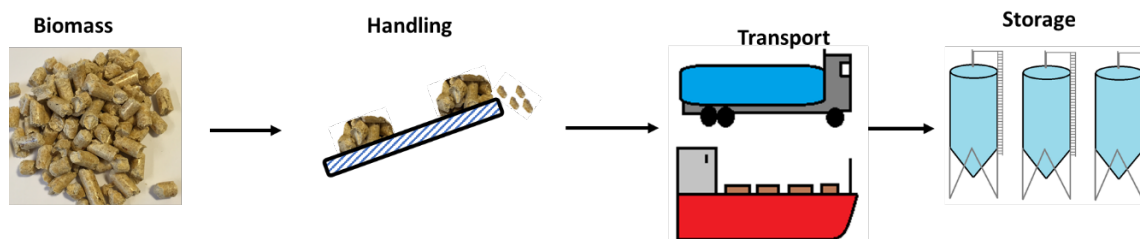


Figure 2.3: The distribution line of wood pellets, from the production to the handling on conveyor belts, transport by ship or trucks to the storage of the pellets in silos.

Hazards during storage and transportation of pellets are: formation of dusts, off-gassing, self-heating and biological hazards [11, 27, 38, 39]. When stored and transported, wood pellets experience off-gassing of carbon monoxide and hexanal [4, 40]. Self-heating of pellets is caused by microbiological processes [27]. Biological hazards are for instance fungi and bacteria forming in the biomass products, which can cause respiratory issues or other health issues [11, 27].

Self-heating is an important mechanism leading to ignition of smoldering fires in pellets during storage, handling, and transport. Other ignition sources could be hot surfaces, or overheating from other sources [27]. The moisture content and temperature of the biomass product are important for the

extent of microbiological processes [41]. During transport with trains, it is critical that the temperature of the pellets is kept below 30 °C to avoid overheating. External conditions, such as weather conditions affect the moisture content inside the storage unit. Warm weather, and solar radiation hitting the surface of the storage unit increases the temperature inside the unit, and when later cooled, condensate tend to form inside, with conditions suitable for microbiological growth, and the risk of self-heating increasing [27]. The time since production, affects the biomass material's ability for self-heating. A fresh pellet is more reactive compared with an older pellet as fresh pellets contain more resin and fatty acids in the first periods after production [27].

Knowledge on the different biomass materials is important, to avoid or reduce the risks of fire from these materials during storing and handling. Several materials have been tested experimentally to find the ignition temperature for smoldering combustion. The ignition temperature is influenced by several parameters, such as experimental setup and type of ignition test. Hadden et. al [42] found that there was an effect of the sample height, and for polyurethane foam to smolder, a minimum sample size was found. In addition, the sample size influenced the smoldering ignition by a cone heater, as sample size increased, ignition temperature of smoldering decreased. Among other parameters studied for smoldering in cellulose materials such as cotton, was the density of the cotton sample [43]. The same trend was found here, as the density of the cotton batch increased, the ignition temperature decreased. Another relevant parameter is the volume fraction of oxygen in the surrounding air during a smoldering combustion as studied by, Malow et.al [44]. They found that the availability of oxygen affects the chemical conversion rate of a bulk material, such as wood chips and coal. The findings indicate that when a silo is flushed with inert gas, so that oxygen concentration in the storage unit is significantly reduced, this will lead to lower the reaction rate and temperature. However, the fire will not be quenched.

There have been several accidents involving smoldering fires in biomass pellets during transport, handling, and storage. During production and handling, incidents have been reported where malfunctions with the conveyer belt caused an increase in temperature of the pellets, leading to smoldering fire in a production hall [45] and in storage units [1]. Common denominators for smoldering combustion in storage units are the difficulty in extinguishing the fire, delayed detection of the smoldering fire, and a large amount of material involved in the combustion [16]. Eckhoff [46], Russo et al. [47], Ogle et. al [48] and Hedlund et.al [1] have all reported smoldering fires in silo storage units. In Esbjerg in Denmark, a smoldering fire started in a storage unit containing wood pellets. The fire spread, and it took nine months for the fire brigade to extinguish the fire [16].

Smoldering fires can lead to gas explosions due to the hazardous off-gases from the biomass material. A pellet factory in Norway experienced a smoldering fire leading to a gas explosion in the storage silo [45]. The case study described by Ogle et. al [48] reported a smoldering fire inside a storage silo for

agriculture grain lasting for weeks. When extinguishment was attempted, several explosions occurred inside the silo. In Russia a large storage unit, consisting of silo cells, experienced a smoldering fire in one of the cells containing moist sunflower seeds in 1987/1988. The smoldering fire in the cell developed into several gas explosions in one cell after another [46].

The experience from these accidents is of importance to ensure a rapid response from fire departments. A quick response in an early phase could hinder the combustion from growing and spreading to other parts of the bulk material. Storage units with materials in risk of combustion should be monitored closely to avoid critical temperature conditions. For better storage, transport, and handling of biomass materials, and measures to avoid/limit the damage to structures, one needs to understand the fundamentals of the smoldering behavior and how smoldering combustion is impacted and develops. The understanding of the mechanisms such as mass loss, air flow is important to understand the smoldering process.

3. Experimental method

In this chapter the experimental method, experimental setup, and materials will be described. This chapter will firstly describe the materials used in this thesis (section 3.1). The experimental method and experimental setup are described in section 3.2. The changes to the experimental setup to measure the air flow is described in section 3.3 and the reduction of the opening of the pipe in section 3.4. The experimental setup for the long-run experiment with refill of mass can be found in section 3.5.

3.1 Materials

Three different types of biomass pellets have been investigated: Two wood based, and one produced from sunflower seed shells.

3.1.1 Wood pellets type A and type B

Two types of wood pellets were used in the experiments. One was produced in Norway, following the Norwegian standard NS3165 [49], and denoted as pellet A. The other originated from Sweden, was produced according to the Swedish standard SS 18 17 20:1998 [50], and denoted as pellet B. Both pellet types were categorized in the same class: class 1. Thermogravimetric Analyzer (TGA), bomb calorimetry, adiabatic test, and permeability tests were carried out for the two types of pellets, and the results are given in Table 3.1. Figure 3.1 shows the two pellet types, pellet A contains bark and has a darker brown color compared with pellet B, which is without bark.

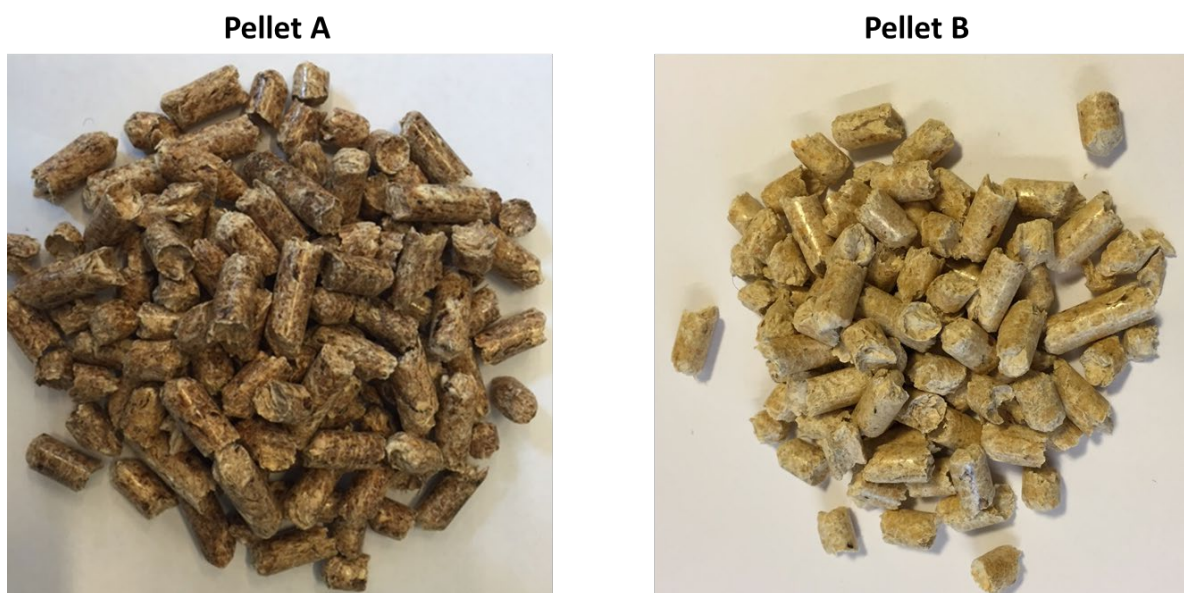


Figure 3.1: The two different types of pellets. Pellet type A is to the left. The pellet itself is darker than pellet B (to the right) due to the content of bark.

Table 3.1: The material properties for pellet A and pellet B.

Properties	Pellet A	Pellet B
Type of wood	20 – 50 % Pine 50 – 80 % Spruce (including bark)	60 % Pine 40 % Spruce
Diameter [mm]	8	8
Pellet density [kg/m ³]	1020	1050
Bulk Density [kg/m ³]	710	730
Porosity [vol%]	31.4	30.3
Higher calorific value [kJ/kg]	18834	17453
Lower calorific value [kJ/kg]	17433	15931
Activation Energy [kJ/mol]	91.4	107.1
Permeability [m ²]	$\leq 2.4 \cdot 10^{-8}$	$\leq 2.1 \cdot 10^{-8}$
Moisture content [wt%]	6.3	7.7
Volatile compounds [wt%]	77	78
Ash content [wt%]	0.46	0.21

3.1.2 Oily pellets

Non-wood pellets are produced to meet the increased demand for renewable energy [6]. An example is the pellets made from shell casings from sunflower seeds. The pellets are made from the residue after the production of sunflower oil and is referred to as oily pellets in this thesis. Compared with wood pellets, the oily pellets have a smaller diameter, but the same length as wood pellets, see Figure 3.2. The major difference is the natural presence of oil in the oily pellets, otherwise the moisture content of the two types of pellets are in the same range. The results from the elemental analysis of the oily pellets are shown in Table 3.2.

Oily pellets



Figure 3.2: The sunflower seed shell casings pellets, a more oil-rich type of pellet, produced from the residue after sunflower oil production.

Table 3.2: The material properties of the oily pellets.

Properties	Oily pellet
Material	Shell casings from sunflower seeds
Diameter [mm]	6.4
Bulk Density [kg/m ³]	620
Higher calorific value [kJ/kg]	18207
Lower calorific value [kJ/kg]	16809
Moisture content [wt%]	7.67
Volatile compounds [wt%]	72.28
Ash content [wt%]	2.15

3.2 Top-ventilated system: onset of smoldering

The smoldering behavior of biomass pellets is described through four experimental approaches, described in sections 3.2, 3.3, 3.4 and 3.5 respectively. The top ventilated system, developed in the EMRIS project, replicating a small-scale storage unit, is described in section 3.2.1 and the experimental method in section 3.2.2.

3.2.1 Top-ventilated system: Experimental setup

The top-ventilated system was developed as a setup that resembles a silo storing biomass. To reduce heat loss, an insulated steel pipe was used, with ventilation only at the top, see Figure 3.3. The thickness of the steel-pipe wall was 0.1 cm, and its diameter 15 cm. The pipe was insulated with 6 cm layer of stone wool. Two different pipe heights were used: a pipe height of 33 cm, denoted as “low pipe” and two pipe modules stacked together with a height of 58 or 63 cm, denoted as “high pipe”. The variation in the height of the high pipe was due to different ways of assembling the pipe at the two different labs where the experimental work was done, see section 1.5.

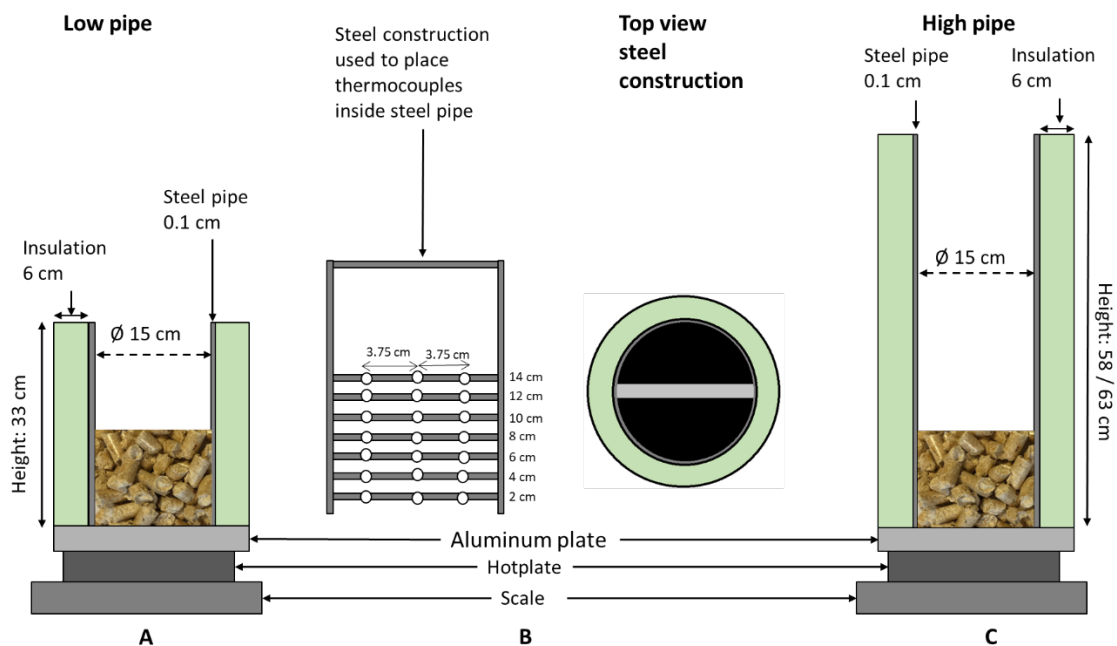


Figure 3.3: The experimental setup, here shown with the variations referred to as low pipe and high pipe. The two different setups contain the same diameter pipe, 15 cm, and is both surrounded by insulation with a thickness of 6 cm. The thickness of the steel-pipe wall is 0.1 cm. The steel pipe is placed in direct contact with the top of the aluminum plate, which is placed on top of the hotplate. The whole assembly is placed on a scale that measure the change in mass during the experiments. Part A)

The low pipe assembly, the height of the pipe is 33 cm. Part B) the steel construction (not to scale) containing all 21 thermocouples. The thermocouples are placed at the cylinder center, and 3.75 cm to the left and right. Each level with thermocouples is 2 cm above the previous one and contains three thermocouples. The levels are from 2 to 14 cm. Part C)

Illustration of the high pipe, the height of the high pipe is 58 / 63 cm.

A traditional cooking plate, denoted as hotplate, was used to heat the sample from below. An aluminum plate with a thickness of 3 cm was used to distribute the heat from the hotplate evenly to the pellet sample. The aluminum plate was machined to allow a thermocouple to inserted at the center at the top of the plate. In addition, the bottom part of the aluminum plate was machined to fit the top of the hotplate, ensuring good contact, and hindering the plate from being displaced during experiments. Below the aluminum plate a thermocouple was fitted at the center of the plate. A thermostat was used to regulate the hotplate, the thermostat was controlled by the thermocouple below the aluminum plate. In the planning phase, both aluminum and steel were tested for distributing the heat from the hotplate.

The tests showed that the aluminum plate functioned better, and therefore the aluminum plate was used in all experiments in this work.

Shielded type-K thermocouples 0.5 mm thick were used to measure temperatures, both at the aluminum plate and inside the sample. A total of 21 thermocouples were placed inside the sample using a steel construction (Figure 3.3B), with three thermocouples at each 2-cm level from 2 to 14 cm above the hotplate. One thermocouple was placed at the cylinder center, and the others 3.75 cm to the left and the right from the center.

During the experiments, the mass was recorded using a scale. The experimental setup is displayed in Figure 3.3. The scale was placed first, followed by the hotplate and the aluminum plate. The insulation was attached to the steel pipe, and the steel pipe placed at the center on top of the aluminum plate before the steel construction was placed inside the pipe. The pellets were added after the steel construction was in place. Figure 3.4 shows the low pipe and the high pipe in the lab.

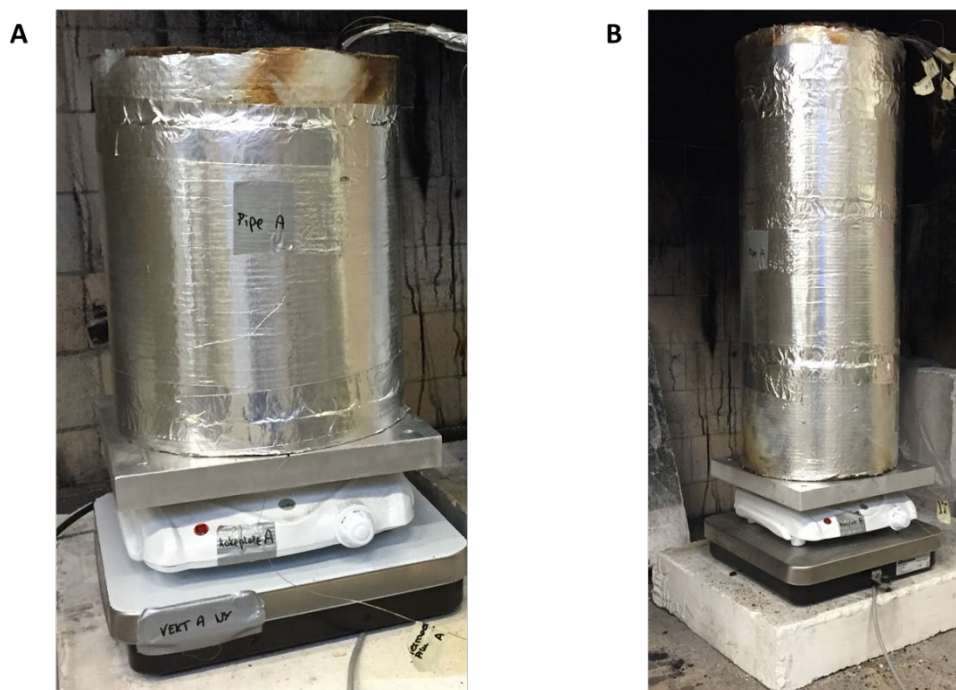


Figure 3.4: The two experimental setups in the lab. Part A) The low pipe 33 cm high setup and Part B) the high pipe setup 63 cm high.

3.2.2 Top-ventilated system: Experimental procedure

Several experiments have been carried out using a top-ventilated system with sample heating from below. Introductory experiments, denoted as initial experiments, were run together with two fellow PhD students, Edmundo Villacorta and Ragni F. Mikalsen. The group's work focused on determining

the conditions necessary to obtain self-sustained smoldering fire in wood pellets. The findings has been reported in a joint article [18].

In the initial experiments, the thermostat setting was 370 °C. As a consequence of heat loss from the aluminum plate to the surroundings, the temperature on top of the aluminum plate was 350 – 360 °C during experiments.

The sample height varied from 6 to 12 cm, the amount of pellets needed to obtain this sample height was weighed, and distributed evenly inside the pipe, which also contained the steel construction (ladder) with the thermocouples. Temperature and mass were recorded every 5 s. Before the hotplate was switched on and the sample was heated, there were two minutes of data acquisition, to allow check of thermocouple operation.

The sample was heated from below, until a predefined cut-off temperature was reached. The cut-off temperature was defined as reached when 2 out of 3 thermocouples at 2 cm above the aluminum plate obtained the predefined temperature. At this point, the hotplate was switched off. The temperature increase within the sample was slow. Therefore, to ensure that a sufficient part of the sample was dried and that the pyrolysis had started, the cut-off criterion referred to the height level 2 cm above the hotplate (aluminum plate), see Figure 3.3. The cut-off temperature was varied over the range 260 – 350 °C, depending on the sample height. Depending on the choice of cut-off temperature, the sample evolved in one of two possible and very different ways, referred to as, non-smoldering or smoldering.

As previously described, this procedure was used to determine if changes to the terms inside the pipe, such as the cut-off temperature, affected the onset of self-sustained smoldering. The external condition changed was the height of the pipe, from 33 cm to 58 or 63 cm. The experimental procedure was the same for both pipe heights, and sample height were equal. However, the cut-off temperature for the high pipe was determined based on the experience from the experiments in low pipe. The cut-off temperature for the high pipe was varied between 220 – 320 °C.

3.3 Top-ventilated system: Air flow in at height 20 cm / 33 cm

The inhomogeneous process of smoldering resulted in a smoldering front that moved upwards through the sample in an elongated bell shape. The analyzed data showed that the smoldering front reached the three thermocouples at each level at different times. It was therefore decided to investigate how air enters and exits the sample through the pipe.

The experimental setup was similar to the setup as Figure 3.3A and is shown in Figure 3.5A, except for the additional measurement position for temperature in the space above the sample where air circulates. These thermocouples were located in the pipe at height 20 cm above the aluminum plate, and in a couple of experiments, at the top of the pipe at 33 cm, as seen in Figure 3.5B-C.

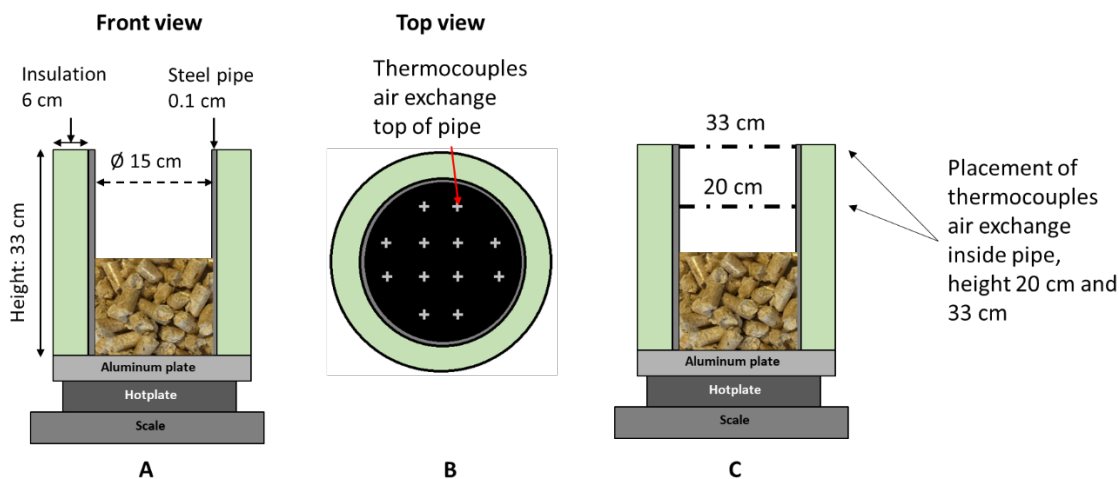


Figure 3.5: The low pipe experimental setup as shown in part A, was used in the experiments with the air flow measurements inside the pipe. Part B) show the thermocouple placement as seen from above. A total of 12 thermocouples were placed inside the pipe at 20 cm height. Part C) show the measurements points as seen from the side. Temperatures that reflect the air flow have been measured 20 cm from the bottom of the pipe. In addition, for some experiments temperatures has been measured at the top of the pipe, at 33 cm in addition to the measurements at 20 cm.

To characterize the air flow above the sample, one would preferably measure air velocity at a number of points. Temperature measurements were chosen as a replacement, since there were several challenges connected to velocity measurements: Attempts were made to measure the velocity of the convecting air, however, the air moved slowly. A handheld air velocity measuring unit was tested; however, the air velocity was too low to obtain a non-zero reading. A bidirectional probe was discussed, however in this small-scale experimental setup the fear was that this would affect the air flow. Other options such as a hot wire was also discussed. Due to the tar in the smoke, which contaminated all measurement equipment, since it condensates on all equipment above the sample, it was considered not to be a suitable method for these experiments. Therefore, only temperature measurements were used.

Temperatures in the air flow were measured by shielded 0.5 mm type-K thermocouples. A steel mesh was used to place 12 thermocouples in the pipe at a height of 20 cm, see Figure 3.6A for the location of the mesh at 20 cm in the pipe. 12 additional thermocouples were placed in a larger mesh, used to measure the air flow on the top of the pipe, at 33 cm, see Figure 3.6B, in a couple of experiments.

The experimental procedure used was similar to the one described in section 3.2.2, with a few exceptions. The sample was heated for a predefined time: 6.5 h. The sample heights were 10 and 12 cm. The mesh was placed inside the pipe, after the pellets had been added. The mesh was placed at 20 cm by placing it on top of the steel construction (ladder) that held the thermocouples used to measure temperatures inside the sample. The mesh with thermocouples at 33 cm was simply placed on top of the steel pipe.

Air flow measurements were performed with two different types of materials, wood pellet type A and oily pellet. In addition, some of the experiments had a reduced air flow obtained by covering the opening of the steel pipe (see section 3.4). In these experiments the duration of heating was varied from 3 to 13.2 h.

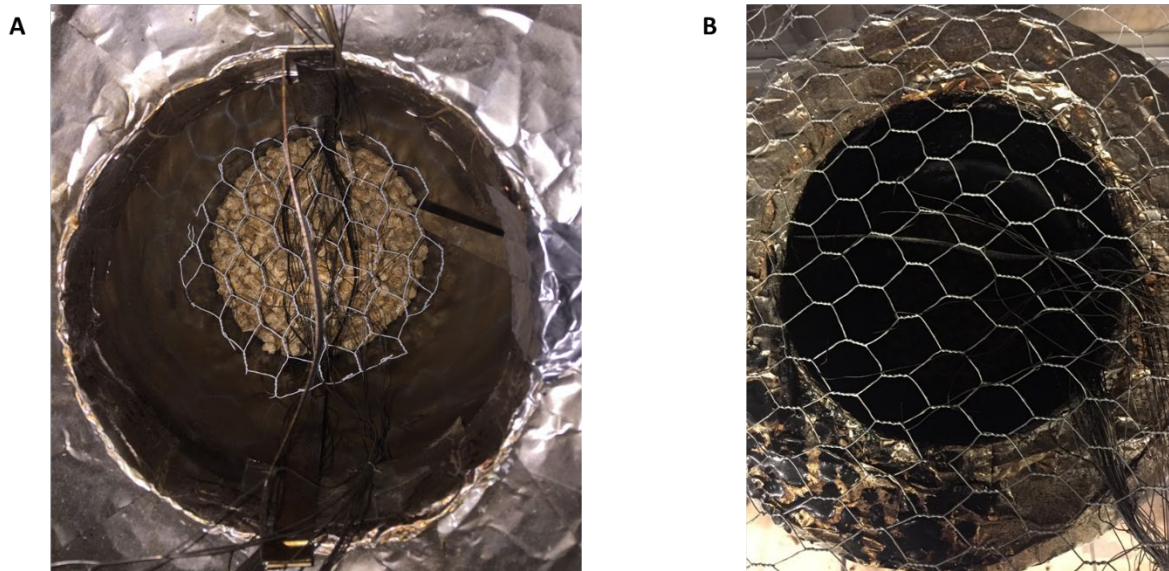


Figure 3.6: The mesh containing the 12 thermocouples used to measure the temperature in the air flow to and from the sample. Part A) The mesh placed at height 20 cm, in this case 10 cm above the pellets sample. Part B) the mesh with thermocouples at top of the steel pipe, at 33 cm. The mesh was folded around the pipe to ensure that the thermocouples stayed at the desired position during experiments.

3.4 Restricted air supply to sample

Smoldering can occur at low oxygen concentrations (10 %) [15]. In a silo storage unit, the oxygen is limited. In the top-ventilated system used in the experiments, air enters the sample from the top. Thus, by reducing the opening of the steel pipe, the oxygen supply is reduced. This allows experiments on how the air supply affects smoldering combustion. Steel plates with cut-outs corresponding to 50 % and 25 % of the opening were used as covers. The cut-out was in the middle of the steel plate, which also allowed easy access to the thermocouple wires, see Figure 3.7. The steel covers forced air flow into the middle of the pipe. The three configurations are shown in Figure 3.8, where the red lines indicate the openings. In Figure 3.8A-C, the thermocouple wires exit the pipe in the lower part of the photos. The first photo shows the standard opening, followed by the opening reduced to 50 % and 25 %, respectively.

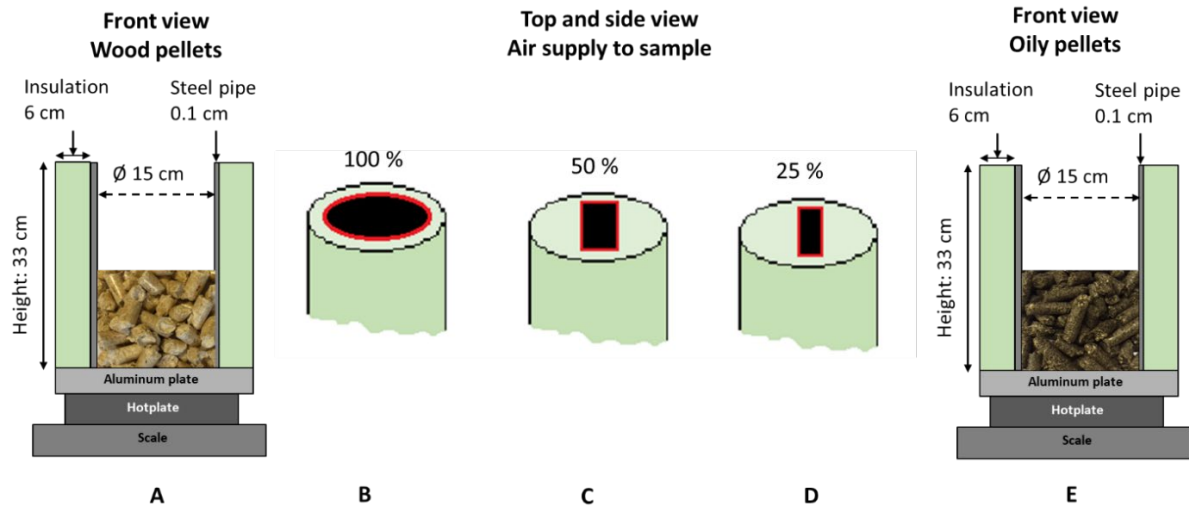


Figure 3.7: The experimental setup with covers at the top of the pipe. Parts A and E show the experimental setup with wood and oily pellets. The experimental setup is the same for both types of pellets. Part B) The air supply to the sample is 100 %, with opening indicated by the red line, there is no reduction in the air supply. This is the standard condition. Part C) The air supply is reduced to 50 %. Part D) The air supply is reduced to 25 %.

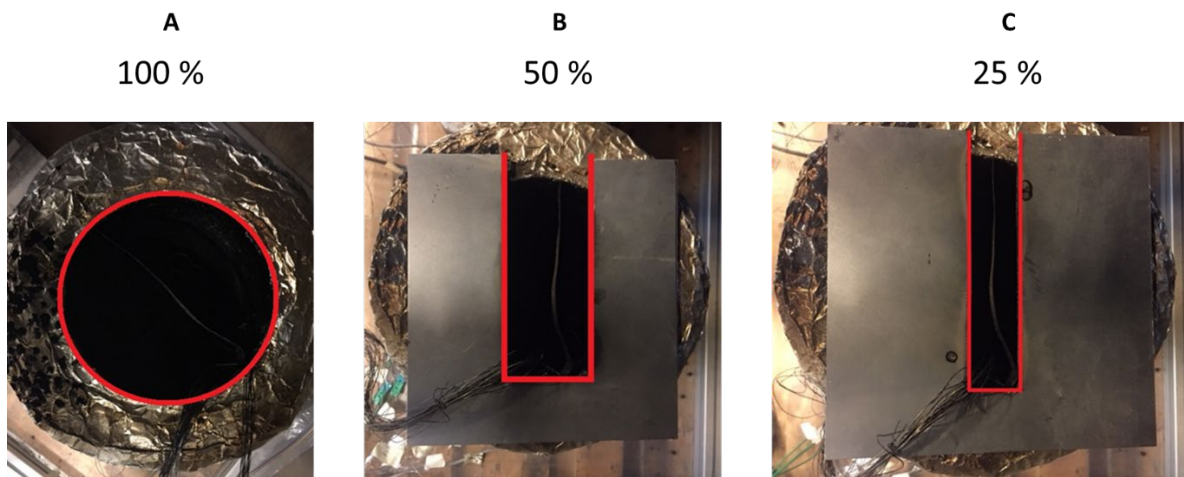


Figure 3.8: Top view of pipe (sample container), with three different openings. From left to right, air access is reduced. Part A) normal conditions, with no reduction in the air supply, the pipe is a 100 % open. Part B) The air supply is reduced to 50 %, a steel plate with a cut-out placed on top of the pipe covering 50 % of the opening. Part C) The air supply to the sample is 25 %. In each case, the red line indicates the opening.

Two different types of biomass pellets were tested: wood pellets and oily pellets. The experimental setup was the same as the one in Figure 3.3A. Both materials were tested in parallel using two identical set-ups, as shown in Figure 3.9, to ensure the same external conditions for each set of experiments. The two set-ups were placed side by side, in the same cabinet with three walls, and an opening on top, with ventilation above. The sample heights were 10 and 12 cm, with heating duration from 3 h to 13.2 h. The variation in the heating time was a consequence of the use of cut-off

temperature as a stop criterion for the 10 cm sample height. In the 12 cm sample height the duration of heating was used. The experiments were heated for 6.5 h, if the result was non-smoldering, the duration of heating was increased by 1 h for the next experiment. Otherwise the experimental procedure was equal to the one described in section 3.2.2.



Figure 3.9: The two experimental setups in the lab. The pipe to the left was used for wood pellets, and the pipe to the right was used for oily pellets. The two assemblies are placed inside a cabinet, which is closed at three sides: left, right and rear sides. The cabinet has an opening at top with ventilation above. This ensures the same external conditions, and the experiments were run in parallel.

3.5 Long-run experiments with refill of pellets

The so-called long-run experiments are a continuation of the standard experiments. During storage and production of pellets, the large units are refilled with pellets during production. The impact of a refill of a silo on a smoldering fire, was replicated with the small-scale experiments. In these experiments, additional pellets was refilled at intervals to resembles an actual storage unit, where fresh pellets are added to a silo already containing pellets. With a smoldering fire inside the silo, the effect of the added, fresh fuel could be investigated.

In the long-run experiments the wood pellet sample was refilled to its initial mass three times a day. The experimental setup the same as shown in Figure 3.3A. However, more thermocouples were used, temperatures inside the pipe were measured up to 20 cm. The idea of the long-run experiments was to allow for several periods of large mass-loss rate. The procedure is displayed in Figure 3.10, the sample was refilled with pellets in intervals of 8 h. The refilling times were 07:00 am, 03:00 pm and 11:00 pm. These intervals were chosen because of the manpower needed to conduct each refill, and the

alarm system in the building. All the refills were conducted manually, meaning that a person needed to be physically present to refill the mass.

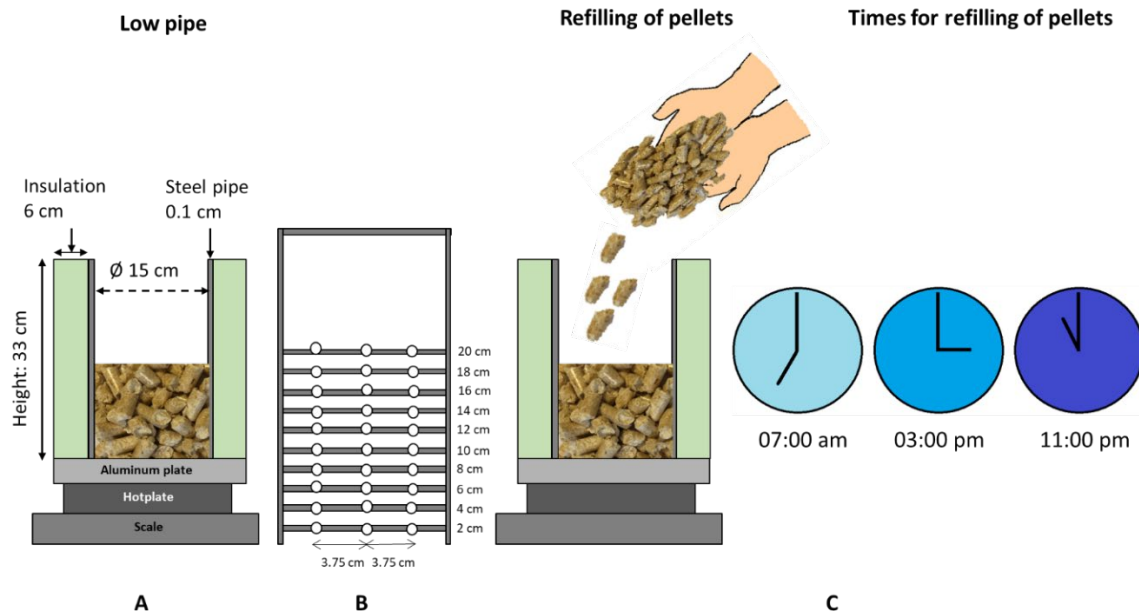


Figure 3.10: In the long-run experiments the low pipe setup is used as displayed in part A. Part B show the thermocouple steel construction, where the number of thermocouples have been increased from 21 to 30 from the initial experiments. The temperature in these experiments is measured from 2 – 20 cm. Wood pellets are refilled to the sample to reach the start weight of the experiment each 8 hours as shown in part C. The refilling times are 7:00 am, 3:00 pm and 11:00 pm.

The refilling extended the duration of the experiment by days and even weeks. The longest experiment lasted for two weeks. The sample height was varied between 10, 12, 14, 16 and 20 cm. The amount of pellets added in each refill was dependent on the amount combusted from the previous measurement, the sample was refilled to its initial mass. However, there were different ways of treating the wood pellets before it was added into the pipe: room temperature fuel (untreated fuel), heated pellets (heated for 15 min at 120 °C) and room temperature fuel added when the external heating was still connected throughout the experiment.

There were different approaches in the long-run experiments. The initial method with the cut-off criteria was used for conducting the first experiments. However, in more recent experiments the criteria were changed to the duration of heating. In the most recent experiments, the external heating was not switched off during the long-run experiments. However, the thermostat settings were in these cases lowered to a temperature of 300 °C. The sample was therefore not heated to such a high temperature. This implies a slower heating of the sample, compared to the previous experiments. By lowering the temperature of the thermostat, and therefore also the temperature of the aluminum plate,

one was able to obtain enough refills to ensure that the sample would not burn out after an intense combustion period, and previous tests showed that the sample needed to be heated to around 300 degrees to obtain self-sustained smoldering combustion.

4. Onset of self-sustained smoldering and intense combustion period

The onset of self-sustained smoldering combustion in wood pellets was investigated to establish the boundaries for obtaining a sustaining smoldering fire. Through a variety of cut-off temperatures, the temperature needed to establish a self-sustained smoldering fire in the lower parts of the sample was found. There were two different outcomes from the initial experiments, non-smoldering and self-sustained smoldering. During smoldering combustion, a chaotic temperature development was observed, however, the mass loss curve indicated a systematic behavior during combustion. The findings from the onset of smoldering and the findings in the intense combustion period will be described in the following chapters.

4.1 Typical smoldering and non-smoldering behavior in the top-ventilated system

There were two different scenarios resulting from the experimental setup, non-smoldering, and smoldering. Typical smoldering and non-smoldering behavior in terms of temperature development and the change in mass is shown in Figure 4.1, in the left column is a non-smoldering experiment (Figure 4.1A and C) and the right column shows a smoldering experiment (Figure 4.1B and D). The top row displays the temperature development in a sample with wood pellets, and the bottom row shows the change in mass. When the external heating was switched on, the temperature inside the sample started to slowly increase upwards in the pipe, from the lower parts and up to the middle or top of the sample depending on the sample height. In the cases shown in Figure 4.1, both samples were heated for 6.5 h. However, only one of them resulted in smoldering fire. The sample height was 12 cm. In such high sample size as 12 cm, the temperature in the top (10 – 12 cm) was not as affected by the external heating at the lower parts of the sample. During external heating, the temperature increased in the lower parts of the sample and when the external heating was switched off, the temperature decreased. In the first phase of the experiment the non-smoldering and smoldering behavior was similar. However, in smoldering cases, the temperature increased after the sample reached the critical point of thermal runaway (TRA), and a self-sustained smoldering combustion was established, as seen in Figure 4.1B. The non-smoldering experiment cooled to room temperature, there was not enough heat generated inside the sample to obtain a self-sustained smoldering combustion, as seen in Figure 4.1A.

After thermal runaway (9 h), the material undergoes a slow smoldering combustion at lower temperatures, see Figure 4.1B. When the combustion front reached the surface of the fuel, where fresh oxygen supply was present, the smoldering entered a new phase, an intense combustion period with

higher temperatures, approximately at 18 h in Figure 4.1B. After the peak, the smoldering combustion slowed down, where it fluctuates, and in some cases reach a second or third peak caused by secondary char oxidation. However, the temperature at the secondary char oxidation was much lower compared to the first intense combustion. The smoldering front moved downwards through the sample, and when the front had moved through the whole sample, the temperature decreased to room temperature. An experiment was finished when all thermocouples measured room temperature.

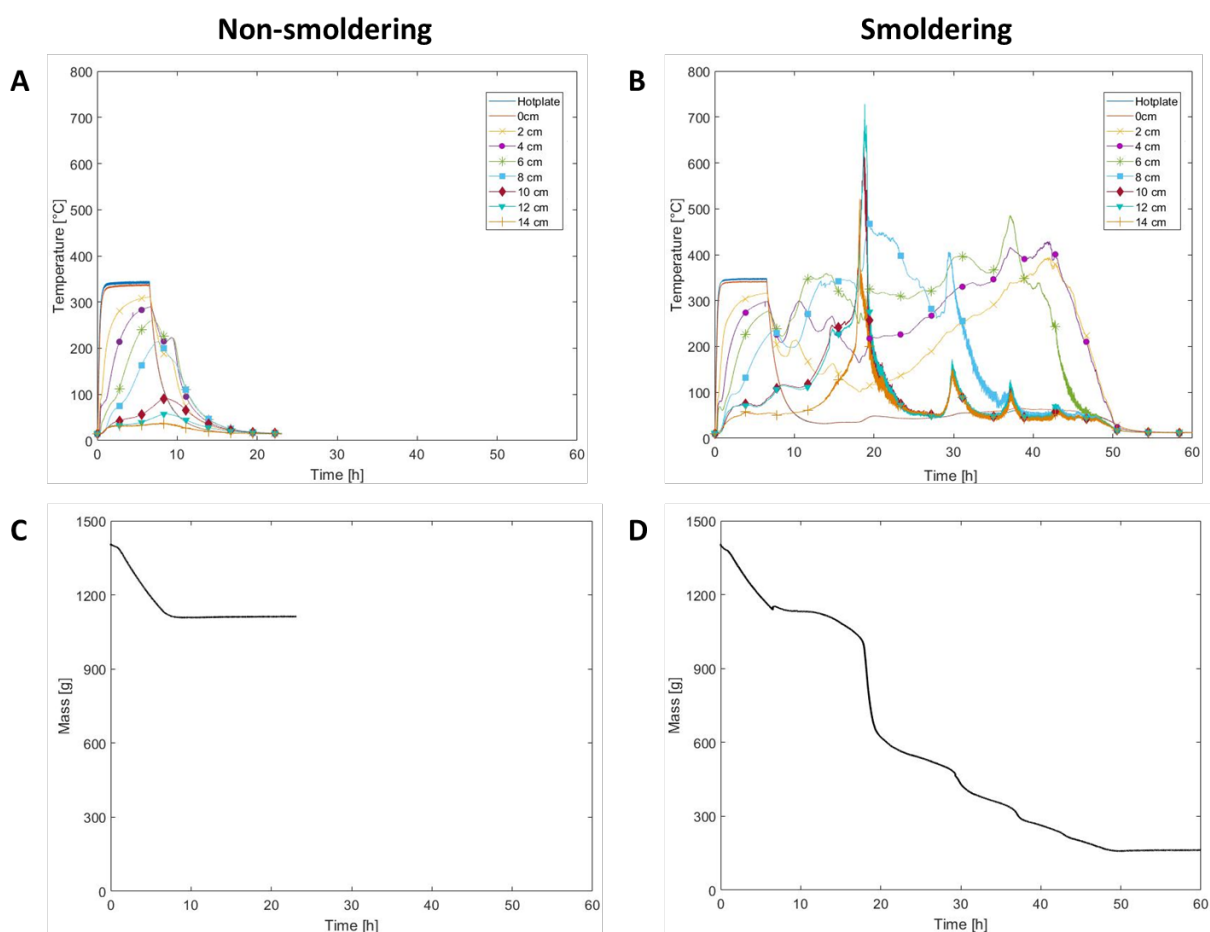


Figure 4.1: A typical non-smoldering and a smoldering scenario in a sample with a height of 12 cm is displayed. Part A) The temperature distribution in a wood pellets sample with non-smoldering. The sample was heated for 6.5 h, the sample did not smolder. The temperature decreased to room temperature after the external heating was switched off. Part B) The sample was heated for 6.5 h, however, in this case the sample with wood pellets smoldered. After the external heating, the temperature decreases until thermal runaway occurred, and the temperature started to increase without any impact from any external sources. The temperature shows an intense combustion period at approximately 20 h, and otherwise a more stable low intensity smoldering combustion until 50 h, where the sample cooled to room temperature. Part c and d show the change in mass during the experiments. Part C) the mass decrease during the external heating, when the external heating was switched off the mass stabilize. Part D) the first period of the mass loss was similar for the two outcomes. After thermal runaway, the mass-loss rate slowly increased at the start of the intense combustion period. There was a rapid increase in the mass-loss rate before it slows down after the intense period. Note: that there is still material left after the smoldering process, the residue consists of ash and charred pellets.

During external heating (6.5 h), the sample was dried and a pyrolysis of the material started, this was seen by the change in mass for both outcomes, see Figure 4.1C and D. When the external heating was

switched off, the mass-loss rate stabilized. For the non-smoldering cases, the mass-loss rate was zero, as the sample cooled to room temperature. In the smoldering experiments, the mass-loss rate is quasi constant during the cooling and during slow combustion of the sample (between 8 – 15 h). However, as the sample reached the start of the intense combustion period, at approximately 18 h (Figure 4.1D), the mass-loss rate increased rapidly, from 0.25 g/min in the slow combustion period to 4.20 g/min during the intense combustion period. This can be seen by the steep slope in the mass loss curve. More detail on the mass loss can be found in section 4.4.

Smoldering is a slow process, a sample with 1 kg of pellets has a duration of approximately 48 h. Pictures of the first 23 h with physical changes to a 10 cm sample with wood pellets, is shown in Figure 4.2. Pictures are from the top of the pipe looking downwards onto the sample, showing important visual changes of the sample during the first 23 h. After this there was no other visual changes in the top view of the sample. In picture A, the pellets were unaffected by the heating. After 5.5 h, (picture B), the external heating was switched off and a change in the pellets were observed. The pellets had started to break apart. Along the pipe wall the pellets had started to change color to light brown. After 9 h (picture C) self-sustained smoldering was established. On the left side of the picture, the smoldering front had reached the surface of the fuel in one area, shown by the black charred pellets and ash. Later, the smoldering combustion was visibly generating more smoke and the temperature was higher, as shown in picture D. After 23 h, the sample consisted of black/charred pellets and ash (picture E). Even though it seems like the smoldering combustion was over, there were still high temperatures inside the sample, and 13 h later the sample had cooled to room-temperature. There were no visible changes to the top view these 13 h.

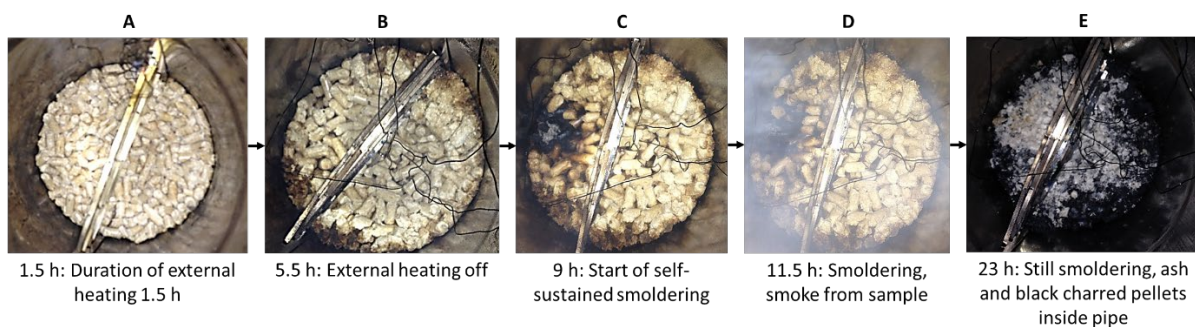


Figure 4.2: Pictures of how the wood pellets are affected during an experiment with a sample height of 10 cm. The total duration of the experiment was 36 h, and the pictures are of the first 24 h. After 1.5 h of external heating, the pellets were unaffected by the heating from below (A). The hotplate was connected for approximately 5 h, and at 5.5 h (B), the outer parts of the sample seems to be affected by the heating, the pellets started to crumble and change color. At 9 h (C) the smoldering front had reached the top of the sample in one small area, as seen by the black pellets and grey ash. At 11.5 h (D) the sample had reached the intense combustion period, the wood pellet produced more visible smoke. At 23 h, the intense combustion was over, and there was a stable smoldering process ongoing in the pipe. However, only ash and black charred pellets was visible (E). The smoldering continued for 13 h, before it cooled to room temperature.

4.2 Residue after non-smoldering experiments with wood pellets

To get a better understanding of how the pellets combust and the effect of heat, the residue after both smoldering and non-smoldering was sorted [51]. In the smoldering experiments the residue consisted of ash and some charred/black pellets. In the non-smoldering experiments, the residue could be divided into four different categories; pristine fuel, partially brown, brown and black/charred, see Figure 4.3. The categories were determined by how visually affected the pellets were by the external heating. The pristine fuel was unaffected by the external heating, there were no changes to the physical appearance of the pellet. The unaffected fuel was in the top part of the sample. Underneath the pristine fuel, changes in physical appearance of the fuel was observed. The pellets had a color change, from beige to partially brown. The next layer consisted of brown pellets, indicating that the heating had affected the pellet. The bottom layer consisted of black/charred pellets, these pellets were located closest to the aluminum plate. The size of the pellets had shrunk and undergone a pyrolysis. The difference in residue from non-smoldering and smoldering combustion was the content of ash. Even though the layer closest to the aluminum plate was combusted, there were no ash present in the residue from the non-smoldering experiments. The occurrence of char oxidation results in ash, however, only pyrolysis occurred in the non-smoldering experiments.

The water content of the pellets was between 7 and 8 wt%, however, during the external heating more mass than the water content was lost. In the non-smoldering cases 9 – 25 % of the mass was lost during the external heating, indicating a pyrolysis of the material, in addition to the drying. The pellets were affected by the external heating, causing a reduction in sample height. Some pellets increased in diameter, and started to dissolve, as an effect of drying, and exposure to moisture vaporization of the lower parts of the sample. The average mass lost during heating for the non-smoldering scenarios where 131.5 g. Three stages of the pellet were studied further in a microscope, see Figure 4.4. The pristine fuel and the brown pellet show more texture on the edges of the fuel. Black/charred pellets had a smoother surface. The black pellets was the closest to the heat source, and therefore also directly exposed for the heat of the hotplate, causing the fibers in the wood pellets to shrink because of water evaporation and pyrolysis. Similar visual color change can be found in smoldering in polyurethane foam [20]. In addition, Rogers et.al [52] reported a black char residue after smoldering in polyurethane foam. This consists with the color change observations in these experiments, where the front leaves black charred pellets.

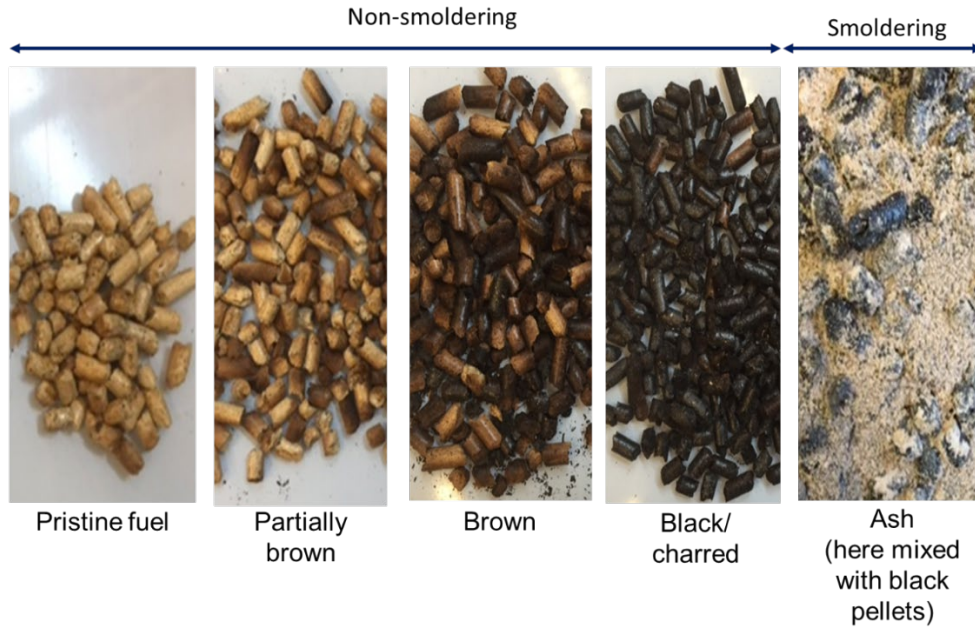


Figure 4.3: The residue after the initial experiments. The non-smoldering experiments had four categories of pellets: pristine fuel: unaffected pellets. Partially brown: pellets that had started to be impacted by the heating. Brown pellets: clearly affected by the heating of the sample. Black/charred pellets: showed that during the external heating, a pyrolysis of the material had started. The smoldering cases had a residue consisting of a mixture of black/charred pellets and ash.

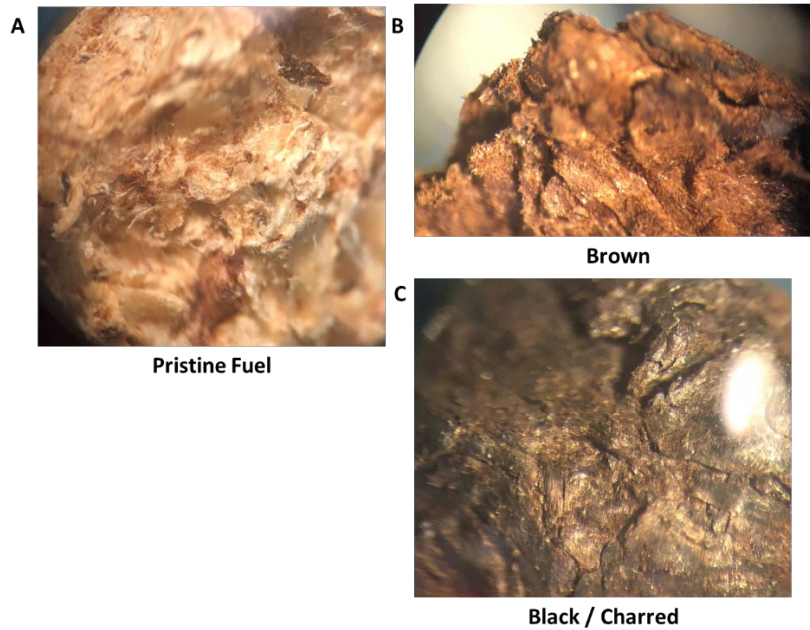


Figure 4.4: The different pellets residue in a microscope. In this case it was looked further at the pristine, brown, and black stage of the pellet. Picture A show the pristine pellet with the light beige color. Picture B is the brown pellet and picture C is the black/charred pellet.

During the onset of smoldering experiments, the sample height was 6, 8, 10 and 12 cm. The residue was sorted for the four different sample heights and the results are shown in Figure 4.5. The samples were heated to predefined temperatures, varied for each sample height, more details can be found in

section 4.3. The residue from the non-smoldering experiments showed a correlation between pristine fuel and sample height. As the sample height increased, the unaffected part of the pellets also increased. Pristine fuel residue decreases with increasing duration of heating. A longer duration of external heating resulted in more pyrolyzed fuel.

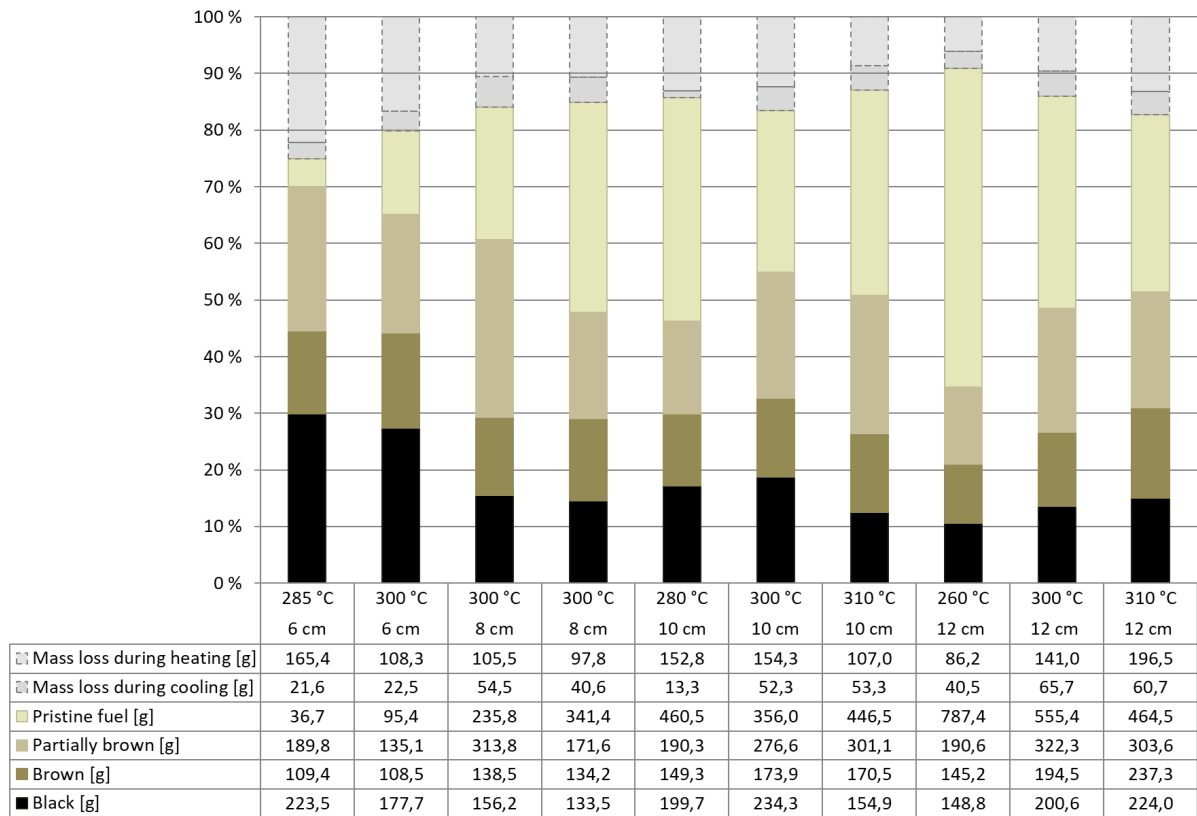


Figure 4.5: The residue from the non-smoldering experiments, where the residue are divided into the four categories, pristine fuel, partially brown, brown and black/charred. The dotted areas at the top represent the mass that is lost during cooling and the mass loss during heating. The figure is used with permission from Madsen et. al [51].

4.3 Onset of self-sustained smoldering

In these experiments two different types of wood pellets (Table 3.1) were tested under the same conditions. Through this work a method to indicate the critical temperature needed to obtain a self-sustained smoldering combustion was found. There were two approaches used, a predetermined temperature criterion, denoted as cut-off temperature, and the duration of heating, the time until the

sample reached the predetermined temperature. The results from this study will be presented in this chapter¹.

A smoldering initiation temperature was found in the experiments with the criteria for the onset of smoldering, where the sample was heated until a predetermined cut-off temperature as described in section 3.2.2. The smoldering initiation temperature was the needed temperature of the lowest part of the sample to obtain a self-sustained smoldering fire. The outcome of these experiments resulted in two different scenarios, non-smoldering, and smoldering. However, there are several parameters present in the experiments, which could affect the end results, such as: height of pipe, duration of external heating, sample height, cut-off temperature and pellet type. Therefore, a statistical analysis of all the parameters was conducted. The statistical analysis showed that the duration of heating was the most significant parameter regarding onset of smoldering in the wood pellets. When the sample was heated for longer, the outcome was more likely to be self-sustained smoldering fire.

From the statistical analysis the limits for the outcomes non-smoldering and smoldering was determined. These limits are indicated with lines for the two parameters cut-off temperature and duration of heating as shown in Figure 4.6 and Figure 4.7. The results from the analysis of the cut-off temperature is shown in Figure 4.6. The basis of the analysis was conducted through equation (1), as the onset of smoldering combustion could depend on a number of different parameters:

$$p = \frac{e^{\alpha_1(x_1 - x_{1,p50}) + \dots + \alpha_n(x_n - x_{n,p50})}}{1 + e^{\alpha_1(x_1 - x_{1,p50}) + \dots + \alpha_n(x_n - x_{n,p50})}} = \frac{e^{\alpha_0 + \alpha_1 x_1 + \alpha_2 x_2 + \dots + \alpha_n x_n}}{1 + e^{\alpha_0 + \alpha_1 x_1 + \alpha_2 x_2 + \dots + \alpha_n x_n}} \quad (1)$$

Pellet A is displayed in the left column, while pellet B results are shown in the column to the right. The top part shows the results from the experiments in the low pipe, while the bottom part shows the results from the high pipe. For the sample to establish a self-sustained smoldering process, the cut-off temperature needed to be high enough to ensure that the heat production inside the sample exceeded the heat loss to the surroundings after the external heating was Switched off. There are differences in

¹In the work in section 4.2 and 4.3, all experimental work were performed in collaboration with Edmundo Villacorta and Ragni Fjellgaard Mikalsen. This work resulted in a joint article where the three first authors contributed equally to the work [18] E. Villacorta *et al.*, "Onset of smoldering fires in storage silos: Susceptibility to design, scenario, and material parameters," *Fuel*, vol. 284, p. 118964, 2021/01/15/ 2021, doi: <https://doi.org/10.1016/j.fuel.2020.118964>.

Some of the work is also presented in Ragni Mikalsen's PhD thesis [19] R. F. Mikalsen, "Fighting flameless fires: initiating and extinguishing self-sustained smoldering fires in wood pellets," 2018.

the results from the two different types of pellets, even though both pellets consisted of wood, the composition of wood varied, and could be a reason for the difference in results. Another parameter is the freshness of the fuel, as Pellet B had been stored for a longer time compared with pellet A. Pellet A has an increasing trend in the cut-off temperature as the sample height increased. An opposite trend was found for Pellet B in the low pipe, as the sample height increased, the cut-off temperature decreased. For the high pipe, the pellet B results show that the trend was more stable, there was no increasing or decreasing trend, and the cut-off temperature was independent of the sample size. The two different pellets had different storage time, and were tested at two different locations, even though pellets were tested at both locations, it could be site differences could have influenced the experiments.

To determine the onset of self-sustained smoldering, the impact of the duration of the external heating was analyzed. The time for the sample to reach the given cut-off temperature varied for the different sample heights. The duration of external heating impacted the onset of smoldering, see Figure 4.7. Pellet A results are in the left column, pellet B in the right column, and the top part is the low pipe, while the lower part is the high pipe. Both pellet types show the same trend, as the sample height increased, the duration of heating increased to obtain a self-sustained smoldering process. This is as expected, to generate enough heat in the sample, a larger volume of the sample needs to have started a pyrolysis process. The lower samples (6 and 8 cm) had a shorter duration of external heating, as these sample reached the cut-off temperature faster, a reasonable assumption is that the lower sample had less mass dry, therefor more rapidly increased in temperature.

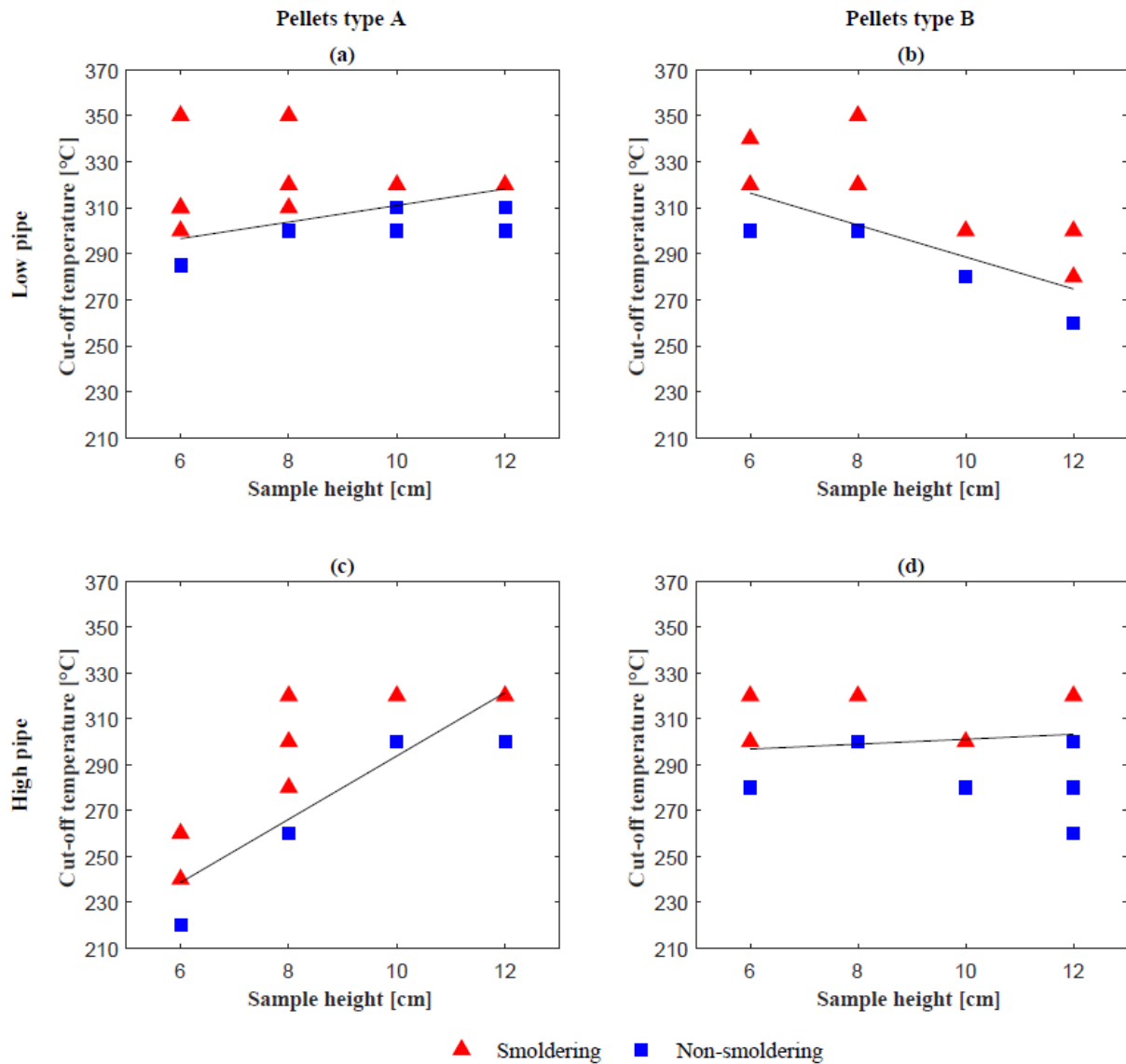


Figure 4.6: The non-smoldering and smoldering experiments, the red triangles are the smoldering cases, and blue squares are the non-smoldering. In addition, there is a statistical analysis for the limit to obtain smoldering representative for both type of pellets and pipe heights. The results for pellet A are shown in the left column, and pellet B in the right column. The low pipe experimental results are shown in the top row, and the high pipe in the row below. The sample height is shown on the x-axis, while the criteria cut-off temperature is displayed on the y-axis. The figure is reused from Villacorta et.al [18] with permission.

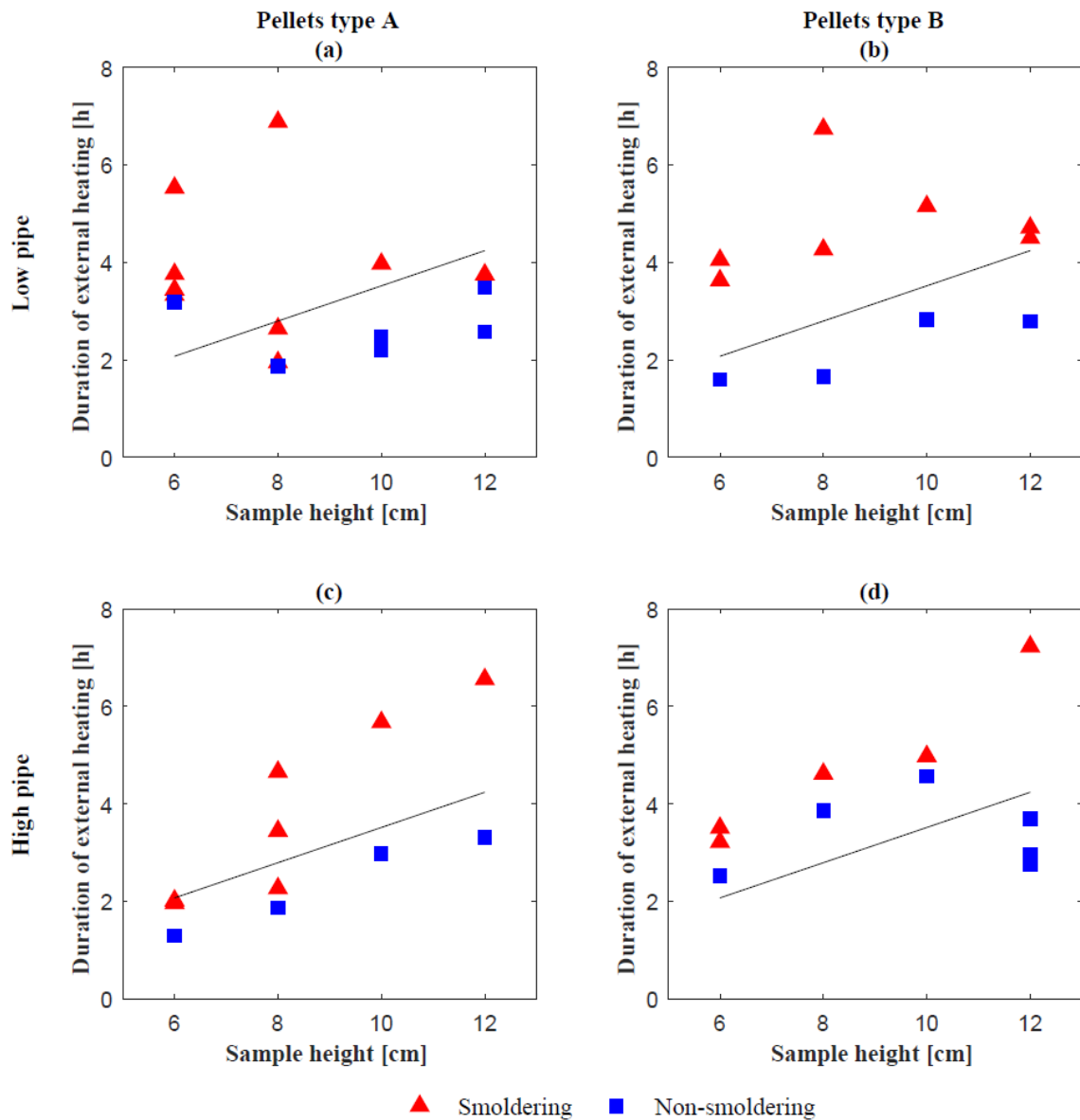


Figure 4.7: Non-smoldering and smoldering experiments with parameter: duration of external heating. The sample height was 6 – 12 cm, and there are two pipe heights. The results from Pellet A is displayed in the left row, and the row to the right is Pellet B. This figure is reused from Villacorta et al [18] with permission. The duration of heating increased with increased sample height.

Logistic regression was used to find the transition regions between smoldering and non-smoldering. Figure 4.8 show the results from two of the models tested: duration of heating and the height x duration of heating. In the first model, Figure 4.8a, the cut-off temperature, pipe height and type of pellet was found to not be significant, while the two significant parameters were the sample height and duration of heating. In the second model, Figure 4.8b, the significant parameters were the height of the sample and sample height x duration of external heating. The second model was the model with the best fit to the observed data. Parameters being $x_1 = \text{sample height}$ and $x_2 = (\text{sample height}) \times (\text{duration of external heating})$. As the sample height increased the duration of the external heating increased. However, the increase in external heating was smaller for the sample heights 10 – 12 cm compared to

the smaller samples, 6 – 8 cm. The external heating increased with 0.5 h when the sample height increased from 10 – 12 cm and by 1 h for 6 – 8 cm. In a large sample the top layer functioned as thermal insulation, ensuring a lesser increase in external heating, in addition to the relationship between surface to volume ratio.

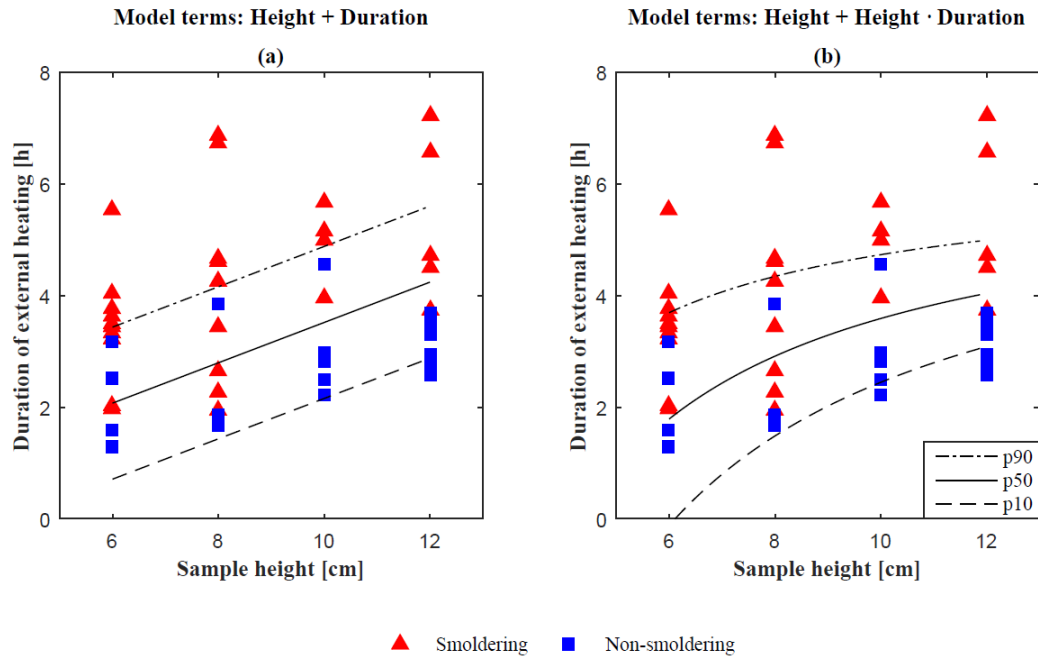


Figure 4.8: Determining the transition regions and finding the significant parameters for the outcomes non-smoldering and smoldering. A) This statistical model with the two significant parameters height and duration of external heating. B) A statistical model with the two significant parameters height and (sample height) x (duration of external heating). The figure is reused from Villacorta et.al [18] with permission.

4.4 Rapid increase in mass-loss rate during intense combustion

For the previously described experiments, the mass loss during smoldering combustion was analyzed. During smoldering combustion, a rapid increase in mass-loss rate was observed close to the intense combustion period, where the sample reached maximum temperature. The increase in mass-loss rate started at the time the temperature of the sample increased significantly, indicating that the intensity of the combustion process increased. The duration of the increased mass-loss rate was until the sample reached the maximum temperature, approximately 19 h (see Figure 4.1b and d). The mass loss for 26 experiments formed the basis for the analysis. The mass loss curve showed similar behavior for the four sample heights, 6, 8, 10 and 12 cm. Mass was lost during the external heating, before the mass-loss rate became quasi-constant during a period with low-intensity combustion. At the start of the intense combustion period, the mass-loss rate increased significantly.

The mass loss curve for an experiment with a sample height of 12 cm is shown in Figure 4.9. The mass loss displays different behaviors and is denoted as before significant mass loss (m_1), during significant mass loss (Δm) and after significant mass loss (m_2) intense combustion period. The start mass is denoted m_0 . The mass loss before the intense combustion was a result of the external heating, causing drying of the material and pyrolysis. During this period the mass-loss rate was low. When the intense combustion started, the mass-loss rate increases rapidly. After the intense combustion period the mass-loss rate was again low. Char oxidation of the fuel occurred during the intense combustion period, some experiments had a secondary char oxidation, see Figure 4.9 at approximately 40 h. A second intense combustion period can be observed at 40 h where the mass is reduced rapidly as in the previous intense combustion period at approximately 25 h, however shorter duration of the intense period, lower temperatures compared to the first intense combustion period, and therefore also a lower mass loss. Such periods of secondary char oxidation has not been further analyzed.

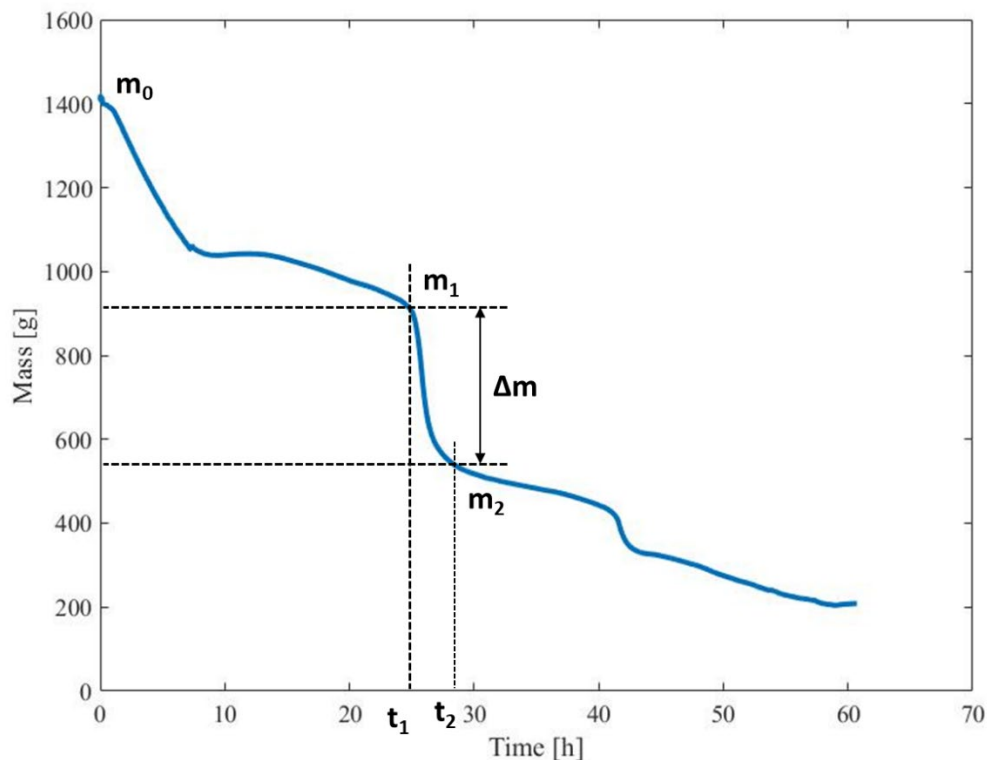


Figure 4.9: Mass loss during self-sustained smoldering in a top-ventilated system. During the smoldering combustion, there was a rapid increase in the mass-loss rate. The total mass loss during this period of intense combustion is indicated as Δm in the figure. Mass at start of the drop is denoted as m_1 , and m_2 is the mass at the end. The initial mass of the sample is denoted as m_0 . The start and end time of the period with intense combustion is indicated by t_1 and t_2 .

4.4.1 Determining the mass loss during the intense combustion period

Two different manual methods were used to determine total mass loss during the period with intense combustion based on the graphs of mass and mass-loss rate as functions of time, respectively. During

smoldering combustion, the mass-loss rate curve reflects the different phases of combustion. It is challenging to determine start and end point of the intense combustion period, as the mass-loss rate is noisy. Therefore, two graphical approaches were used to determine the start and end point of the mass loss, the quantitative values for m_1 and m_2 was found from the average start and end time found in the two approaches. The two methods are described in detail below.

Construction based on mass as a function of time

The construction based on mass as a function of time is shown step by step in Figure 4.10. A portion of the mass loss curve around the rapid decrease in mass was. A tangent (1) fitted to the steepest part of the curve was drawn, as shown in Figure 4.10A. Two additional tangents ((2) and (3)) were drawn along the mass curve before and after the period where it decreased rapidly (Figure 4.10B). The intersections indicated the start (t_1) and end (t_2) time of the period of intense combustion (Figure 4.10C).

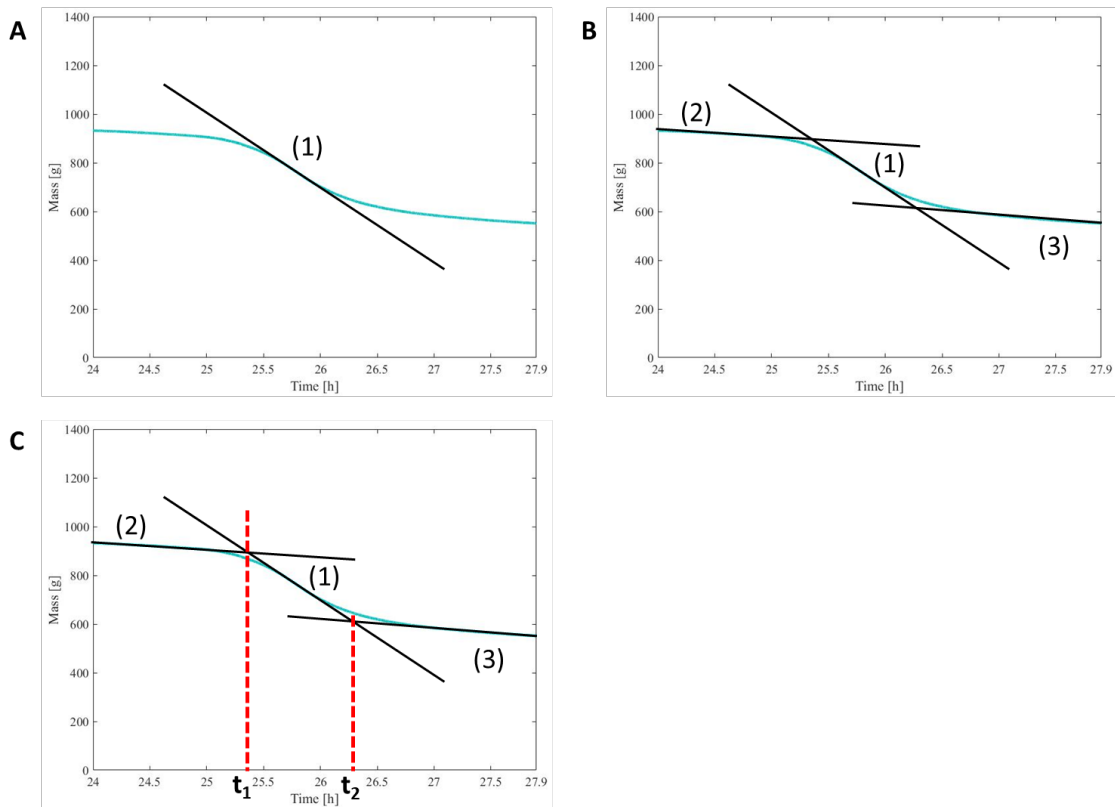


Figure 4.10: Method using the mass curve, to find the total mass loss during the period of intense combustion. A) The start point was to draw a tangent following the steepest portion of the mass curve (1). B) The next step was to draw two more tangents to follow the curve before (2) and after the steep portion (3). C) From the two intersections, the start time and end time were found.

Construction based on the mass-loss rate as a function of time

The second method used the mass-loss rate as function of time, the method is shown step by step in Figure 4.11. The mass-loss rate curve was smoothed by a running average over 600 sec, the noisy data before smoothing is displayed in the top right corner of the figure. A portion of the mass-loss rate curve, focusing on the intense combustion period, is shown in Figure 4.11A. Two tangents (1) and (2) were drawn along each side of the peak (Figure 4.11B). Two additional tangents (3) and (4) were drawn along the curve before and after the intense combustion period (Figure 4.11C). The two intersections resulted in the start (t_1) and end (t_2) time of the intense combustion period (Figure 4.11D).

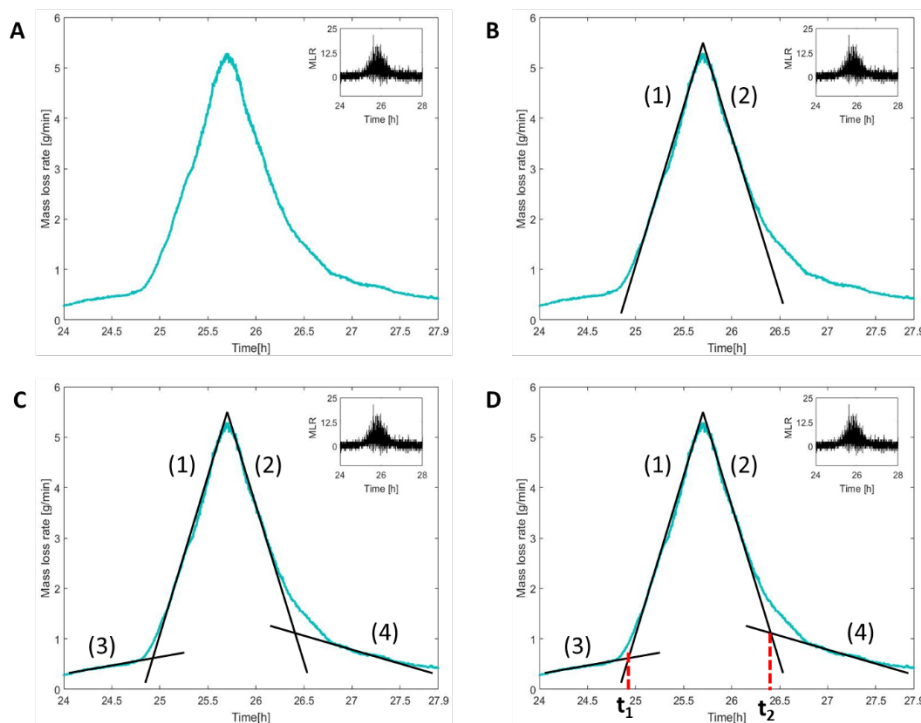


Figure 4.11: The second method used the mass-loss rate curve. The rate was smoothed over 600 s, to reduce the noise sufficiently that the start and end time of the intense combustion period could be determined. The mass-loss rate before smoothing is shown in the upper right corner. A) The mass-loss rate during the part of the experiment where the intense combustion occurred. B) First, two tangents were drawn along the slope of the curve at each side of the top, marked with (1) and (2). C) Second, tangents were drawn along the curve before (3) and after (4) the period with the highest mass-loss rate. D) From the intersection of the tangents, the start (t_1) and end (t_2) time was found.

The two methods were used to find the start (t_1) and end (t_2) time of the intense combustion period, and the corresponding mass was found from the recorded mass based on the average start and end time found in the two methods. There were variations in the time found by the two methods. The average difference for t_1 found for the two methods was 12 minutes. For t_2 the average time difference was 6 minutes. The larger difference in the start time was caused by the duration of the external heating. In some experiments, the intense combustion period started before or right after the hotplate was

switched off, causing difficulties to separate between mass loss caused by drying of the material, and the mass loss from a self-sustained intense smoldering combustion.

4.4.2 Mass loss during the intense combustion period

The duration of the intense combustion period was short compared with the overall length of the smoldering experiments, 0.5 and 1.5 h, compared with 30 – 60 h.

The method described above was used to find the mass reduction for the intense combustion period, in addition, the total mass loss before and after the drop could be determined. Variations with parameters as the experimental design, material, and sample height, might affect the size of the total mass loss. Figure 4.12 shows the total mass loss during the intense combustion period as a function of sample height. The total mass loss increases with increasing sample height and was independent of the parameters: pellets type and the experimental design. It was therefore determined to conduct a correlation analysis to confirm the relationship between the different parameters. A correlation analysis [53] was conducted to determine the dependency on the parameters: pipe height, sample height, pellet type and mass loss during intense combustion, through a multiple linear regression [53]. The dependency of the parameters was determined by the regression, where a value close to 1 show that they correlate and would affect the mass loss during intense combustion. The results are shown in Table 4.1, where only the sample height affected the size of the mass loss during the intense combustion period.

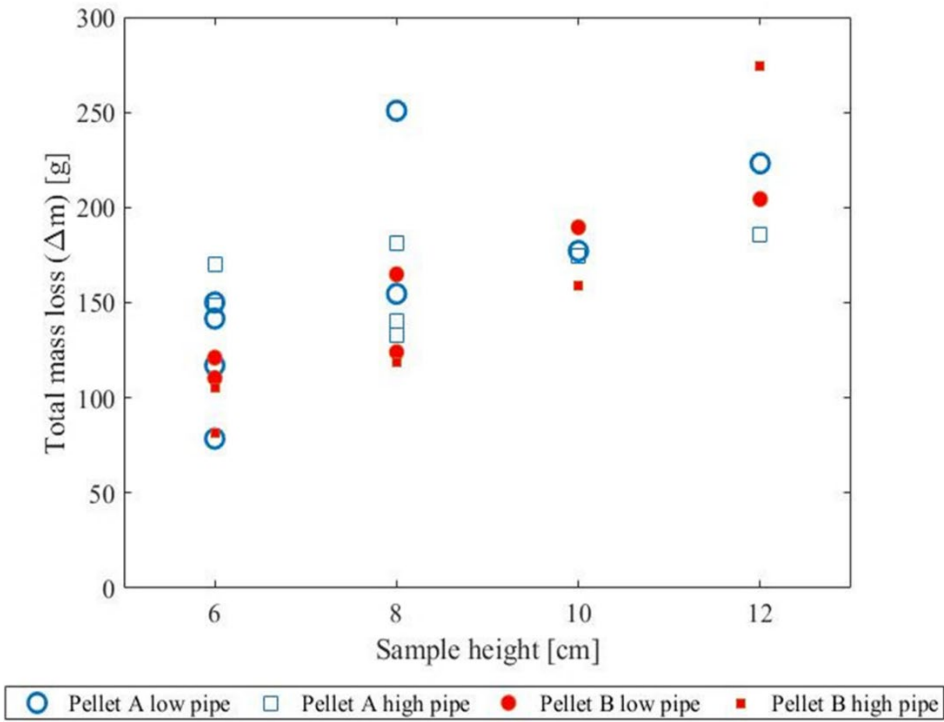


Figure 4.12: Total mass loss during intense during combustion in two different types of wood pellets. The sample height varied from 6 - 12 cm (left to right). The height of the steel pipe was indicated with a circle for the low pipe setup (33 cm) and a square for the high pipe (63 cm). The unfilled markers show pellets type A, while the filled markers show the results for pellet B. As the sample height increased, the size of the total mass loss increased.

Table 4.1: Correlation analysis of the parameters in the wood pellets experiments with smoldering, the size of the total mass loss during the intense combustion period. See further explanation in the main text.

	Pipe Height [Low / High]	Pellet type [A/B]	Sample height [cm]	Δm [g]
Pipe Height [Low / High]	1			
Pellet type [A/B]	-0.0120	1		
Sample height [cm]	0.0776	0.0284	1	
Δm [g]	-0.0185	-0.1217	0.7253	1

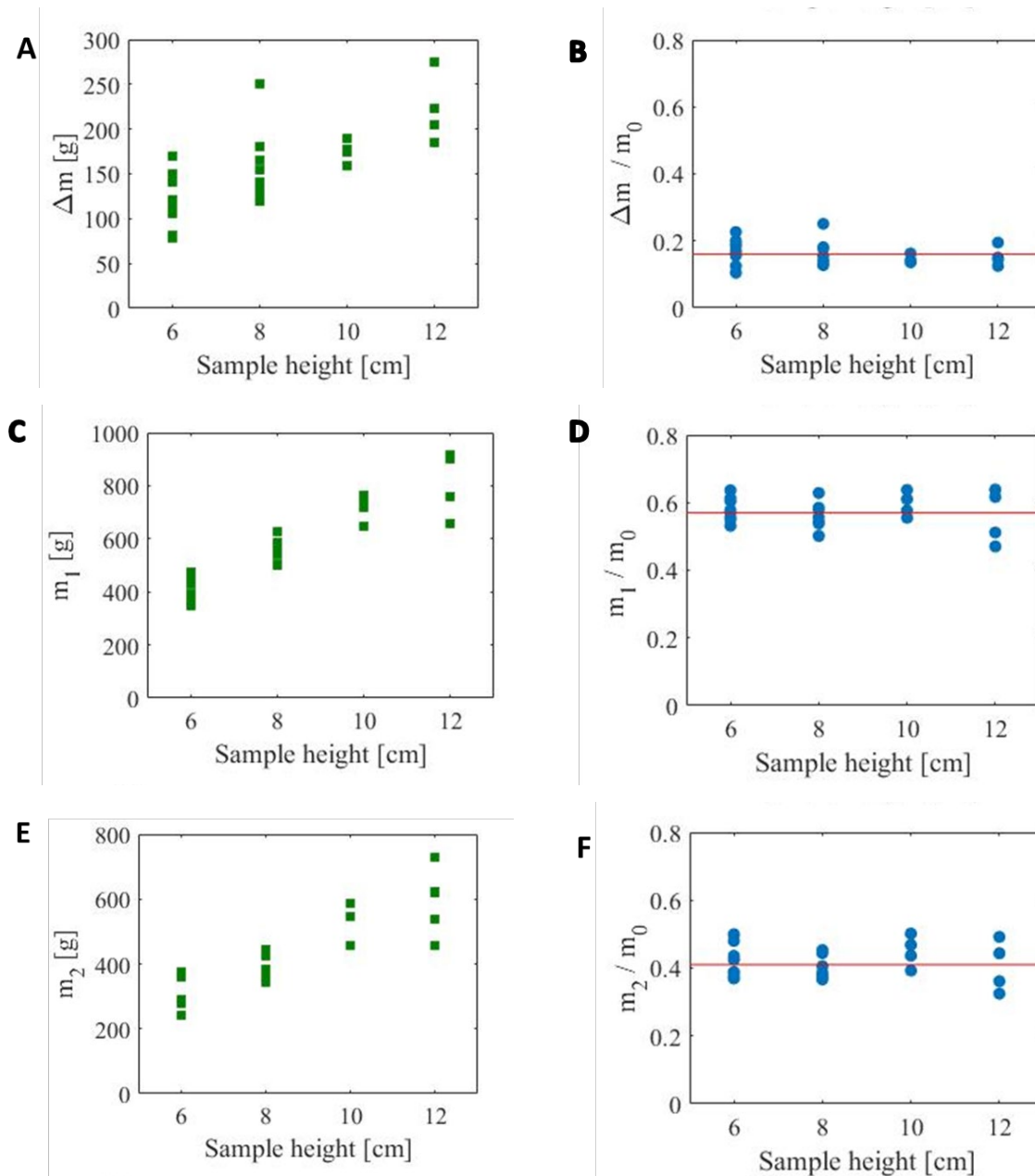


Figure 4.13: Three characteristic mass measurements, as defined in Figure 4.9. All of them increased with increasing sample height, as shown in figure A, C, and E. When these quantities were normalized with initial mass, they are approximately independent of sample height as shown in B, D, and F. The results show a mass loss of 15 % during the intense combustion phase (B). After the first phase with the external heating and low intensity combustion there is approximately 55 % of the sample left, meaning 45 % of the total mass was lost during this period (D), leaving 40 % of the sample (F) at the end of the intense combustion period. NOTE: the y-axis in figure A, C and E differ

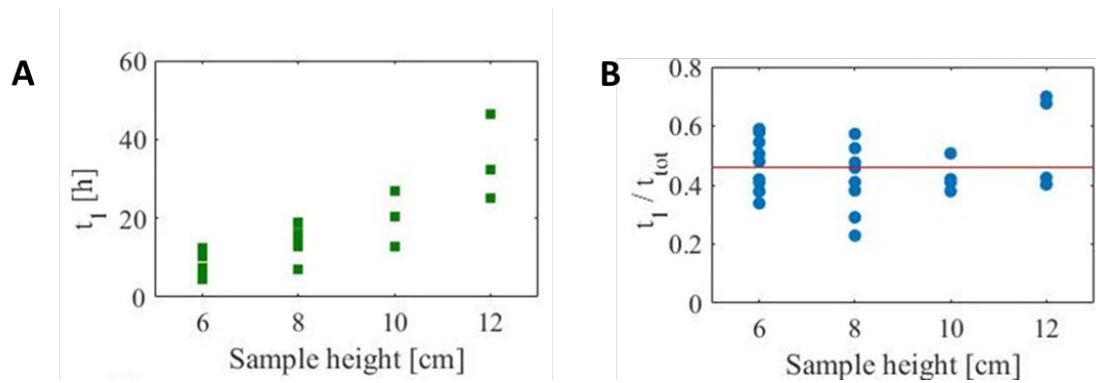


Figure 4.14: As time until the start of the intense combustion period as a function of sample height, see Figure 4.9. Time rescaled by the total duration (t_{tot}) of the experiment as a function of sample height, with an average value of 0.46 ± 0.11 .

The results show a systematic trend in the mass loss behavior during these experiments. Several factors were changed in these experiments such as the sample height (varying from 6 – 12 cm), wood pellets from two different manufacturers, and the height of the steel pipe, 33 or 63 cm. Despite all these changes, the sample mass behavior displayed a systematic trend, as shown in Figure 4.13. During external heating and the low intensity combustion leading up to the intense combustion period, 45 % of the total mass was lost (see Figure 4.13D). During the short intense combustion period, 15 % of the mass was lost (see Figure 4.13B), leaving 40 % of the mass (see Figure 4.13F). The start time of the intense combustion period (t_1) showed an increasing trend with sample height. Rescaling the start time with the duration of the experiment, showed that the intense combustion period occurred when 45 % of the experiment had been carried out (see Figure 4.14A). After the intense combustion period, approximately 50 % of the experiment remain. An overview of the different phases of a typical experiment is shown in Figure 4.15. In the first phase, the mass-loss rate was low, it increased during the intense combustion period, and decreased below the initial value afterwards, as shown in Figure 4.16. The mass-loss rate during the external heating and low-intensity combustion is higher for the lower samples heights and decreases with increasing sample height. This can be explained by the durations of the low intensity combustion. For the lower sample heights (6 – 8 cm) the time from shut-off of the hotplate to the intense combustion period is shorter than the higher sample heights (10 – 12 cm). All samples loose approximately the same percentage of mass during this initial phase, however, due to the longer duration of the initial phase for the higher samples, the average mass-loss rate is lower during this phase before the intense combustion period. The change in mass-loss rate during intense combustion could be explained by the access of air, as the intense combustion occurred the front had reached the surface of the fuel, the fresh air to the combustion zone increases the burning rate, increase the temperature and causing a larger mass loss over a short duration of time.

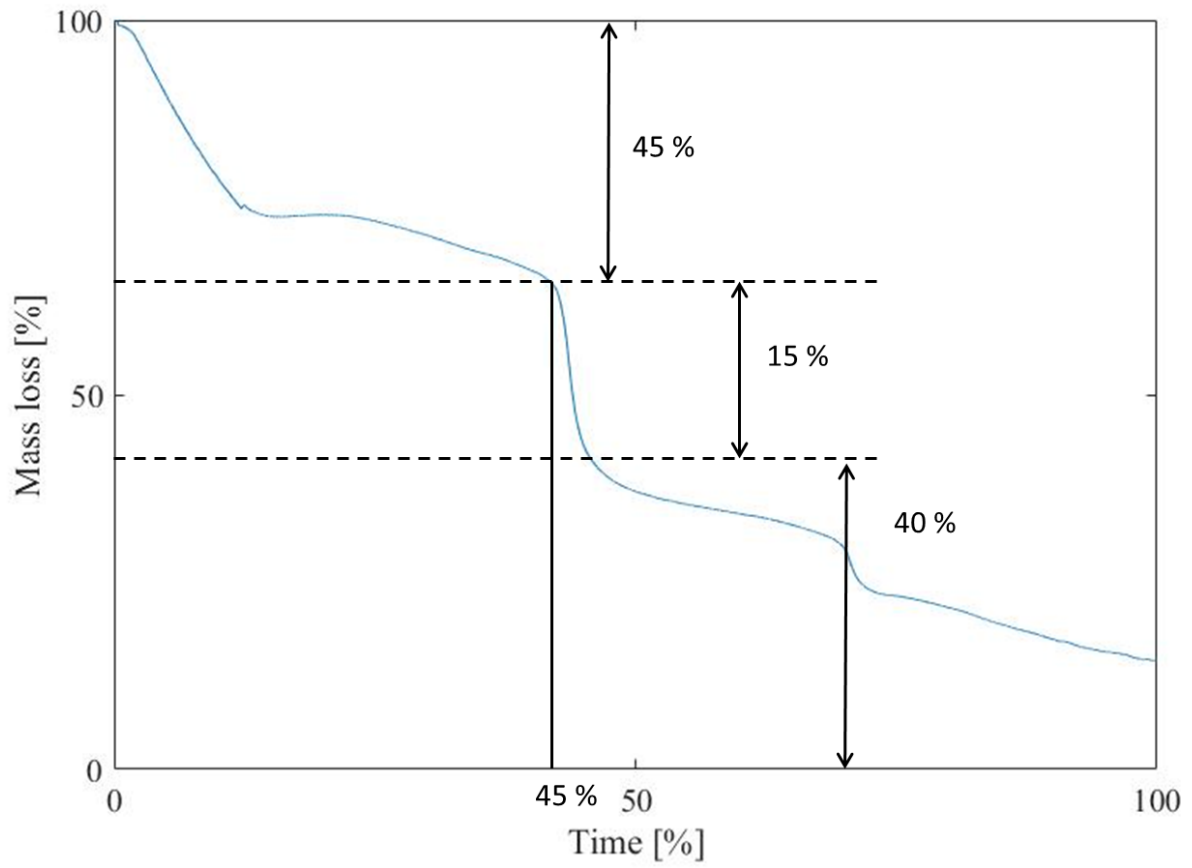


Figure 4.15: Overview of the different stages in terms of sample mass during smoldering experiments: before, during, and after the intense combustion period. 45 % of the mass was lost before intense combustion, 15 % was lost during the intense combustion, afterwards the intense combustion period 40 % was left.

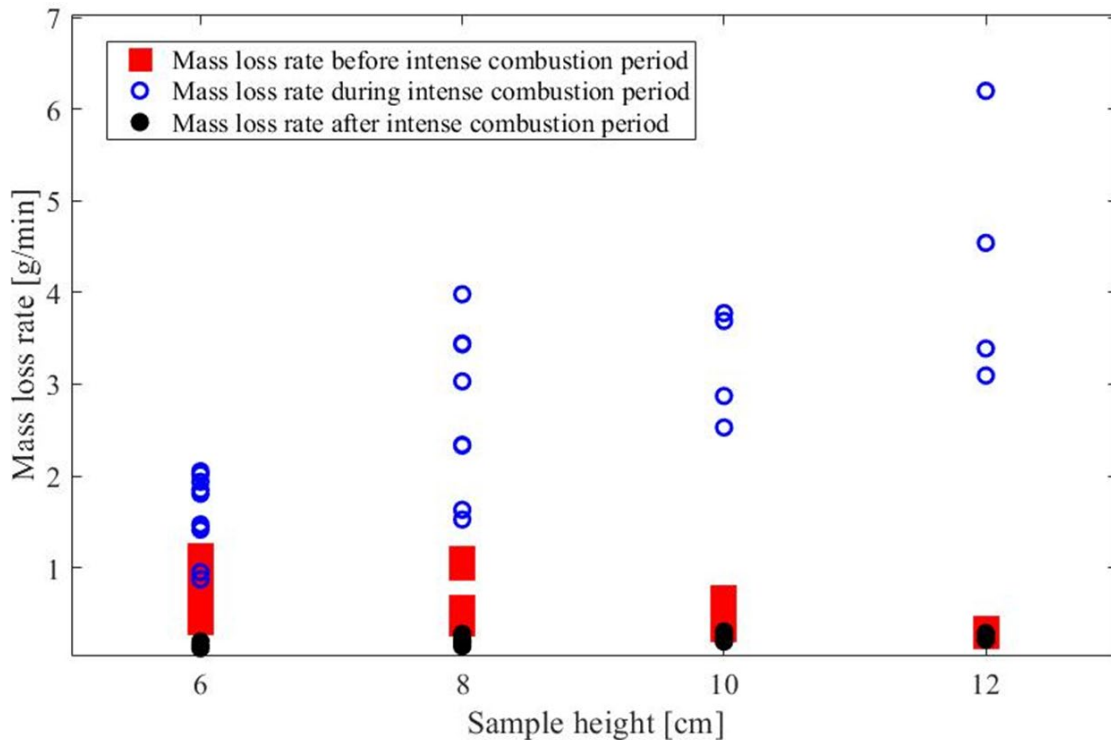


Figure 4.16: Mass-loss rate during the three different stages of the smoldering process in wood pellets in a top-ventilated system. As the sample height increased, the mass-loss rate increased. The highest values for the mass-loss rate were obtained during the intense combustion period for the largest sample heights (12 cm).

4.4.3 Conditions needed for the intense combustion period to occur

The mass-loss rate increased before the sample reached the intense combustion period where the high temperatures occurred, see Figure 4.1 B and D. For the sample to undergo an intense combustion period, three conditions need to be fulfilled: the combustion front needs to reach the surface of the fuel, a hot core area has to be established inside the sample, and the entire sample needs to have a temperature above 200 °C during the first phase. The three conditions are discussed in detail below.

For an intense combustion to occur, the smoldering front must have reached the upper surface of the fuel at the level of the maximum sample height, ensuring that the front has a fresh supply of oxygen before burning downwards through the sample. As the sample was heated, the pellets expanded, and shrunk. The height of the sample after heating could differ from the initial height, due to physical changes of the pellets. Therefore, the height of the sample must be estimated to determine if the smoldering front has reached the surface of the fuel. Figure 4.17 shows how wood pellets are affected by smoldering combustion inside the sample. Along the pipe wall the pellets have swelled and started to crumble. In the picture to the right the pellets had started to change color.



Figure 4.17: Physical changes of the wood pellets. The pellets were affected by the heating of the sample and the pyrolysis front. The pellets along the pipe wall have broken apart, and in the picture to the right there has been a color change from beige to light brown.

To estimate the height of the sample, the temperature measurements were used, the temperatures were recorded every 5 sec. As a thermocouple is exposed to the surrounding air or smoke in the pipe, the data show more scatter (larger and more rapid variations). This can be seen from temperature and standard deviation, see Figure 4.18. The timeline was from the start of the experiment, until the intense combustion period. The temperature for each layer in a 12 cm high sample is shown in the left column. Temperature graphs for all the three measurement points in each layer are shown. The three first layers (2 cm – 6 cm) has similar temperature development, and higher temperatures when the hotplate is disconnected. The second group of the sample (8- 12 cm) show a lower temperature during external heating. However, during the self-sustained smoldering process all the temperature graphs show similar trends of temperature development. Close to the intense combustion period, the temperature in the lower parts of the sample decreases (2 – 6 cm), while 8 – 12 cm increase in temperature. At the time of the intense combustion period, it is reasonable to assume char in the lower levels of the sample, as shown in the residue from non-smoldering samples (section 4.2). As the smoldering front has passed this part of the sample, and the front is moving upwards through the sample, it is natural for the lower parts of the sample to cool.

The standard deviation for the temperature at the center of each layer, with a running average of 2 min, is shown in the right column in Figure 4.18. The standard deviation increased for the first 2 h, at 2 cm during the external heating, probably due to the internal regulation control of the hotplate. The hotplate switched on and off to obtain a given temperature and it is likely that the lowest part of the sample could be somewhat affected by the temperature regulator. When the hotplate was on the temperature increased rapidly, and when the hotplate was off the temperature increases slower. In the layers from 2 to 8 cm, the standard deviation was low until the intense combustion period, indicating

that the thermocouples were located inside the sample, and not affected by surrounding air flow. The standard deviation at 12 cm increased at 10 h, which could indicate that the thermocouple was being exposed to surrounding air or smoke, caused by the fluctuations of cool air and warm smoke. This indicates that the sample height had decreased below 12 cm. At 10 cm (around 25 h), there was a large increase in the scatter, indicating an exposed thermocouple and a decreased sample height in the middle of the sample.

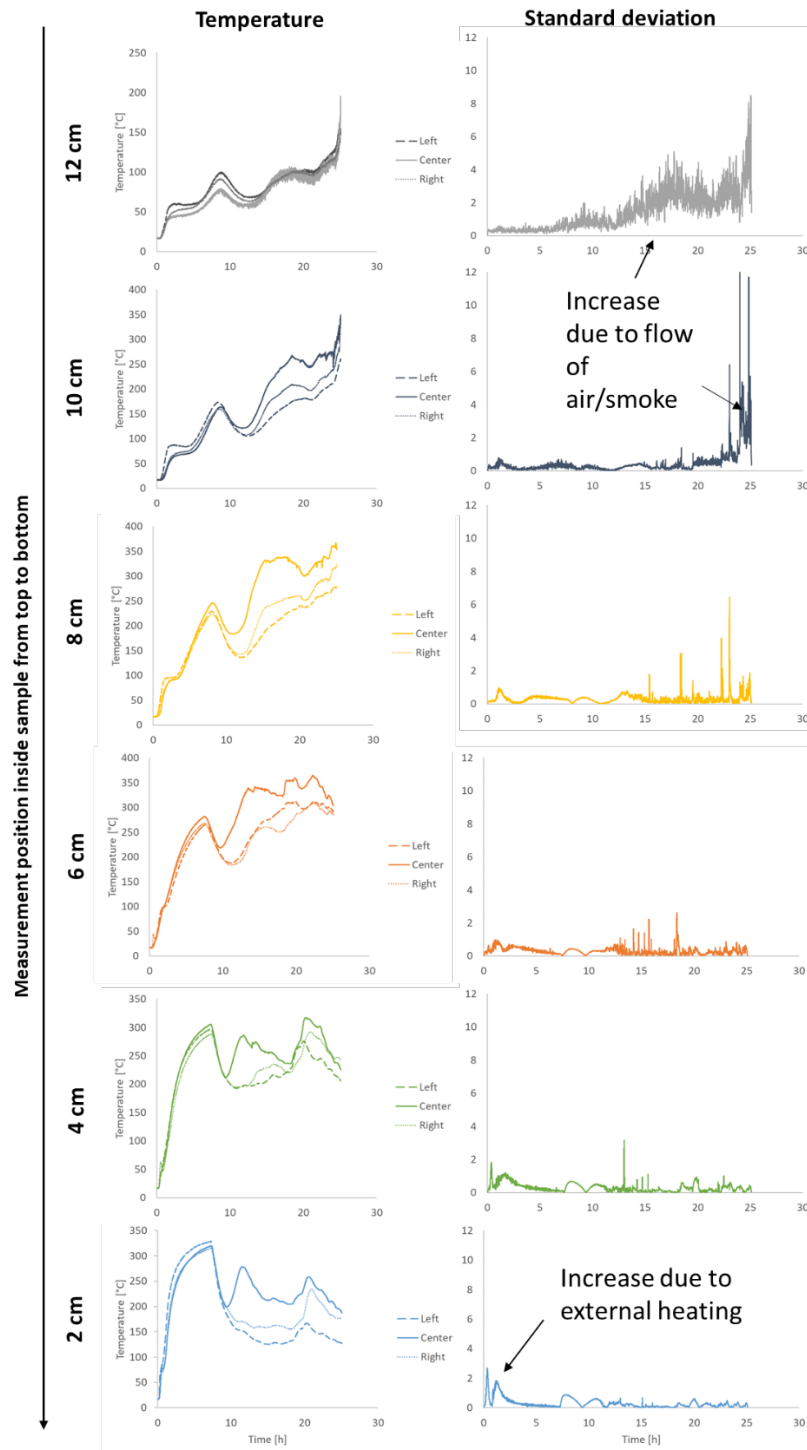


Figure 4.18: Temperature for each measurement position (left, center and right) in the left column and standard deviation for center temperature in the right column for a 12 cm sample. The time scale is from the start of the experiment until the intense combustion occurred (t_1). The curves are display from top (12 cm) to bottom (2 cm).

Estimation of the height of the sample was done by comparing the standard deviation of the temperatures, as shown in Figure 4.18. An increase in noise in the measurements indicate a thermocouple in air, and the noise is caused by the air and smoke passing along the thermocouple. The standard deviation in the middle of the sample increased at 10 and 12 cm, indicating that the height at

the middle of the sample had shifted from 12 to below 10 cm during the first 30 h, as shown in Figure 4.19 the lines indicate the change in sample height during the first 30 h of the experiment. Analysis of the temperature evolution for the three different sides left, right and center in similar plot as shown on the right-hand side of Figure 4.18, showed an uneven combustion front. There were distinctly more noise present at 8 cm after the intense combustion period, reflecting a further decrease of the sample height in the middle. On the right side, a rapid decrease in sample height occurred during the intense combustion period, corresponding with the location of the hot core area at the start of this combustion period. The left side decreased in height when approaching the intense combustion period, however, the decrease was more stepwise. The temperature in this region was lower than at the center and to the right.

The time for various parts of the sample to reach temperatures 200 °C, 300 °C and 340 °C are displayed in Figure 4.19a-c. Figure 4.19a show how the sample reached a temperature of 200 °C, layer by layer, before the intense combustion period. A temperature of 300 °C was found at the center of the sample from 2 – 10 cm, as seen in Figure 4.19b. The left side of the sample showed unconnected positions reaching a temperature of 300 °C, while the right side, 6 – 10 cm had a temperature of 300 °C. This could indicate that the front moves out of the vertical plane of temperature measurements, it also indicates a more curved front moving upwards the pipe. It is reasonable to assume that due to the material and the random distribution of pellets inside the pipe, there is a creating of pathways inside the sample. These could affect how the front moves through the material, based on the air flow access. Only a core at 6 – 10 cm in the middle of the sample reach a temperature of 340 °C, before the intense combustion period (Figure 4.19c).

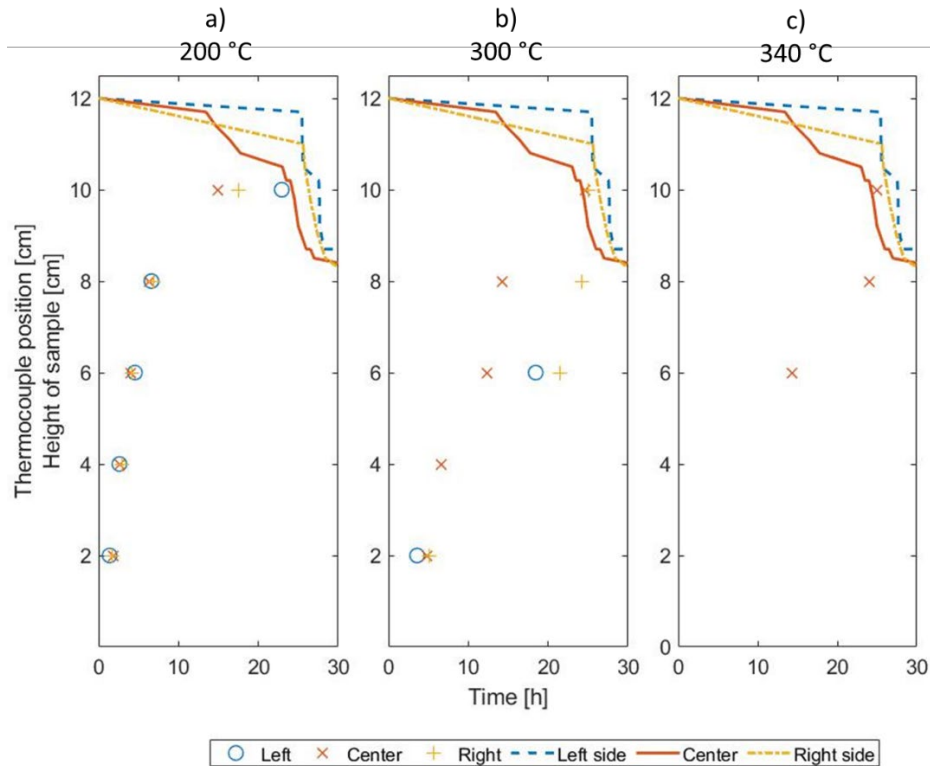


Figure 4.19: The time until various parts of a 12 cm sample reached temperatures of 200 °C (a), 300 °C (b) and 340 °C (c). The lines indicate the estimated change in sample height left, center and right. The height in the center of the sample decreased during the low-intensity smoldering, while the left and right decreased closer to the intense combustion period at 25 h.

After the external heating was switched off, the sample cooled, until thermal runaway occurred, and self-sustained smoldering was established. In most cases this phase had a low-intensity smoldering, which lasted until the conditions necessary to obtain intense combustion were fulfilled. The temperature of all the thermocouple situated inside the sample had to at some point exceed 200 °C before the intense combustion period occurred, as shown in Figure 4.20. However, since the temperature fluctuate, the temperature could be below 200 °C at the start time of the intense combustion, as shown in Figure 4.20A, where 13 out of 15 thermocouples had a temperature equal to or above 200 °C. Figure 4.20B-D shows the temperature until the intense combustion period. External heating of the pellets caused the first temperature top, and after external heating was switched off (3 h 43 min) the sample cooled, until thermal runaway (5 h 35 min).

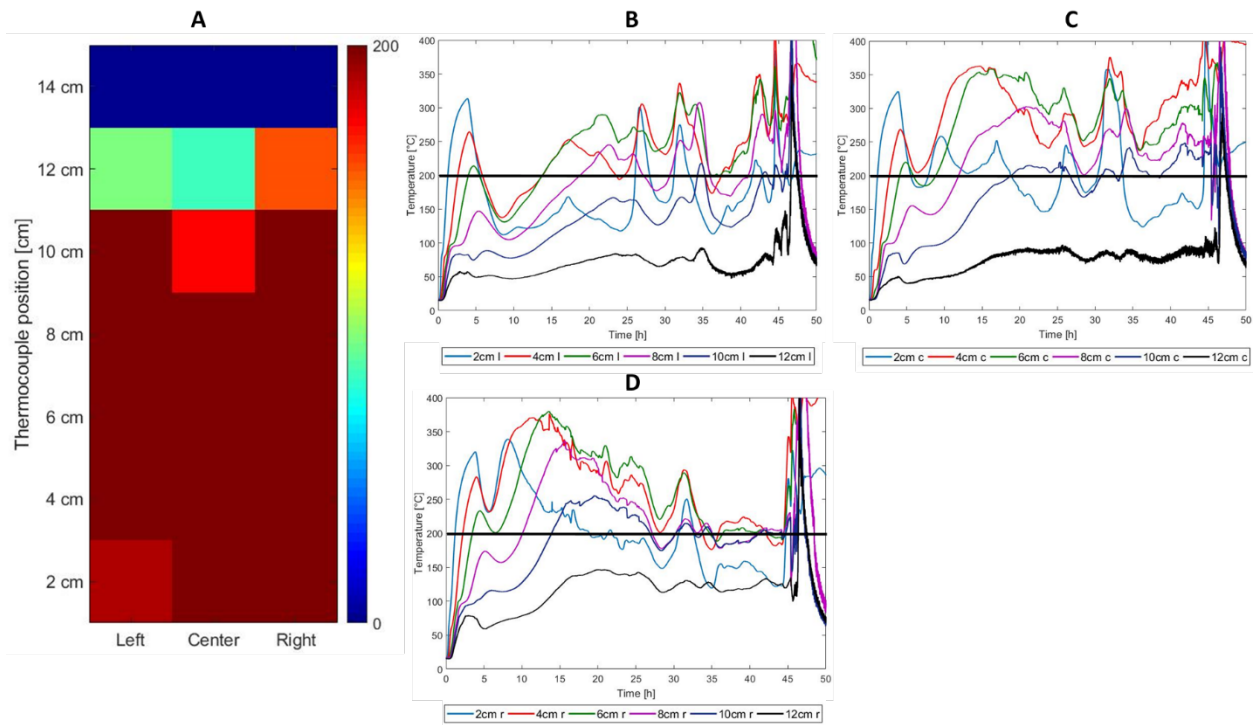


Figure 4.20: Temperatures in a sample with height 12 cm. A) Temperatures at the start of the intense combustion period. The temperature scale was 200 °C as maximum value. The temperature was 200 or more for 13 of 15 thermocouples inside the sample. Part B, C, D show the temperature development in the sample, from the start of the experiment, until the end of the intense combustion (47 h). The figures are divided into the temperature measurements on the left side (B), in the center (C) and on the right side (D).

The third condition is a hot core area inside the sample. A region with temperature above 300 °C was defined as hot in this thesis, because at 300 °C there are physical changes to the pellet, the color changes from light beige to black [54]. The position of the four highest temperature values are indicated by black, dotted lines in Figure 4.21. The shape and location of the hot core was determined for all the experiment. The hottest positions were situated close together, forming a hot core/hot spot inside the sample. The hot core varied in shape and position. However, the three with highest temperatures had a clear L-shape in a most of the experiments. The thermocouple with the highest temperature was in the center of the sample in 20 out of 24 experiments. A series of long-run experiments were conducted, where additional fuel material (wood pellets) was added to the sample at intervals, the results from these experiments are described in section 7. Similar hot spots were found in these experiments.

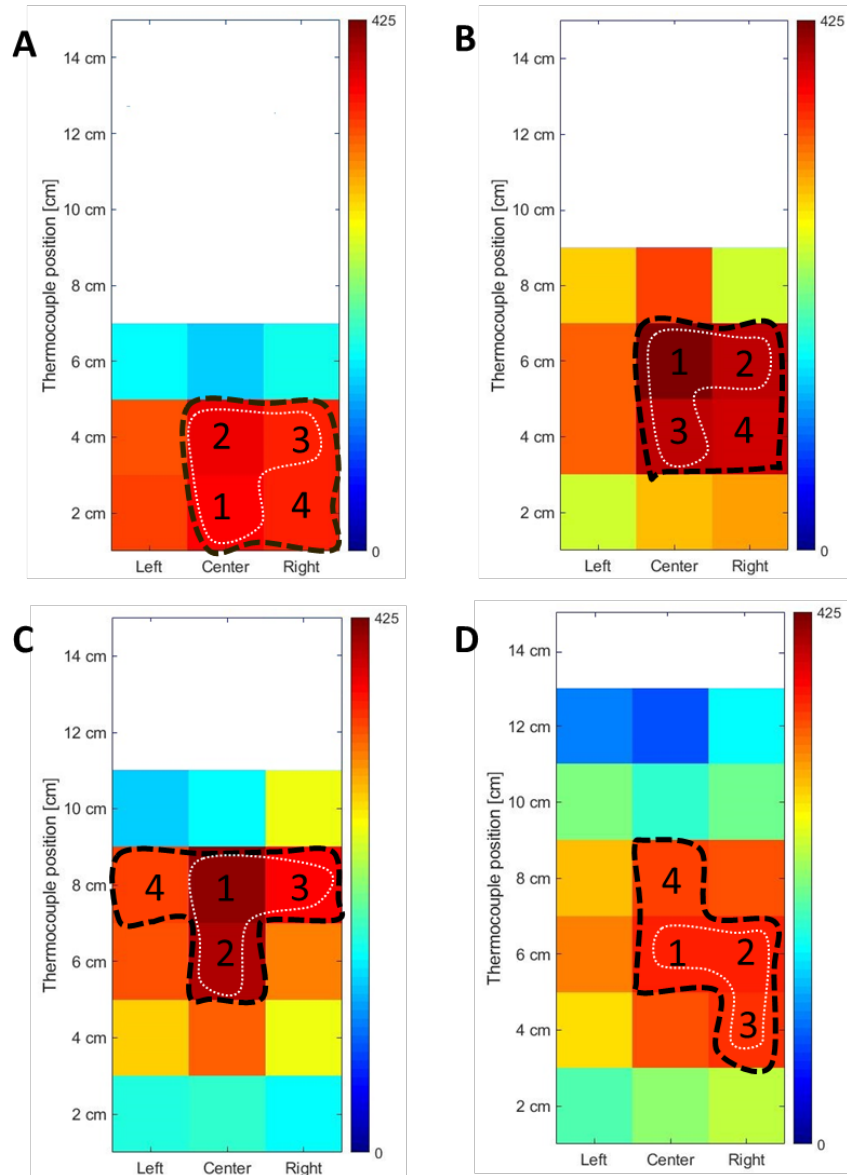


Figure 4.21: Temperature distribution at the start of the intense combustion period for experiments with sample heights from 6 - 12 cm. A warm core area was found, the area exceeds a temperature of 300 °C and was established shortly before the intense combustion period. The temperature scale has 425 °C as upper limit since this was the maximum temperature during the initial phase (before the intense combustion period). A) 6 cm sample. B) 8 cm sample. C) 10 cm sample height. D) 12 cm sample.

The three findings: the combustion front reaching the top of the sample, a hot core, and the whole sample reaching a temperature above 200 °C, are conditions needed for intense combustion to occur

4.5 Mass-loss rate during external heating as an indicator of non-smoldering or smoldering

During external heating, mass was lost due to drying of the material and beginning pyrolysis processes. During smoldering combustion, the mass loss was systematic, however the mass-loss rate during heating was lower than during the intense combustion period. From this observation it was speculated that the mass loss during external heating could be used as an indicator for determining if the sample would smolder or not. A total of 46 experiments, 18 non-smoldering and 28 smoldering was the basis for the analysis. The sample height ranged from 6 – 12 cm as described in section 4.3.

4.5.1 Method for finding the duration of the first mass-loss phase of the smoldering and non-smoldering experiments

The method used in this analysis is the same as the method used in section 4.4.1. The mass loss during external heating was found manually from the mass-loss curve for each of the experiment, during the initial phase, marked with an oval in Figure 4.22A. The initial phase is shown in Figure 4.22B. Tangents (1) and (2) were drawn along the slope of the curve as shown in Figure 4.22C. The intersection between the two tangents indicated the end of the initial phase. The mass at this point (marked in Figure 4.22D) was found from the dataset.

In the previous section (4.4) two methods were used to find the mass loss during intense combustion, focusing on the mass curve and the mass-loss rate respectively. In this analysis of the initial phase, Savitsky-Golay² filtering [55, 56] was used to smoothen the noisy mass-loss data, see Figure 4.23A. However, there is more scatter in the initial phase of the experiments (Figure 4.23B) compared to the intense combustion period, and therefore it is difficult to find the end of the phase by using the mass-loss rate. During this phase, the external heater was connected, and the temperature of the hotplate was kept in a pre-set interval by turning the hotplate on and off. Observations showed an increased amount of scatter in the mass-loss rate during external heating, see Figure 4.23B. Therefore, only the mass curve was used in this analysis.

² Savitsky-Golay smoothing is a mathematical least-squares method to remove noise from measured data. The filtering is based on the method of least squares polynomial [55] A. Savitzky and M. J. Golay, "Smoothing and differentiation of data by simplified least squares procedures," *Analytical chemistry*, vol. 36, no. 8, pp. 1627-1639, 1964. [56] R. W. Schafer, "What is a Savitzky-Golay filter? [lecture notes]," *IEEE Signal processing magazine*, vol. 28, no. 4, pp. 111-117, 2011..

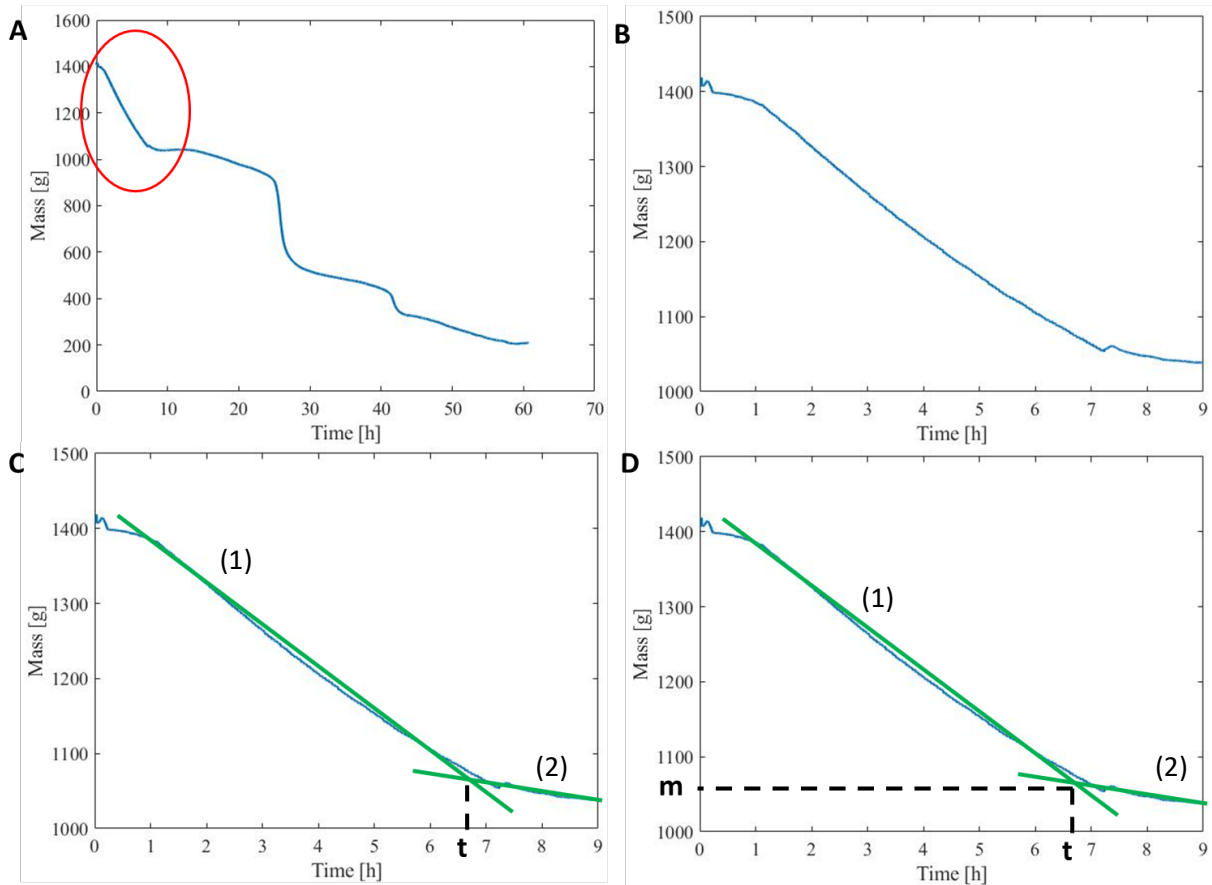


Figure 4.22: Method used to find the end of the first phase for both non-smoldering and smoldering experiments. The experiment shown in the figure is a smoldering experiment with a sample height of 12 cm. A) Mass curve for experiment. The initial phase is shown with a red oval. B) Mass during external heating, from start $t = 0$ h to $t = 9$ h. C) tangents (1) along the curve and tangent (2) where the curve had stabilized. D) The end time of the initial phase was found from the intersection of tangent (1) and (2).

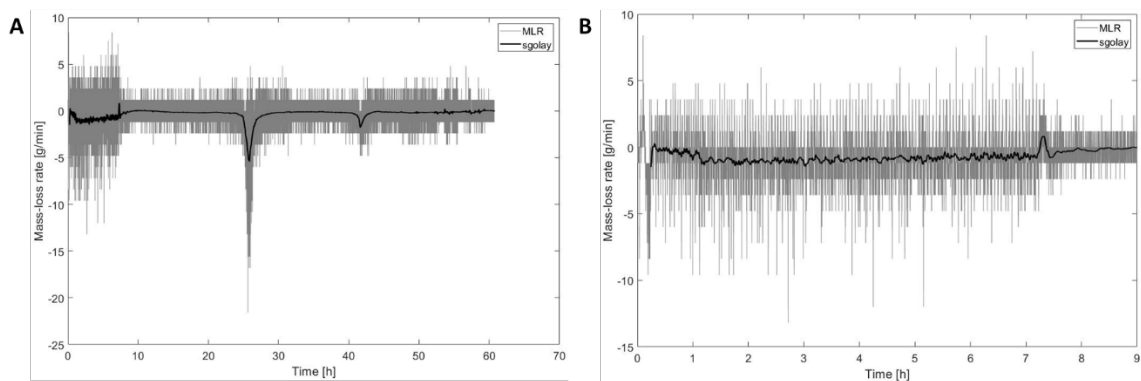


Figure 4.23: The mass-loss rate in a 12 cm high sample, calculated from the mass curve. The light grey area is the raw data, the data has significant noise. The black line is the smoothed of the data, obtained with Savitzky-Golay filtering by a 9th order polynomial and a frame length of 25 min. A) The entire experiment, from start to end. The smoothed curve shows more variations in the early phase of the experiment than after external heating. B) The first phase of the mass loss. Even though the frame length is 25 min, (even longer frame lengths showed similar results), the noise in the start phase makes it difficult to determine the end of the initial phase, from the mass-loss rate curve.

4.5.2 Results from the mass loss in the initial phase

During the initial phase of the experiments showed, mass loss was due to pyrolysis and drying of sample. The criteria for switching off the external heating was a pre-determined cut-off temperature (section 3.2.2). The cut-off temperature varied from 260 °C to 350 °C. A higher cut-off temperature resulted in longer external heating. In addition, the sample height was varied from 6 to 12 cm and the height of the steel pipe was 33 cm or 58/63 cm. The size of the mass loss during the first phase of an experiment is denoted Δm_s and is shown in Figure 4.24 as a function of the time till the end of the initial phase. There are two categories: smoldering (red circles) and non-smoldering (blue squares). The duration of the first mass-loss phase affects the onset of smoldering combustion. A longer duration of heating results in a longer initial mass-loss phase and increases the likelihood of smoldering combustion. In the non-smoldering experiments the time was short, and the average mass loss was 162 ± 43 g. The average mass loss for the smoldering experiments was 282 ± 108 g. Observations indicate that a mass loss over 250 g would result in a self-sustained smoldering process, and below 100 g in non-smoldering. Between 100 g and 250 g, the results are inconclusive.

A correlation analysis [53] was conducted to find the correlation between the parameters and the outcome in the experiments: height of pipe, sample height, end time of initial phase, smoldering or non-smoldering as outcome and the size of the mass loss during initial phase. The results are shown in Table 4.2. There is a correlation between the end time and the size of the mass loss, as seen in Figure 4.24. There is a small correlation between the end time and the outcome, the same is shown for the mass loss, which is confirmed by Figure 4.24, where a longer duration of first mass loss phase and higher mass loss resulted in smoldering. In addition, the size of mass loss was correlated with cut-off temperature. A longer duration of external heating leaves a dryer sample, and the pyrolysis zone was larger, the sample was more prone to smolder. The correlation analysis confirms the findings shown in Figure 4.24, but also confirms that sample height is not an impacting factor. The findings indicate that one can predict a smoldering experiment, by calculating the mass loss. A mass loss above 250 g in this top-ventilated test set-up would result in self-sustained smoldering, independent on sample height. It could also be an indicator of a strong enough pyrolysis process, and not simply drying of the sample, that is needed to ensure a smoldering combustion.

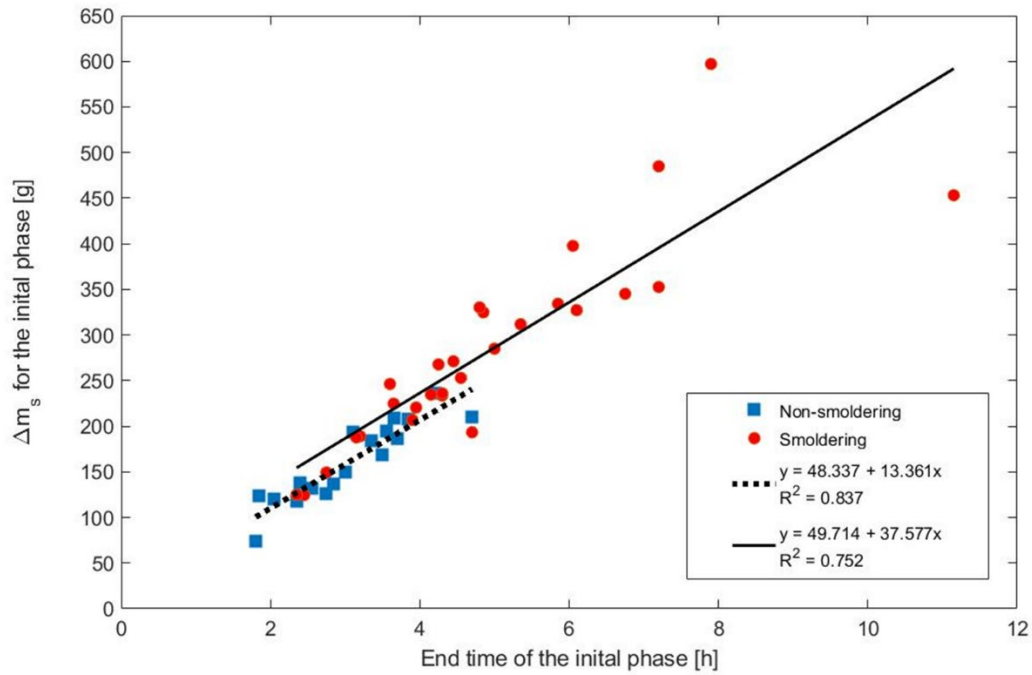


Figure 4.24: The size of the mass loss in the initial phase as a function of the time it ends. The blue squares represent non-smoldering experiments, while the red circles are the smoldering experiments. In general, the smaller the mass loss, the smaller the likelihood of a smoldering.

Table 4.2: Correlation analysis for the parameters and the outcome from the mass loss during the initial phase.

	Smoldering [Yes / No]	Sample height [cm]	Pipe height [Low / High]	End time initial phase [h]	Δm_s [g]	Cut-off temperature [°C]
Smoldering [Yes / No]	1					
Sample height [cm]	-0.18872103	1				
Pipe height [Low / High]	-0.08908708	0.11149412	1			
End time initial phase [h]	0.510153057	0.32346	-0.0097825	1		
Δm_s [g]	0.561277874	0.16999302	-0.1782383	0.90684096	1	
Cut-off temperature [°C]	0.404152724	0.00960781	-0.446146	0.47922617	0.4792262	1

5. Oily pellets from sunflower seeds

The residue after production of sunflower oil is used as a biomass product and processed into cylindrical pellets. The residue consists of sunflower seeds casings. In this analysis they are denoted as oily pellets due to their natural content of oil. The oil content could have an impact on the smoldering behavior, and therefore experiments with wood pellets and with oily pellets were run in parallel.

Wood pellets and oily pellets are both biomass materials, however their material properties differ. A thermogravimetric analysis of these materials showed similarities in physical properties (Table 3.1 pellet A, and Table 3.2), but differences in shape and size. Oily pellets had a smaller diameter compared with wood pellets, but similar length, with average length 17.5 mm for wood pellets and 17.3 mm for oily pellets. These materials are transported and handled in the same way, in storage containers, silos etc.

The experiments with oily pellets were conducted using the same experimental setup as for wood pellets, see section 3.2. The setup is shown in Figure 5.1. Two experiments were run in parallel, one pipe with oily pellets and the other pipe with wood pellets. By conducting the experiments in parallel, the external conditions were equal for each set of experiments. Pipe A contained wood pellets and pipe B oily pellets. Both had the same number of thermocouples in the steel construction to measure the temperature inside the sample (see section 3.2.1). The sample mass was different for wood and oily pellets due to differences in bulk density. In these experiments, the main concern was to ensure same volume-to-surface ratio, which lead to a difference in mass. All the experiments with oily and wood pellets were conducted with the same experimental method as described in section 3.4, and sample heights were 10 and 12 cm.

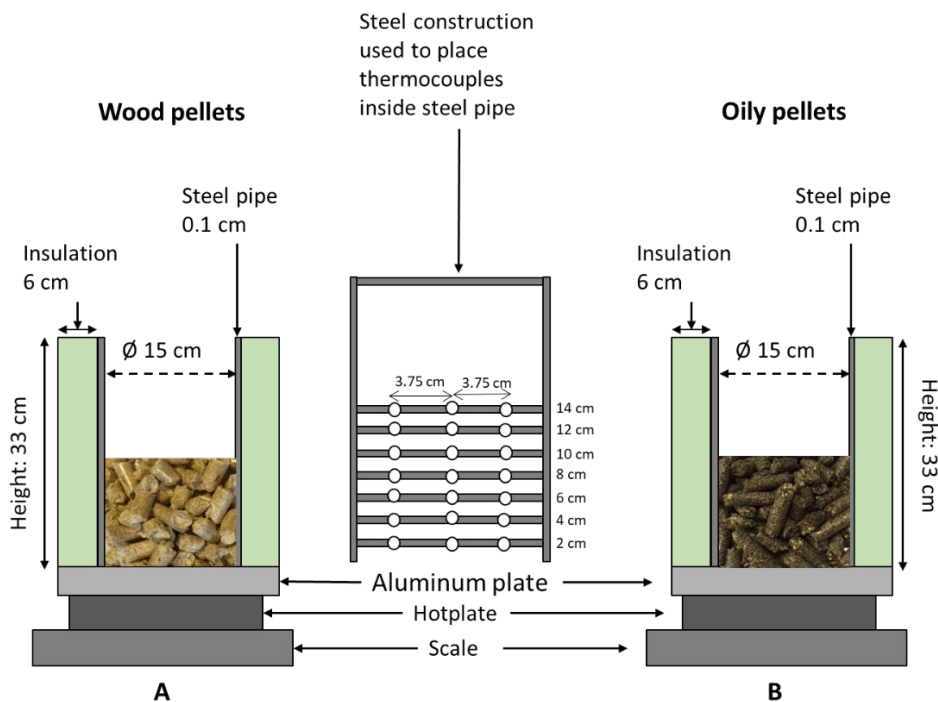


Figure 5.1: Illustration of the two setups with the wood pellets and oily pellets. This is the same experimental setup as for the previous experiments in low pipe, see 3.2.1. Pipe A contains wood pellets and pipe B oily pellets. The two setups are identical, with exception to the content.

5.1 Smoldering behavior of oily pellets

Typical smoldering combustion in oily pellets in this top-ventilated system is shown in Figure 5.2. Temperatures (Figure 5.2A) and mass loss (Figure 5.2B) are shown for a sample height of 12 cm. Figure 5.2A show the center temperatures of the sample. The external heating lasted for 6.5 h. After external heating was switched off, the temperature decreased until thermal runaway (around 9 h), and self-sustained smoldering was established. The temperatures increased slowly, resulting in a low-intensity combustion from 10 - 24 h. The lower parts (2 – 6 cm) displayed decreasing temperatures from 15 h until 24 h. At approximately 24 h, the temperature increased rapidly in the upper parts of the sample, and an intense combustion occurred. The intense combustion had a duration of approximately 16 h. This is a much longer period than previously found in wood pellets, where the average duration was between 0.5 and 1.5 h (section 4.4). Maximum temperature was reached in the second peak and measured at 6 cm. The duration of the experiment was approximately 50 h.

In Figure 5.2B the mass loss for the oily pellets is shown. During the external heating mass was lost due to drying of the material and pyrolysis of the lowest layer of the sample (2 – 4 cm). After the external heating (from 8 h), the mass-loss rate was slow, and the mass seemed to be stable until the intense combustion period from approximately 24 h. Here, the mass-loss rate increased rapidly. The

slope decreased again at 40 h and the slow mass-loss rate was until the sample reached room temperature.

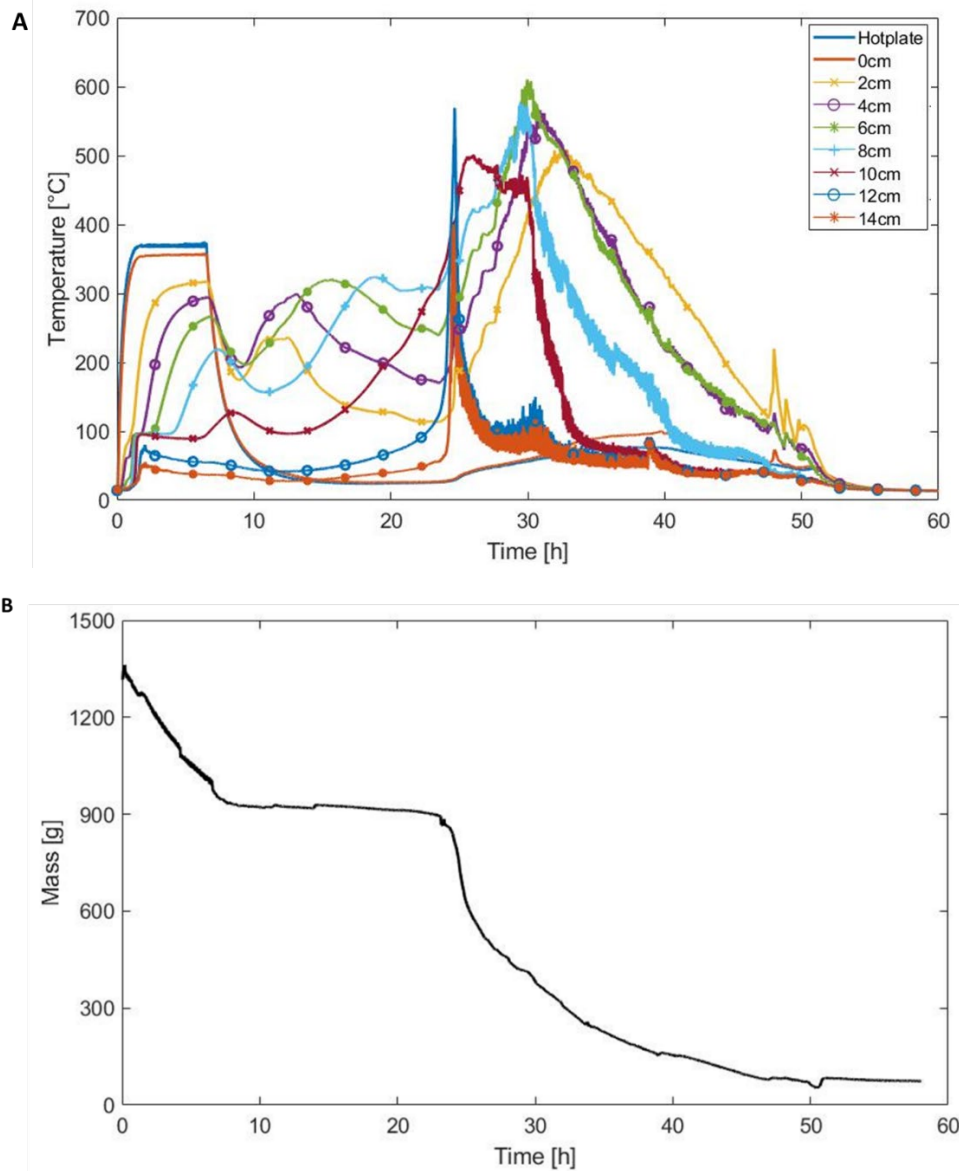


Figure 5.2: Typical smoldering in a 12 cm high sample of oily pellets heated for 6.5 h. A) Temperature distribution at the center. After the external heating was switched off, the temperature decreased until the sample reached thermal runaway. After self-sustained smoldering was established, a low intensity combustion occurred until 24 h, where an intense combustion period started. B) Mass loss during smoldering combustion in oily pellets, followed a similar trend as for wood pellets (see Figure 4.1D). First mass was lost due to external heating (6.5 h) followed by a quasi-constant mass loss (from 8.5 h – 24 h). A rapid increase in mass-loss rate occurred around 24 h.

5.2 Comparison of wood pellets and oily pellets

Since wood and oily pellets are handled and stored in the same way, it is natural to compare these two in the top-ventilated system, which resembles a small-scale silo storage unit. The experimental setup and procedure were equal, two experiments were run in parallel to ensure as similar external

conditions as possible. There are two aspects of the data which will be compared in the following sections: temperature and mass loss.

5.2.1 Temperature distribution inside sample

The temperature evolution differs for wood and oily pellets. By averaging the temperatures in the center of the sample from 2 – 12 cm, the different combustion scenarios for the two materials becomes evident. Figure 5.3 shows an example. The sample height was 12 cm. Both samples were heated for 6.5 h before the external heating was switched off. The temperature evolution during the first 8 h was similar for the two types of pellets. Both were dominated by the external heating, and the average temperature in the center of the sample (2 – 12 cm) differed only slightly during this period.

After external heating was switched off, the samples cooled until thermal runaway. While wood pellets reached the lowest temperature after external heating and the start of thermal runaway at around 8 h, oily pellets reached this point closer to 9 h. This led to a cooler sample as self-sustained smoldering was established. Figure 5.3, shows how the two materials behaved differently after start of thermal runaway. The temperature of the wood pellets increased more rapidly, and three short intense combustion periods occurred at approximately 18, 30 and 38 h. Oily pellets had a peak, before a stronger intense combustion was established with a longer duration from 24 h – 35 h. After the intense combustion period, the oily pellets sample cooled to room temperature.

The main trends of the temperature development are shown through the average temperature of the center of the sample, as shown in Figure 5.3. A complete overview of the maximum temperature scan be found from each specific test. The maximum temperature peak in wood pellets was 728 °C and occurred at approximately 19 h. Oily pellets first maximum temperature peak (occurred at 12 cm, on the left side of the sample) had a temperature of 612 °C and occurred at approximately 25 h. The second peak in oily pellets had a higher average maximum temperature due to higher temperatures in the whole sample at this point, but the peak was 610 °C, similar to the first maximum temperature peak. Note that these values are significantly larger than the values in Figure 5.3. Both wood and oily pellets had lower temperatures close to the aluminum plate (2 – 4 cm). This reduced the average temperature at maximum peak.

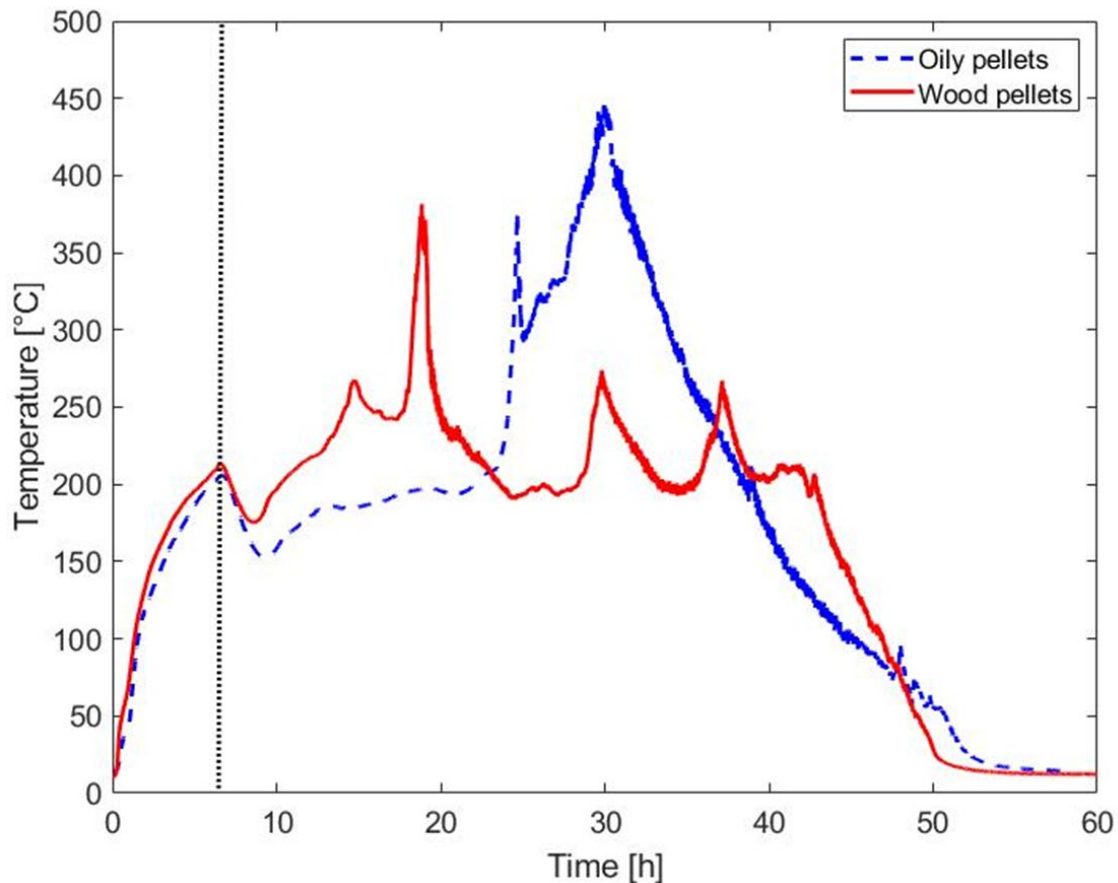


Figure 5.3: The average temperature at the center of a sample with wood pellet (solid red line) and one with oily pellets (blue dotted line). The two materials were heated for 6.5 h (black dotted vertical line), after heating wood pellets display three short intense combustion periods, while oily pellets had one short peak, followed by a long intense combustion period until the sample was consumed.

The intense combustion period differs from wood pellets to oily pellets. Wood pellets have a relatively short intense period, the most intense combustion was located at the top of the sample as shown in Figure 5.4. The total duration of an experiment was approximately 48 h, and the intense period was only 1 – 2 h (Figure 5.4A). During the intense combustion, there were layers of the sample with stable temperature, in this case at 2 – 8 cm, as seen in Figure 5.4B. The upper parts (14 cm) of the sample reached intense combustion first, followed by 10 cm and 12 cm. The sample height was 12 cm, however, pellets have a tendency to swell, and the height could have increased to 14 cm, or slightly below 14 cm, therefore the first peak occurred at 14 cm instead of 12 cm. The movement of the smoldering front in wood pellets, showed a surprisingly non-symmetrical combustion. Meaning it did not follow highest temperature from 14 and down to 2 cm. The temperature was measured in a vertical plan in the center of the sample, a maximum temperature could be located away from the thermocouples. Another possible explanation could be a change in sample height by the affected pellets during the initial phase. Afterwards, the smoldering front moved as expected, layer by layer, downwards from 8 to 2 cm.

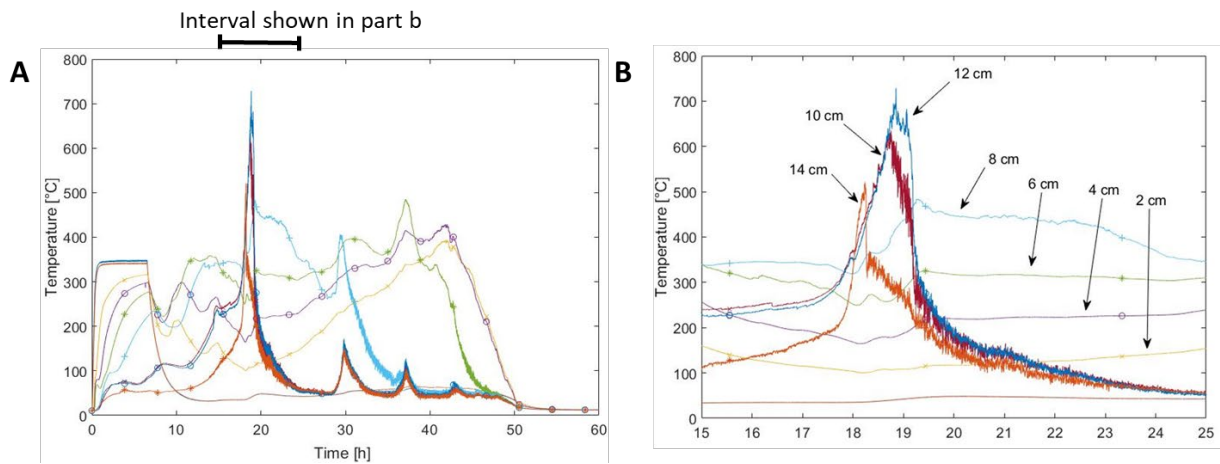


Figure 5.4: Intense combustion period of a 12 cm high sample with wood pellets. Measurements at the sample center for height 2 – 14 cm. Part A) Temperatures during the entire the experiment. B) The intense combustion period for the same experiment as in part A. During the intense combustion, the temperature in the lower parts from 2 – 6 cm was stable. The most rapid increase in temperature occurred in the upper part of the sample (10 – 14 cm). However, the different heights reached the maximum temperature at different times. 14 cm reaches the peak first, followed by 10 cm and then 12 cm. There is a non-systematic trend in the temperature distribution during the intense combustion period.

Oily pellets have a longer intense-combustion period, as seen in Figure 5.5A. The duration of the intense combustion period was from approximately 23 h until the last part reached peak temperature at approximately 33 h. The duration of the intense combustion period was approximately 10 h, while the duration of the intense combustion period for wood pellets was approximately 1 h. The combustion zone moved systematically from the top at 14 cm to the lower part of the sample at 2 cm during the intense combustion zone, see Figure 5.5B.

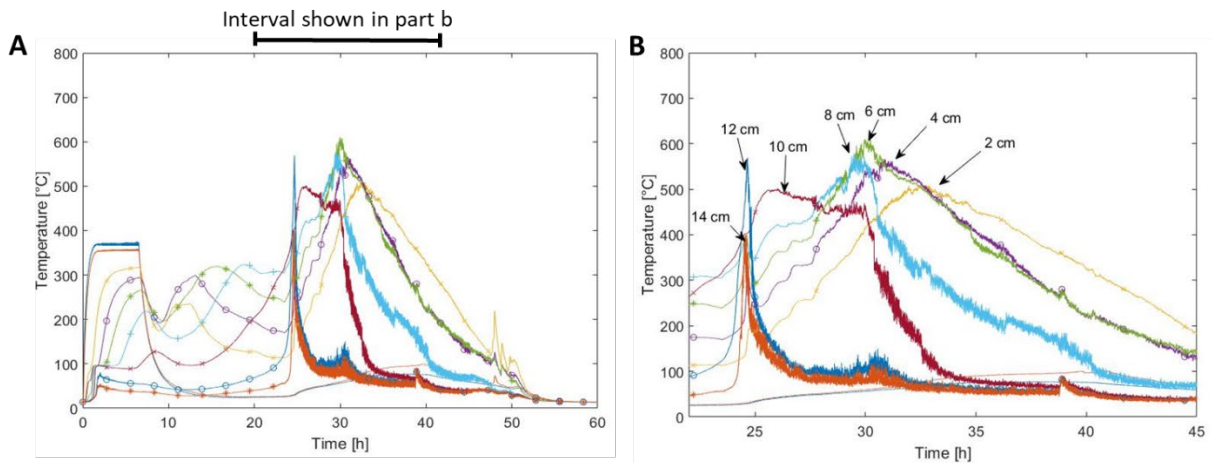


Figure 5.5: Intense combustion period for an oily pellet sample. Part A) Temperatures during the entire experiment. Part B) The intense combustion period for the same experiment as in part A. The sample reached temperature peaks systematically, the combustion zone moved from the top to the bottom of the sample.

The intense combustion period evolved differently for wood and oily pellets. A short intense combustion in the upper layers of the sample was found in wood pellets. Oily pellets had intense combustion moving from one layer to the next, starting at the top and working its way down to the bottom of the sample. Directly after the intense combustion period in the oily pellets, the sample cooled to room temperature. The sample was completely combusted, with only ash and charred residue left. The short intense combustion periods in wood pellets caused the sample to undergo a low-intensity combustion for several hours after the intense combustion period, before the sample cooled to room temperature.

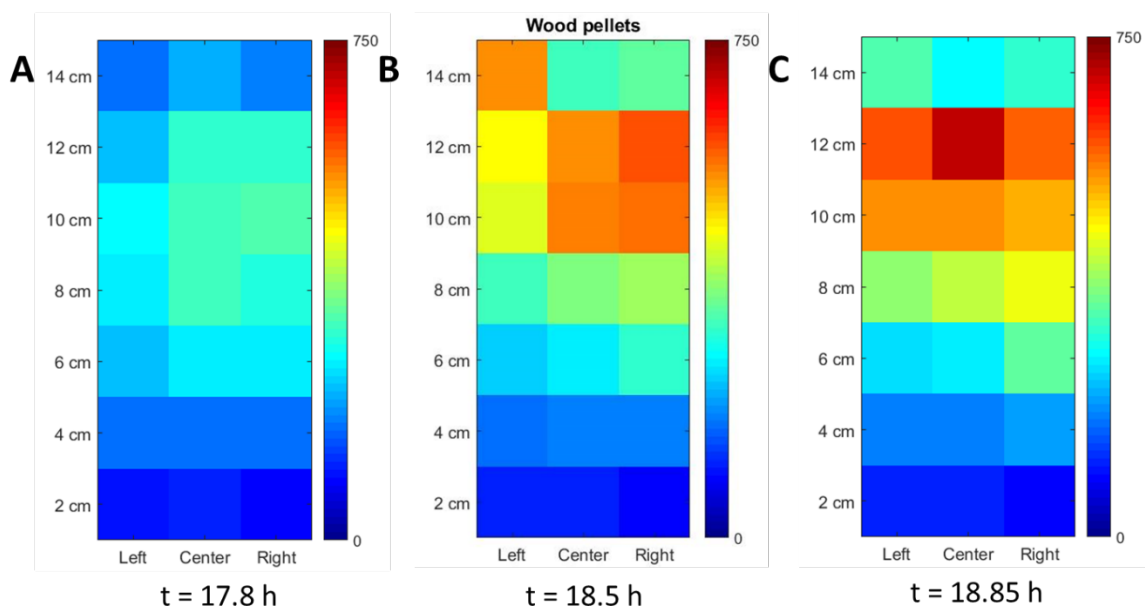


Figure 5.6: Temperature inside a wood pellet sample with a sample height of 12 cm, same experiment as Figure 5.4. The x-axis shows the placement of the thermocouple from left to right, while the y-axis shows the steps in the steel construction containing the thermocouples (section 3.2.1). The color-coding runs from 0°C - 750 °C. A) Temperature at beginning of intense combustion period. Note the warmer area at 8 - 12 cm center and right. B) The temperature inside the sample during the rapid temperature increase, a warm area was located at the top of the sample. In addition, a warm area was found on the left side above the sample (14 cm). C) At maximum temperature (12 cm center), there was a warmer zone in the upper layers (10 – 12 cm). The lower parts (2 – 4 cm) of the sample were cooler.

The temperature distribution during intense combustion shows a clear difference between the two materials. Wood pellets had a short intense combustion located in the upper part of the sample as shown in Figure 5.6, with highest temperatures at the top and center. The temperature distribution in oily pellets is shown in Figure 5.7. A hot spot at 8 – 10 cm was found at the start of intense combustion period (Figure 5.7A). Figure 5.7B show the temperature distribution at the maximum temperature peak. Overall, the maximum temperature was lower for oily pellets. However, a larger part of the sample was hot. The lowest part (2 cm) of the wood pellets was cooler than the oily pellets (compare Figure 5.6C and Figure 5.7C). The intense combustion period lasted longer, resulting in higher temperatures over a longer period for the oily pellets. Wood pellets had one intense combustion

period with high temperatures, followed by several smaller ones, where the temperatures were lower than the first maximum temperature peak.

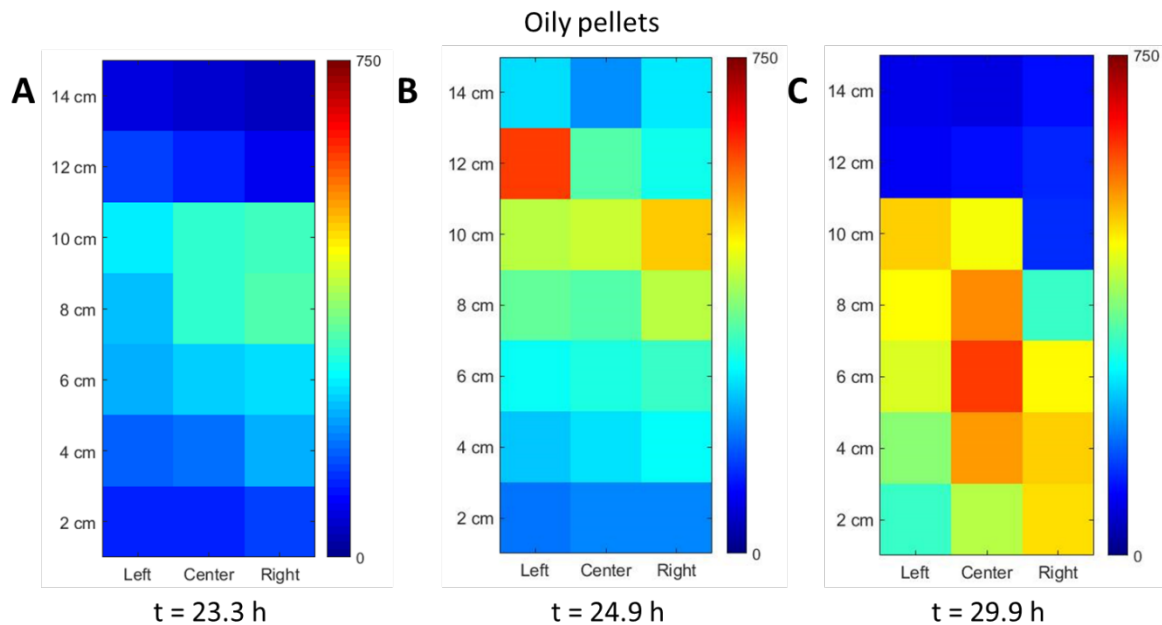


Figure 5.7: The temperature in a 12 cm sample with oily pellets during the intense combustion period (same experiment as in Figure 5.2 and Figure 5.5). The x-axis shows the position of the thermocouples from left to right. The y-axis shows the thermocouple position upwards along the pipe at each level in the steel construction (section 3.2.1). The color coding runs from 0 °C to 750 °C, as in Figure 5.6. Part A) The temperature distribution at the start of intense combustion period where there was a clear tendency for warmer areas at the center and to the right. The warmest area was located near the top of the sample B) The maximum temperature peak at 24 h. It was located at 12 cm and to the left, with a temperature of 612 °C. Most of the sample was relatively hot, the coolest part was located at 2 cm. Part C) The maximum temperature peak in oily pellets was at 6 cm with a temperature of 610 °C. This was later in the intense period at 30 h, the upper parts (12 cm) had cooled, while the warmer areas were from 4 – 8 cm, (8 – 10 cm right side had cooled).

The initial phase (external heating of the sample) is equal for both materials. The temperature difference for T_{cut} (temperature when hotplate was switched off) was 5 K. The average temperature for the three thermocouples at 2 cm when the external heating is switched off was $320 \pm 14 \text{ °C}$ for oily pellets and $315 \pm 8 \text{ °C}$ in wood pellets (Figure 5.3). There were larger variations in the temperature for the oily pellets compared with wood pellets. After the external heating, the temperature decreased in both samples, until they reached thermal runaway.

The thermal runaway temperature differed for the two biomass materials. The temperature was higher in the wood pellets, above 200 °C (see Figure 5.8A). The hot region at thermal runaway, was at 2 – 6 cm, and the thermal runaway first occurred at 4 cm. The hottest region of the oily pellets were situated lower in the sample, at 2 – 4 cm, and the region was smaller than for wood pellets. The oily pellets decreased to a lower temperature before reaching thermal runaway, as shown in Figure 5.8B, the temperature was below 200 °C at the center of the sample at thermal runaway.

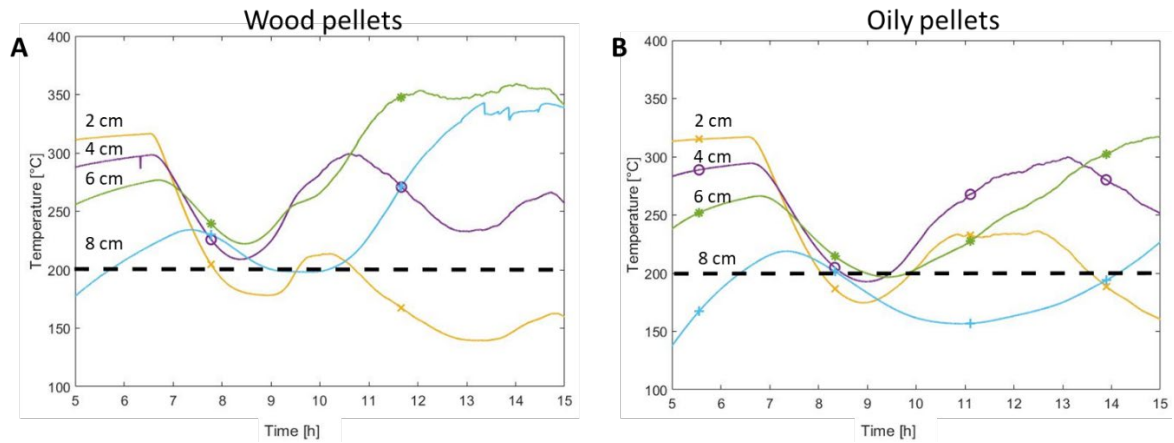


Figure 5.8: Thermal runaway for wood pellets (same experiment as shown in Figure 5.4, and Figure 5.6) and oily pellets (same experiment as shown in Figure 5.5 and Figure 5.7), 200 °C is marked with a dotted line. A) The thermal runaway in wood pellets. The thermal runaway occurred at 4 cm first, followed by 2 cm and 6 cm. The temperature at the first thermal runaway was above 200 °C. B) the thermal runaway in oily pellets occurred in the lower parts of the sample at 2 – 4 cm and at the time of thermal runaway, the temperature in this part was below 200 °C.

5.2.2 Mass loss during smoldering combustion

The mass-loss curves for both wood pellets and oily pellets are shown in Figure 5.9. Both types of pellets lost mass during external heating (0 – 6.5 h). The mass loss was quasi-constant during low-intensity combustion at 8 – 18 h (wood pellets) and 8 – 24 h (oily pellets). The wood pellets reached intense combustion at 18 h, a rapid increase in mass-loss rate occurred, before the mass-loss rate slowed down at approximately 19 h. The sample experienced smaller temperature peaks until the end of the experiment (see Figure 5.3). The oily pellets had a longer period with a low mass-loss rate compared with wood pellets, from 8 h to 24 h. The intense combustion period started at 24 h, see Figure 5.3, and had a longer duration. The total mass loss was $90 \pm 1.9 \%$ for oily pellets, and $89 \pm 3.4 \%$ for wood pellets. The mass loss of oily pellets was larger compared to wood pellets, see Figure 5.9.

During the first phase of the experiments, an interesting observation on the mass loss was made. There was a difference in how the external heating affected the materials. The mass loss during heating as a function of duration of the external heating (t_{cut}), showed a larger mass loss for oily pellets compared with wood pellets, see Figure 5.10. This is particularly evident for 6.5 h as duration of external heating (which was used for most of the experiments).

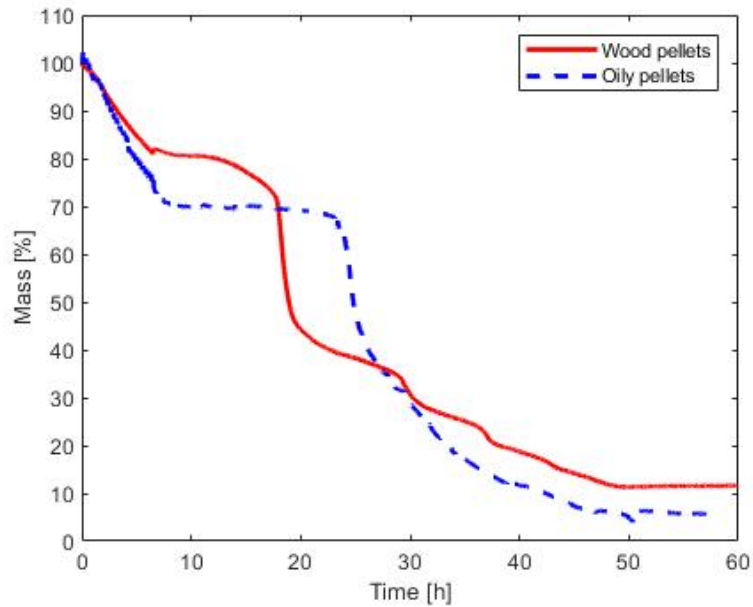
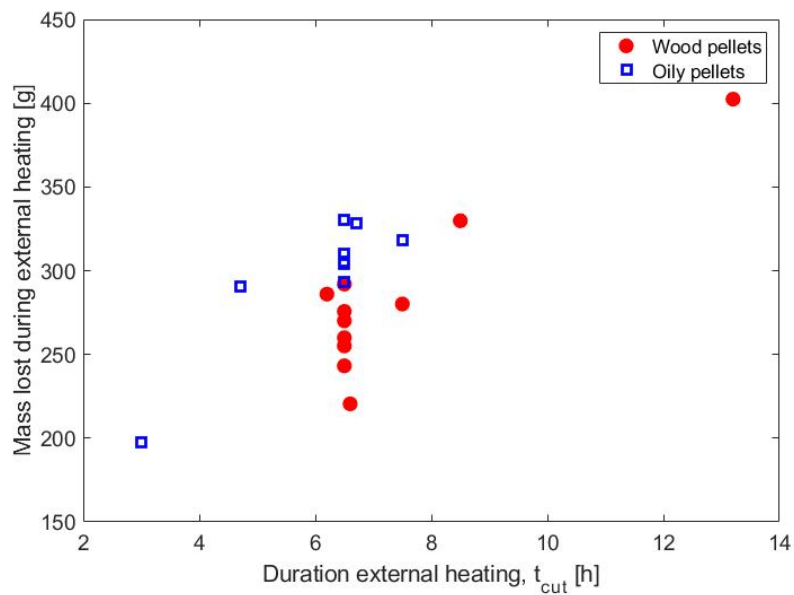


Figure 5.9: Mass loss during smoldering for wood and oily pellets. Same experiments as shown in Figure 5.3. The curves indicate that the oily pellets lost more mass during external heating than the wood pellets. In addition, the intense combustion period occurred later, but lasted longer. Total consumption of mass is larger for oily pellets than for wood pellet in these two experiments.



6. Air flow above the sample and effect of coverage of pipe

Observations of the combustion front showed different velocity in different parts of the sample, it is assumed that the variation of smoldering front is caused by the access of air. The form of the pellets and the random distribution in the pipe causes pathways inside the sample, which could cause a front to move faster in one part of the sample than the opposite side. It was therefore determined to investigate the air flow movement in the top-ventilated pipe. Investigation of air flow in and out of the pipe has been conducted through temperature measurements.

6.1 Temperature of sample and air flow in at the height 20 cm

The air flow in the pipe was measured using thermocouples at 20 cm of the pipe covering the opening of the pipe, at a height of 20 cm inside the steel pipe. The experimental setup is described in section 3.3, but is briefly repeated here: low pipe (33 cm), top ventilated, with temperature measurements along the centerline of the pipe. A mesh containing 12 type-K thermocouples was placed in the at the height 20 cm, figure 3.5 and 3.6 is repeated for clarity (Figure 6.1).

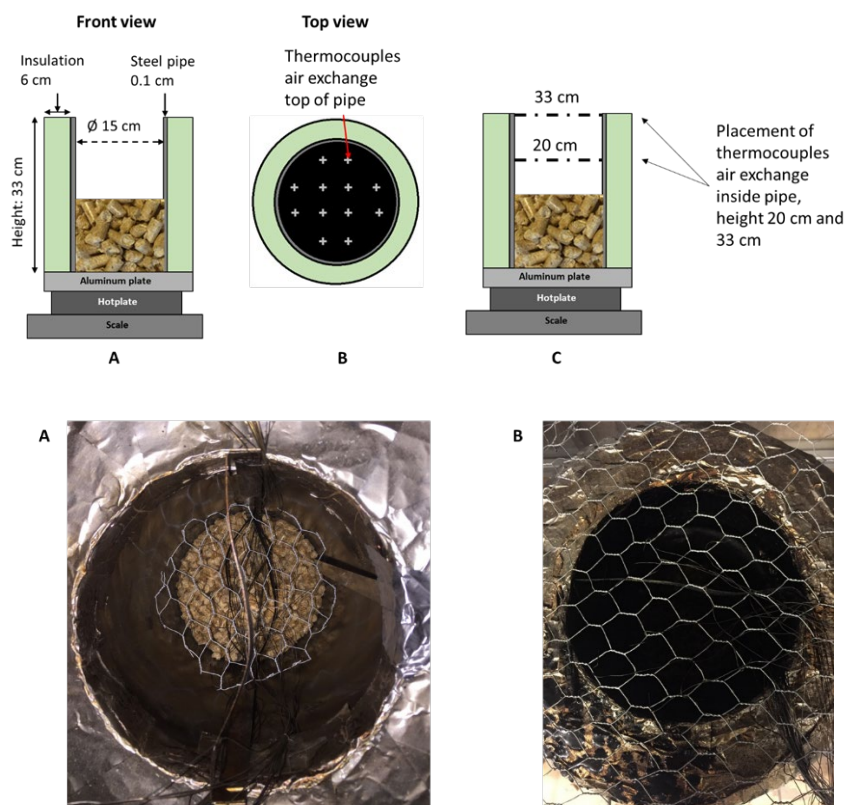


Figure 6.1: Figure 3.5 and Figure 3.6 repeated for clarification of the experimental setup. Top shows an illustration of the steel pipe and location of mesh. The two bottom pictures show the meshes placed inside pipe and on top of pipe.

A representative example of measured temperatures in wood pellets and temperatures in the air at height 20 cm is displayed in Figure 6.2. The sample was heated for 6.5 h, and typical temperature curves for smoldering in wood pellets are shown in Figure 6.2A. After the external heating was switched off, the sample temperature decreased until thermal runaway. A self-sustained smoldering combustion was established around 10 h. Low-intensity combustion lasted until 20 h, where an intense smoldering combustion started. This is shown by the rapid increase in temperature, and the sample reached maximum peak temperature of 635 °C. After the intense combustion, from approximately 22 h, a low intensity combustion occurred, with lower temperatures, until the sample cooled to room temperature.

The temperatures at 20 cm height is shown in Figure 6.2B. The temperatures at 20 cm height and the sample follow the same trend. Thermocouples were 10 cm above the sample and exposed to air and smoke. Temperatures were not affected by the external heating of the sample, as seen in the measured temperature from 0 - 6.5 h. During the first 20 h of the experiment the temperature was below 50 °C. As the sample reached the intense combustion period at 20 h, the air flow temperatures increased, following the temperature development of the sample. After the intense combustion, the temperatures varied between 50 and 100 °C, with three smaller peaks corresponding to those of the sample.

Temperatures in the sample and air flow differs significantly. The average maximum temperature for the pellet samples was 587 ± 41 °C, while the air flow temperature peak was 259 ± 42 °C. The difference was 328 K. The temperatures were similar to the temperature at 12 – 14 cm, these thermocouples were also located above the sample height, see Figure 6.2A and B. The maximum temperatures measured at 12 and 14 cm were 389 °C and 254 °C for the experiment in Figure 6.2. The maximum temperature of flowing air at 20 cm height was 233 °C. Thus, the temperature of the flowing air decreased as the height above the sample increased, which is a reasonable consequence of heat loss and mixing of warm smoke and cool air.

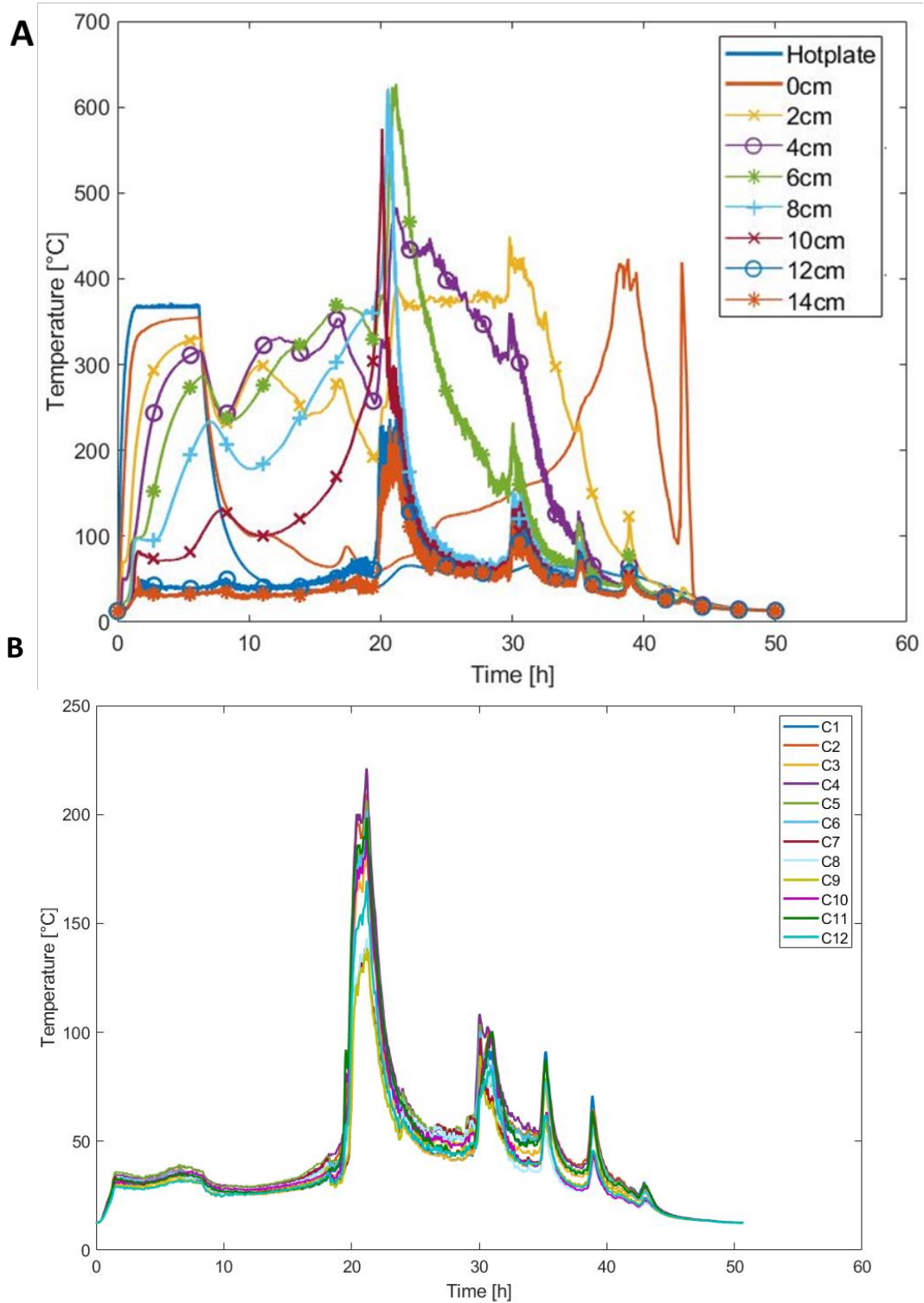


Figure 6.2: Temperatures in a 10 cm wood pellet sample with corresponding temperatures at 20 cm. The y-axis limits range is different in the two figure parts, with the highest temperatures in part A. A) Temperatures at the center of the sample. The temperature was fluctuating through the phases of self-sustained smoldering leading up to an intense combustion period (20 h) followed by low-intensity combustion (from 21 h) until extinguishment (45 h). B) Temperatures at 20 cm height. The temperatures of the flowing air were smoothed by Savitzky-Golay [55] filtering with a 9th order polynomial and a frame length of 30 min.

6.1.1 Warm and cold air flow in the pipe

Temperature data shows positions in the pipe at 20 cm that were warmer and others that are colder than the average temperature. Even though, the direction of the flowing air is not measured, the temperatures indicate the flow direction. Warm positions indicated smoke moving upwards, while cold positions indicated downward motion. The criteria used to sort warm and cold positions was the average temperature of the 12 measurements points. If the temperature was higher than the average temperature, the position was denoted as warm, and denoted as cold if the temperature was lower. The criteria were used to describe how the air flow at height 20 cm change with time. The temperature of the air flow each hour is shown in Figure 6.3. It is reasonable to assume that an average value of the times would likely show similar trend, with small variations, but overall, the same stable areas of warm and cold temperatures. Figure 6.3A shows the placement of the thermocouples at the net and their location along the x-axis in Figure 6.3B and C. The air flow in the pipe fluctuated. Several positions in Figure 6.3 vary between cold (blue) and warm (red) throughout the experiment, while others remain stable either warm (C2, C4, C5 and C6) or cold (C3, C9 and C12).

Further analysis of the data in Figure 6.3B showed that some positions that were constantly warm or cold throughout an experiment. The constant positions are shown in Figure 6.3C with color, while the frequently changing colors are grey/black. During smoldering combustion (see Figure 6.2) four positions were categorized as warm throughout the experiment, these were C2, C4, C5 and C6. This warm zone was located along the pipe wall, see top view of the pipe in Figure 6.4, red color. Three positions were categorized as cold throughout the experiment, these were C3, C9 and C12, located in the center of the pipe (Figure 6.4, blue zone). Through the analysis of the recorded temperatures in the at 20 cm height, it was found that the surrounding air entered the sample in the middle, while smoke from the combustion exit along the pipe wall. This is an unexpected finding since a more a reasonable assumption would be hot smoke rising in the center and cold air entering along the pipe wall. A possible reason for this finding could be that the steel pipe is affected by the temperatures inside the sample and makes it easier for warmer air flows to be established around the outer edges of the sample. The air flow will be discussed in more details in section 8.3.

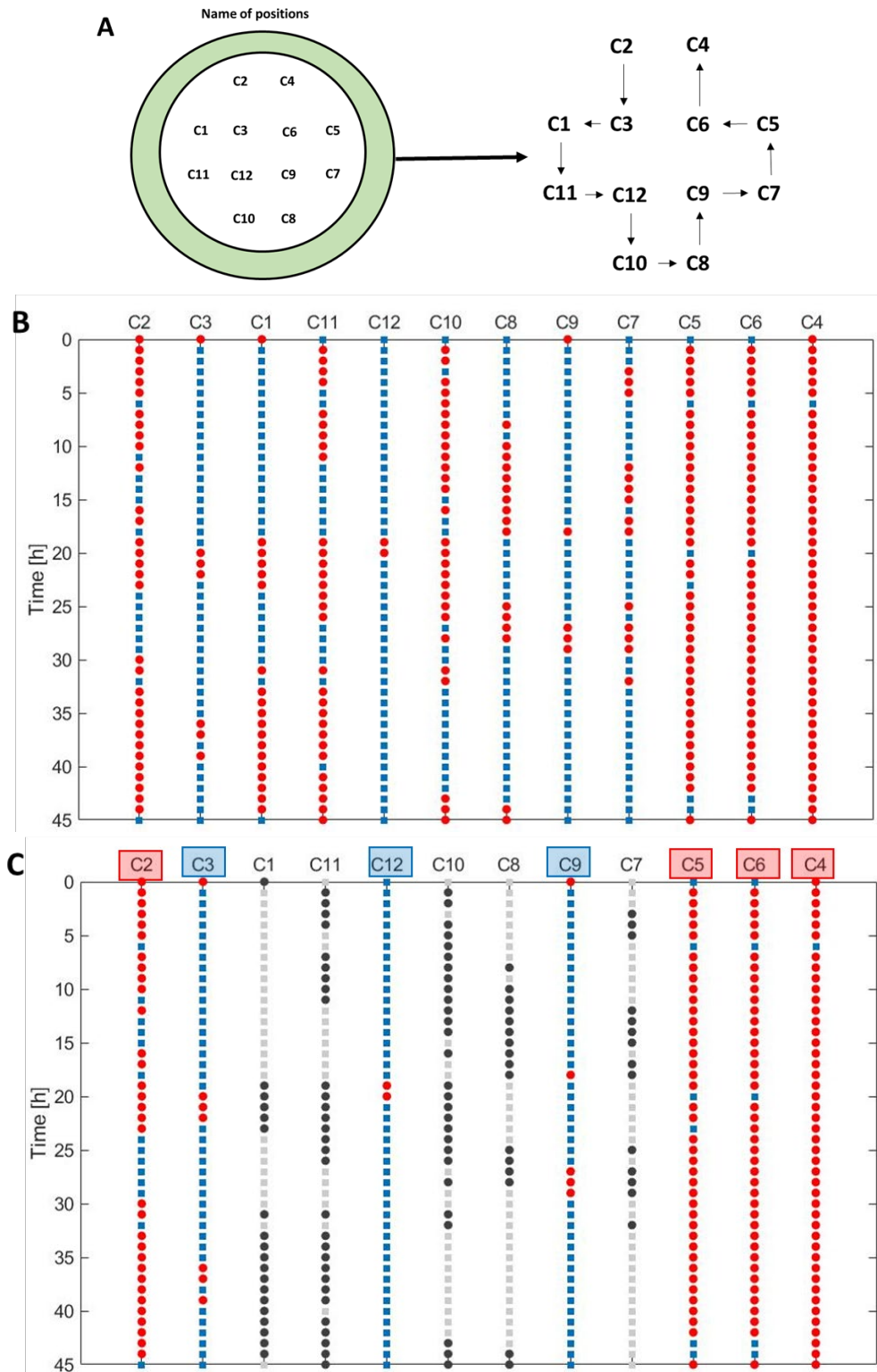


Figure 6.3: Temperature each hour at the height 20 cm, same experiment as Figure 6.2. Blue squares are the cold temperatures and the red circles are the warm temperature. A) Placement of thermocouples at 20 cm. B) The temperatures fluctuate during the experiment, hour by hour, thermocouples vary from cold to warm and the other way around. C) Sorted by stability, warm/cold zones (red/blue) and fluctuating zone (grey and black). The light grey was determined as cold and the black was warm. Four positions (C2, C4, C5, C6) were warm during the experiment. Three positions (C3, C9, C12) were stable cold during the entire experiment.

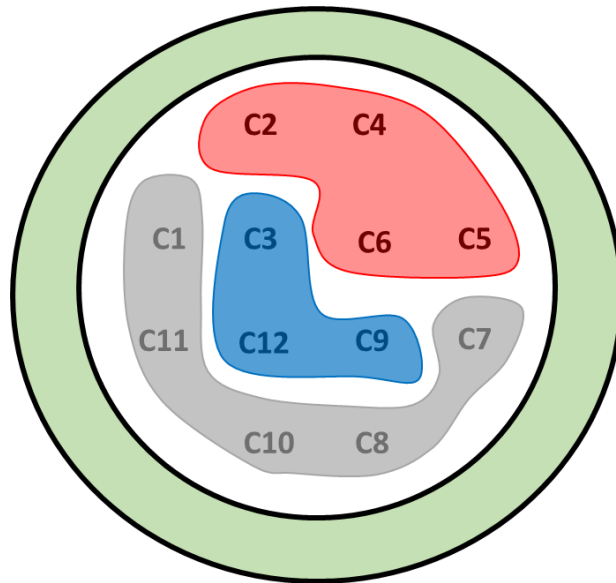


Figure 6.4: The overall picture as for warm and cold zones during the smoldering combustion for the experiment shown in Figure 6.2. Red indicates the warm zone located along pipe wall. Blue indicates the stable cold positions, located in the center of the sample. The grey areas indicates the measurement points fluctuating between warm and cold throughout the experiment.

6.1.2 Temperature in and above sample

The temperature above sample was affected by the smoldering behavior inside the sample. As the temperature increased rapidly inside the sample, the temperature of the air flow increased. The temperature followed the same peak trend (Figure 6.2).

Figure 6.5 show the temperature of the air flow at 20 cm in the pipe during the first intense combustion period (a selected time interval from Figure 6.2B). During the intense combustion period for the experiment in Figure 6.2, a larger section of the air flow was denoted as warm, 8 out of 12 thermocouples were warm during the intense combustion phase in this experiment. Overall for all experiments, a 50 / 50 division of warm and cold thermocouples was found during intense combustion.

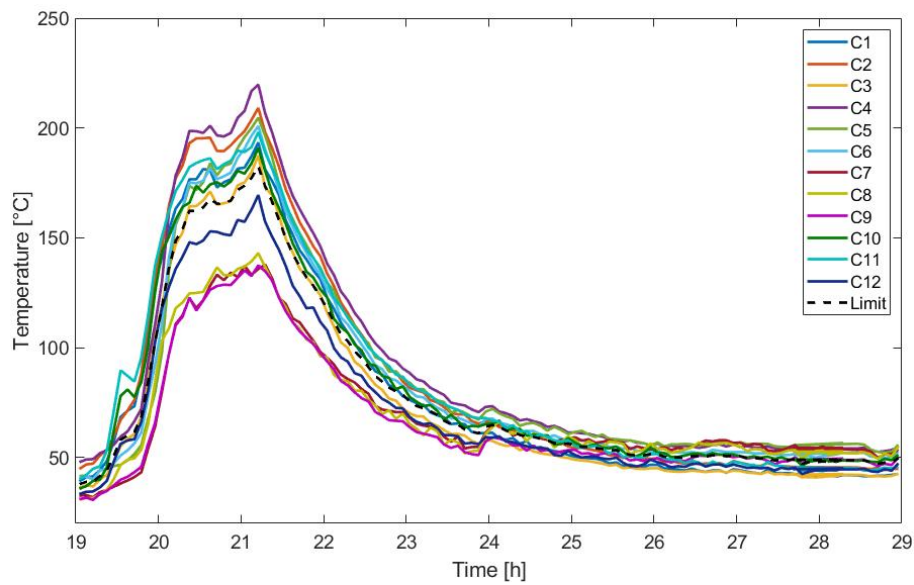


Figure 6.5: Temperatures at 20 cm in the pipe. The temperature with a running average of 5 min. The limit is the average temperature of measured temperatures. The temperatures above the limit are denoted as warm, those below as cold. In this case, 8 thermocouples are denoted as warm during the intense combustion phase. The temperature difference between warmest and coldest positions was approximately 100 °C.

The trend in warm and cold zones for all 11 experiments is shown Figure 6.6. The basis for determining the warm and cold areas were based on the findings for all experiments as Figure 6.3C. This was evaluated for all experiments. The grey area shows the positions that alternate between warm and cold throughout the experiments. In some of the experiments, the top of the pipe was partially covered, however, these experiments had the same tendency for stable warm and cold regions. An overview of all the experiments can be found in Figure 6.7.

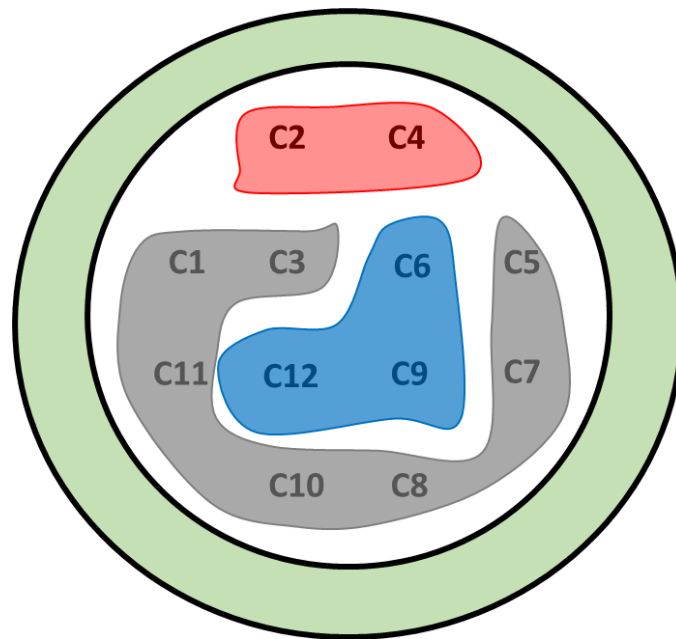


Figure 6.6: The temperature distribution trend in the cross-section of the pipe. The red area was stable hot in more than half of the experiments, the blue area was cold in more than half of the experiments. The grey area was fluctuating during the smoldering experiments. The smoke exits along the pipe wall, while the cold air enters in the middle of the pipe. This is opposite of the first assumption of the air flow.

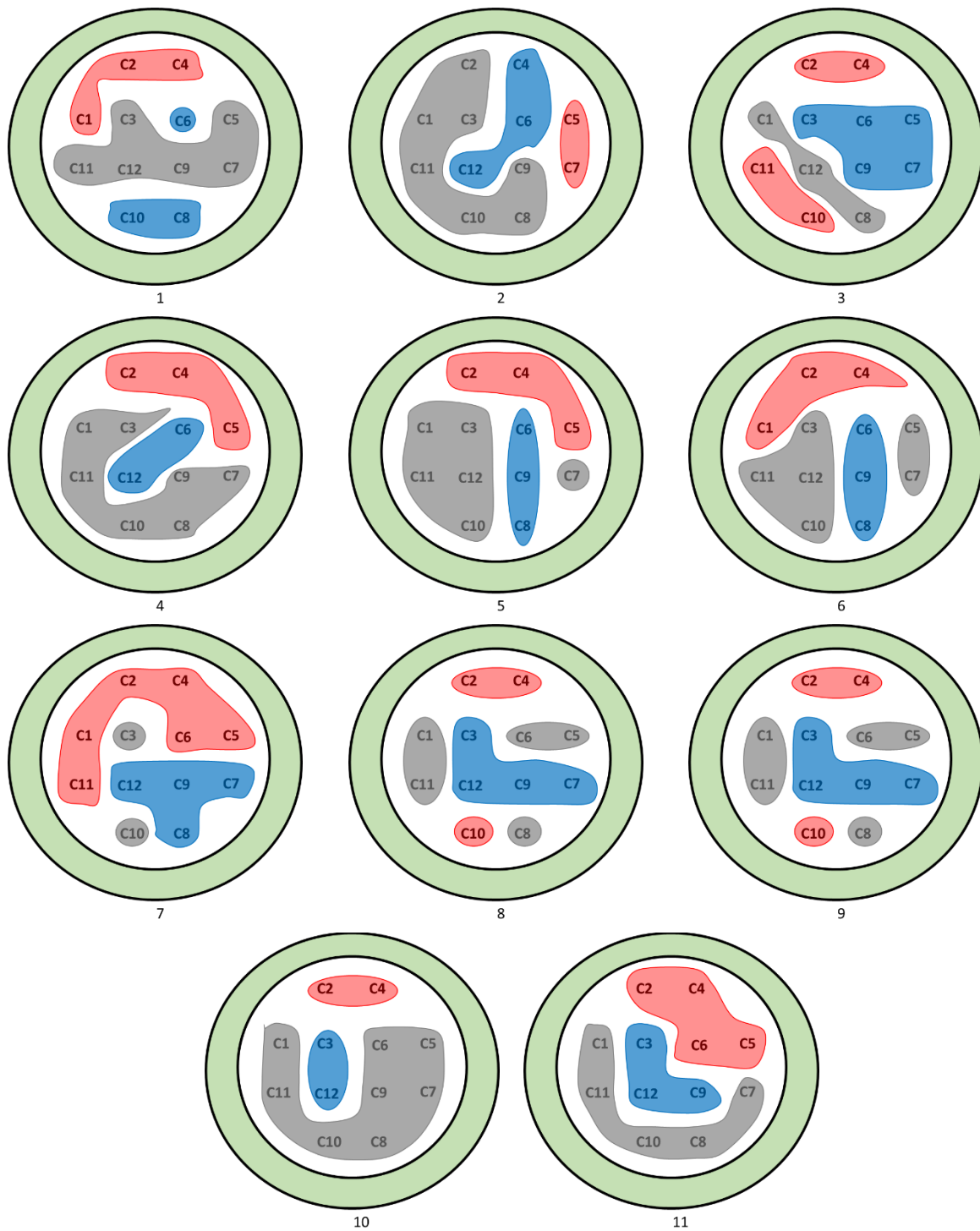


Figure 6.7: The warm and cold zones for the 11 experiments with temperature measurements above the sample.

6.1.3 Temperature in sample and air flow at peak temperatures

The maximum temperature of the sample and the temperature of the air flow at peak temperature show how the exchange of air occur in the pipe. Sample height was 10 cm, and lower thermocouples measured the temperature up to 14 cm, 4 cm above the sample, see Figure 6.8A. At the maximum

temperature of the sample, (6 cm to the right), one notes a significant lower temperature in the air flow above this point (see 10 – 14 cm center and right). Low-temperature and oxygen-rich air from the surroundings enters the sample above the warmest combustion zone, while the warm smoke exits on the opposite side, as demonstrated by higher temperatures above the sample (12 – 14 cm left). The peak temperature of the sample was 635 °C, while the temperature at 8 cm to the left, were 578 °C. There was a 57 °C difference between the two sides, and the warm smoke exited above the left side of the sample. Temperatures measured at 20 cm level display a consistent pattern, see Figure 6.8B. The warmest areas were in the left part of the pipe, while the cooler air entered in the center and to the right, above the region where the highest temperature in the sample were recorded.

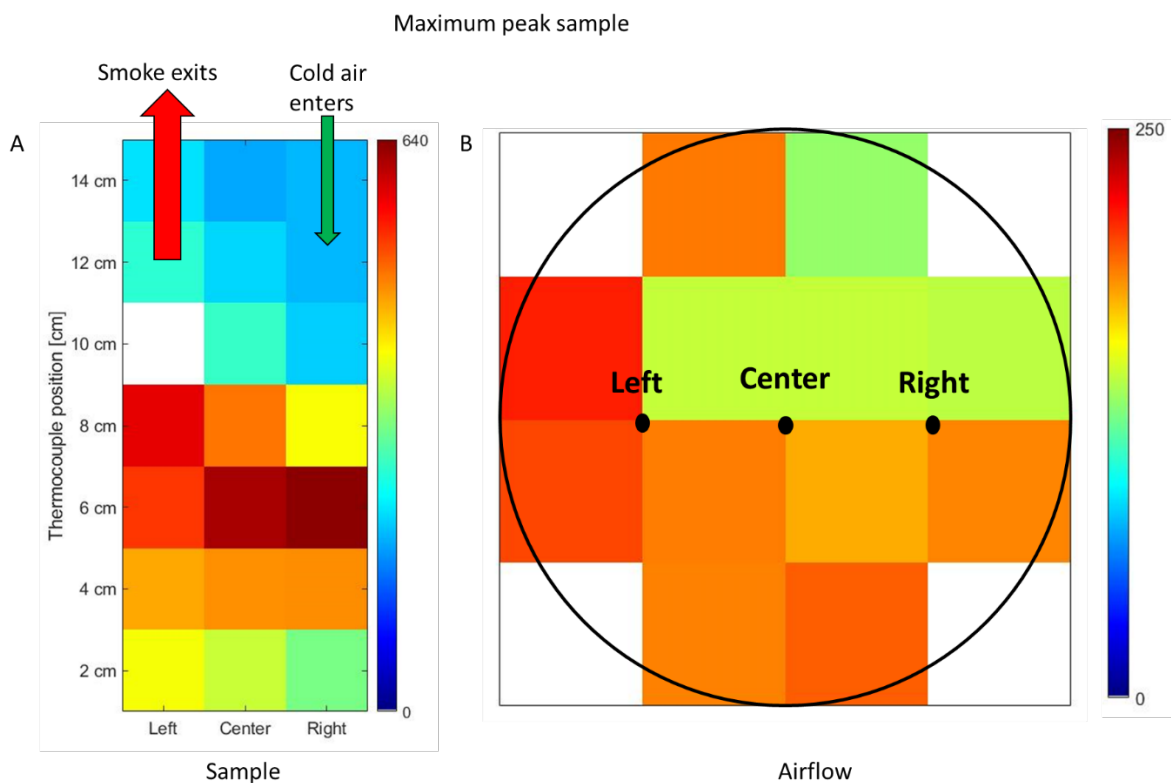


Figure 6.8: Sample and air flow temperatures for a 10 cm sample of wood pellets (same experiment as in Figure 6.2) at the maximum temperature peak for the sample. Note: The temperature scale is different from the sample (640 °C) to the air flow (250 °C). The white spot at 10 cm left is a broken thermocouple. A) The temperature of the sample (side view), B) The temperature in the pipe at height 20 cm (top view).

Smoldering is an oxygen deprived combustion process, where the available oxygen determines the combustion rate. As described in section 4.4, the intense combustion period occurs when the smoldering front reached the surface of the fuel increasing the oxygen supply to the sample. When this happened, the combustion rate increased, and higher temperatures combined with a rapid mass loss was observed. Oxygen access is vital for the smoldering combustion to grow, meaning that the hot spot inside the sample seems to be affecting the air flow. The hot spot needs air, therefore, the cold air

entering the pipe is consumed by the hot spot inside the sample and the smoke generated by the combustion is then pushed out on the opposite side as shown in Figure 6.9.

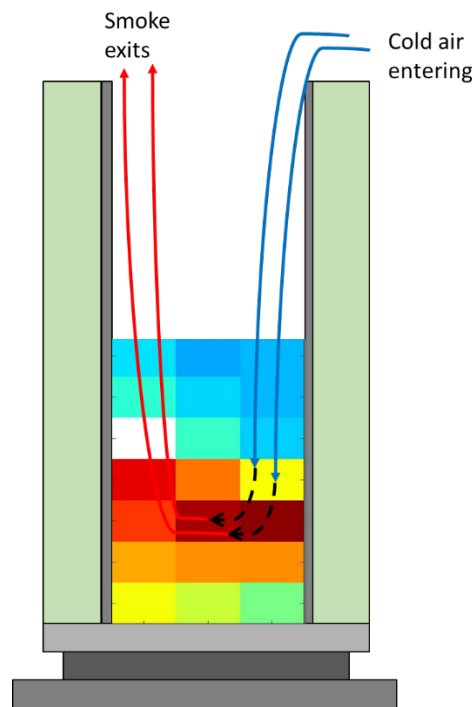


Figure 6.9: Air-flow movement in pipe and sample (same temperatures of sample as Figure 6.8)

The number of thermocouples in the steel construction was increased to include temperature measurements at 20 cm in the vertical measurement positions as in sample. Temperatures of a 12 cm sample of oily pellets, with thermocouples at 14 and 20 cm (above the sample) are shown in Figure 6.10A. The warm smoke exits opposite from the warmest position of the sample located at 14 cm left. Swelling of the pellets could cause an increase of sample height and the condensate could cause a hardened surface at the top of the sample. Based on this, it is likely the sample height has increased to 14 cm, causing the high temperatures at this location. Based on the measured temperature, it is assumed that the surrounding, oxygen-rich air entered the warm zone, contributing to the intense combustion. The smoke exited at the opposite side, warmer temperature measurements above the cooler areas of the sample, as supported by Figure 6.10B, where the warmest area was located on the right side. The surrounding air enters the sample on the left and close to the edge. In this experiment the opening on top of the pipe was reduced to 50 %, all air flow in and out of the top of the pipe was forced to the middle of the pipe.

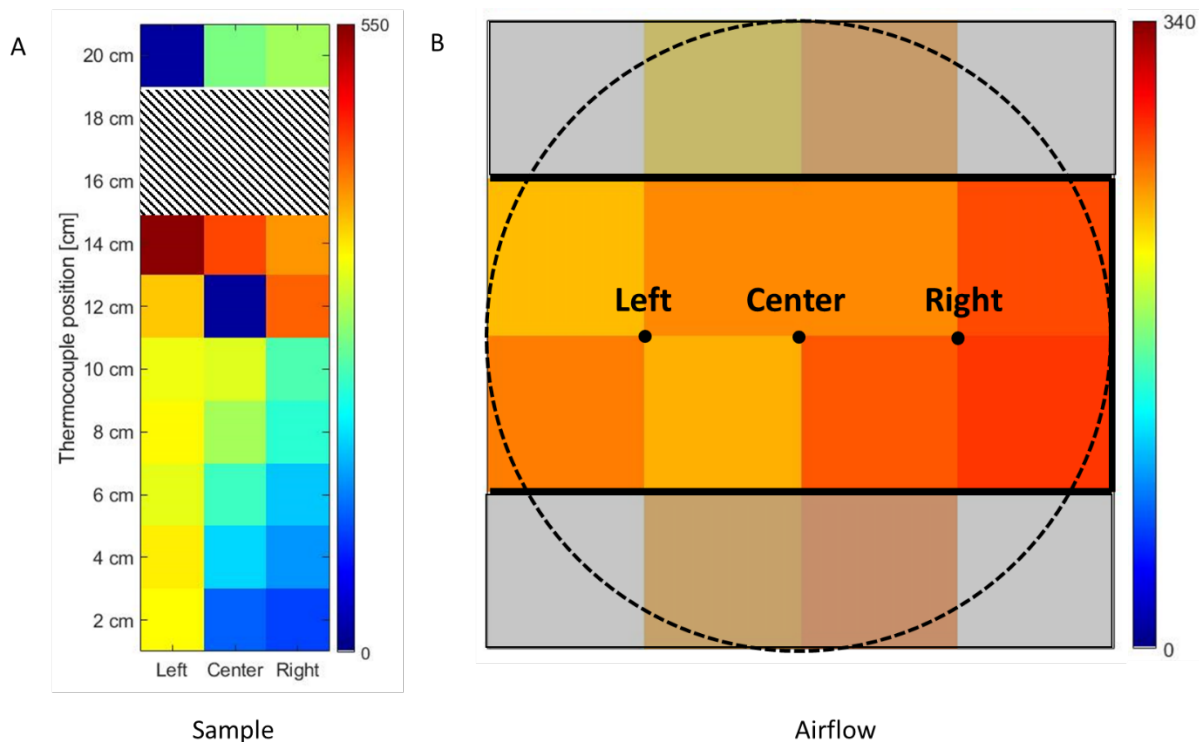


Figure 6.10: Temperatures in a 12 cm sample with oily pellets. Temperature measurements from 2 – 14 cm, and at 20 cm in the steel construction. The pipe opening was reduced to 50 % Note: the temperature scale for the sample (550 °C) and the 20 cm level (340 °C) differ. A) temperature in the sample, the warmest position was at 14 cm to the left. At 20 cm, the coolest position is to the left. The thermocouple at 12 cm center was defect (dark blue). B) Air flow temperatures at height 20 cm. The smoke exits close to the pipe on the right side, while the cooler air enters to the left, close to the pipe wall, and closer to the center. Air enters the warmest part of the sample and exit over the cooler part of the sample.

6.1.4 Temperature of steel pipe

In the experiments conducted in section 4.3 with the high pipe (58/63 cm), the temperature development along the steel pipe was measured by three thermocouples placed between the steel pipe and the insulation. The thermocouples were 25, 35 and 50 cm from the bottom of the pipe, thus markedly above the sample. Temperatures in a 12 cm sample and at pipe wall are shown in Figure 6.11. During external heating, the aluminum plate (hotplate) temperature increased, when the external heating was switched off, its temperature decreased to room temperature (Figure 6.11A). An intense combustion close to the aluminum plate at 0 – 2 cm increased its temperature in some of the experiments. The temperatures at the pipe wall are shown in Figure 6.11B, the highest temperature was found at 25 cm, while it decreased with height. When the sample was heated, the temperature at the pipe wall increased, as expected since the steel pipe rested on the aluminum plate. During the slow combustion, the temperature of the steel pipe was below 50 °C. The steel pipe was affected by the temperature peaks of the sample. During the intense combustion (25 h), part of the sample had high temperatures and heated the walls of the steel pipe. However, the temperatures were in the range of air flow temperatures and in addition temperature of the pipe is similar during the experiments, except for

the peaks. Therefore, it is unlikely that the steel pipe affects the smoldering combustion of the sample or the air flow above the sample. If had been the case, the temperature of the steel pipe had been higher than the temperature of the sample.

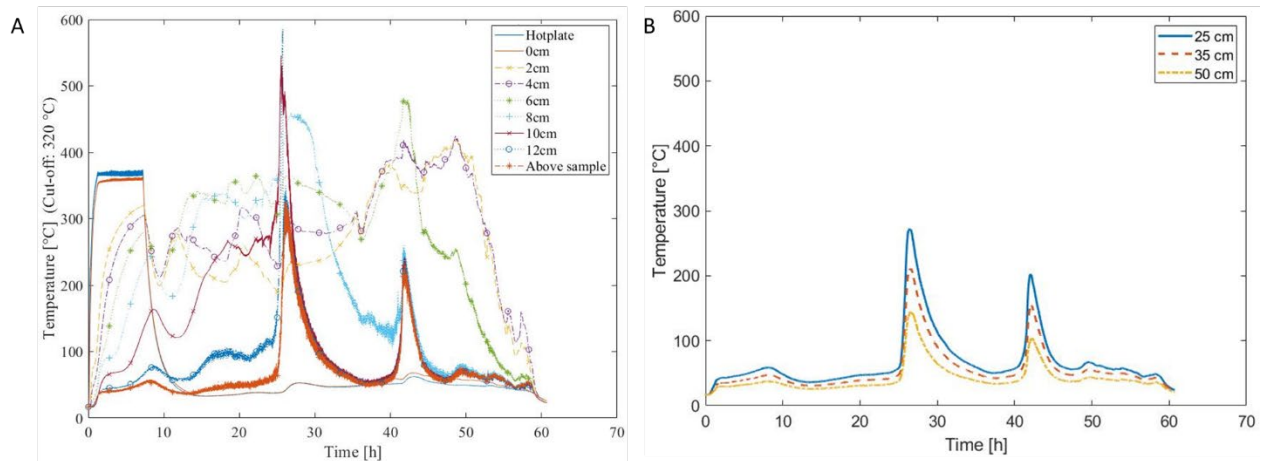


Figure 6.11: Part A) Temperatures in a 12 cm sample of wood pellets in high pipe (58/63 cm). B) The temperatures at the steel-pipe wall during the experiment, measured at heights 25, 35 and 50 cm. The sample temperatures show two temperature peaks, corresponding peaks were found for the steel pipe (25 h and 40 h). The highest temperature of the pipe was found closest to the surface of the sample, and it decreased with increasing height. During the low-intensity combustion, the temperature at the steel-pipe wall was below 50 °C.

6.1.5 Air flow on top of the pipe (33 cm)

The temperatures at the opening of the pipe (33 cm) reflect air flow movement from the surroundings and smoke leaving the sample. However, only one of the experiments gave proper results, the other had problems with the thermocouples. Therefore, this section only shows some preliminary results on the air flow at the top of the pipe. The temperature distribution at the top of the steel pipe is shown in Figure 6.12. Temperatures were lower than at 20 cm, as expected. The same trend as for the pipe-wall temperatures (see section 6.1.4) is found during slow combustion, with low temperatures. Peaks in temperature was found during intense combustion of the sample (20 h).

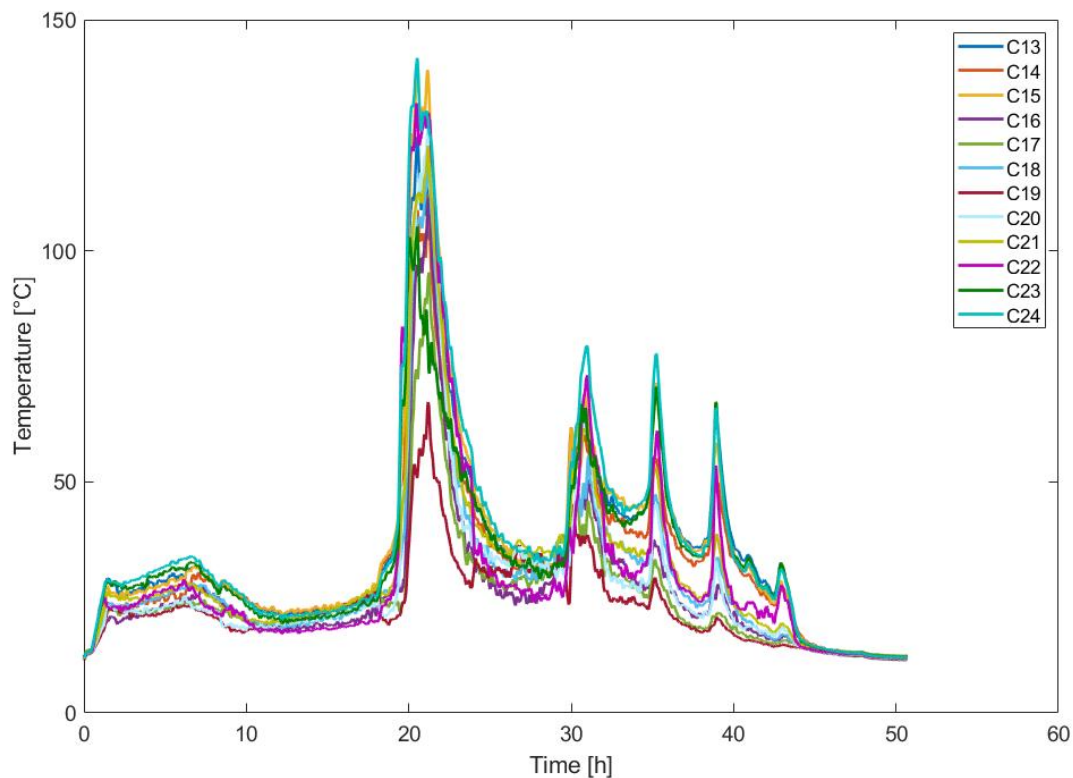


Figure 6.12: Temperature distribution at the top of the pipe (same experiment as shown in Figure 6.2 as a function of time. The temperatures were smoothed using Savitzky-Golay [55] filtering, with a 9th order polynomial and a frame length of 45 min. Due to more scatter in the measurements on top of the steel pipe than inside the pipe, the frame length was increased with 15 min. Note: The temperature at 33 cm was lower than at 20 cm (Figure 6.2b). However, a similar trend was found, with an increase in temperature during intense combustion.

The temperature at the top of the steel pipe was measured using thermocouples fixed to a net that covered the opening of the pipe, with the same thermocouple positions as for the cross-section. The temperatures at 33 cm, hour by hour, are shown in Figure 6.13. The temperatures at the top of the pipe were more stable than at 20 cm. This can be seen from the measurement positions C14, C15, C13, C23 and C24, where the temperatures were high during the experiment. The other positions (C16, C17, C18, C19, C20, C21 and C22) had low temperatures the whole experiment. The stable warm area was larger on top than at 20 cm. Hot and cold zones are shown in Figure 6.14. The warm smoke exits to the left and towards the top, along the pipe wall, while the cold air enters on the right side and to the bottom. The cold zone u

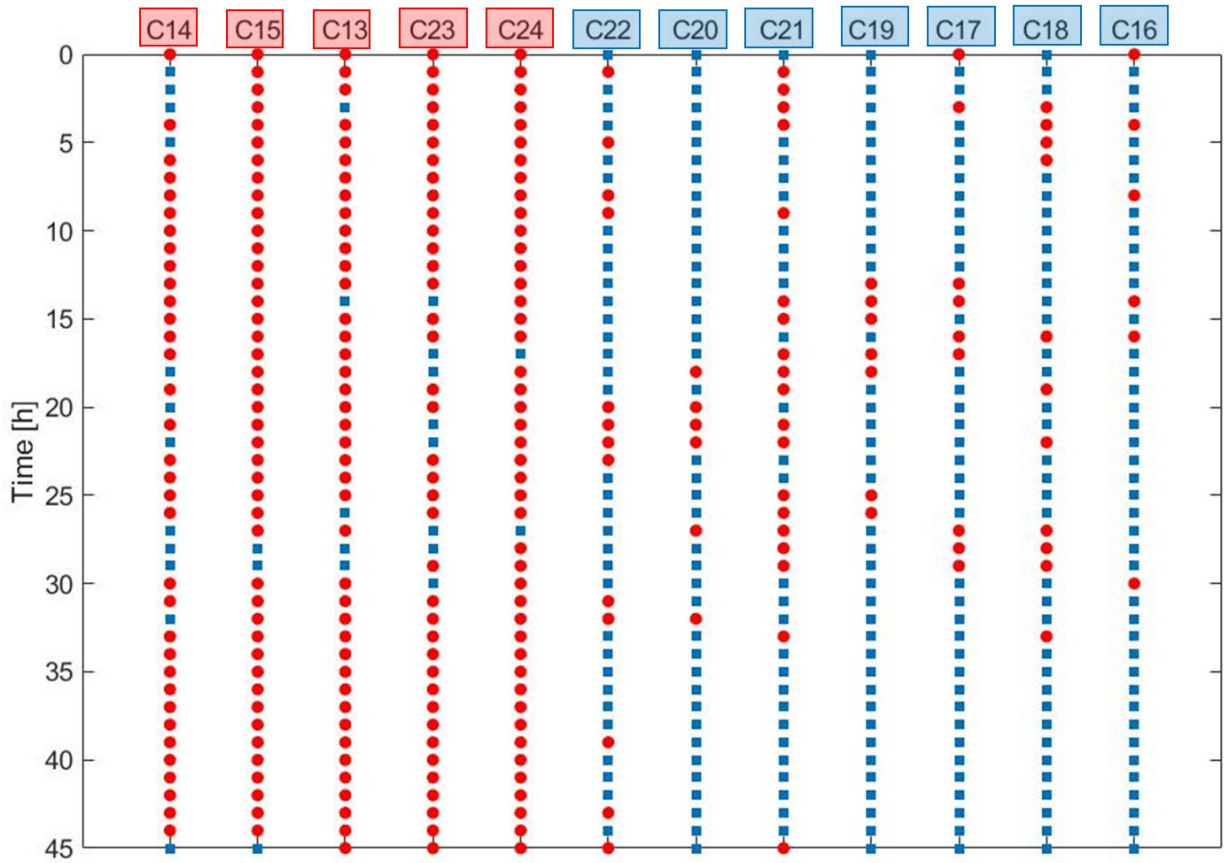


Figure 6.13: Temperature distribution at the top of the steel pipe (33cm) for the experiment in Figure 6.2 and Figure 6.12. Measurement points with high (red) and low (blue) temperatures are both grouped into rather compacted zones. Both warm and cold zones were stable at the top, there were merely a few variations in the position of the boundary between the zones.

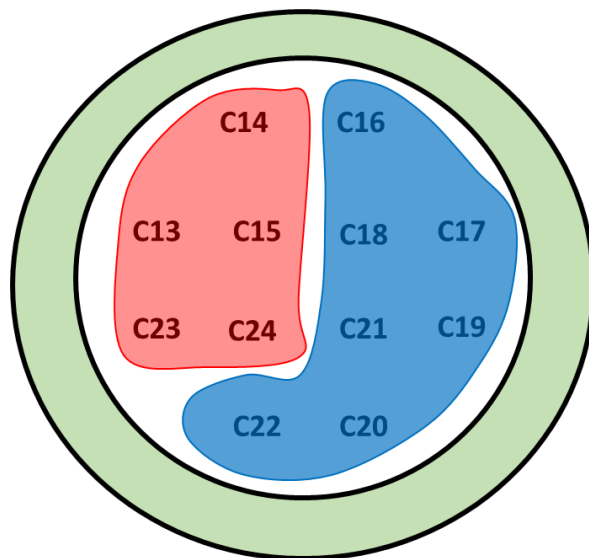


Figure 6.14: Cold zone and warm zone at top of the pipe, for a 10 cm sample of wood pellets (the same experiments as shown in Figure 6.13). Cool air entered at one side and warm smoke exited on the opposite side.

The largest impact on the air flow temperature was found during intense combustion. In addition, the surrounding air entered on the same side as the intense combustion zone in the sample, while the warm smoke exited on the opposite side. This was unexpected since a reasonable assumption would be that warm smoke exits from the warmest part of the pellet sample.

6.2 Impact of top coverage on smoldering combustion in pellets

In the series of experiments with wood and oily pellets, the top of the pipe was covered to reduce the air supply to the sample. Wood pellets and oily pellets were tested in groups of two, one pipe with wood pellets and one with oily pellets to obtain identical external conditions (see section 5). The air flow was reduced by covering the top of the steel pipe, reducing the opening to 50 % and 25 % of the original opening. Steel plates with a cut-out was used to cover opening of pipe, details were described in section 3.4. The location of the cut-out was for practical reasons located at the center of the pipe, to easily get all the thermocouple wires out of the pipe. Therefore, all air entering and exiting the sample was forced to the middle of the pipe. The method used resulted in a symmetrical situation.

In the preliminary experiments, a plastic material was used as coverage of the pipe. It was observed that water evaporated from the sample, condensated on the coverage, before dripping back to the sample, see Figure 6.15 (red circle). This water affected the top of the pellets sample. In the non-smoldering experiments, the pellets at the top had hardened in contact with water. The effect of coverage on smoldering combustion of the two biomass materials, wood and oily pellets, will be discussed in the next sections.



Figure 6.15: Condense on plastic coverage of the steel pipe. The condense is marked with a red circle. The condensate dripped down on and affected the top layer of the sample.

6.2.1 Effects of coverage of opening for a sample height of 10 cm

Reduced opening of the top of the pipe changed the smoldering behavior. An experiment of sample height 10 cm with wood pellets had delayed intense combustion when the pipe opening was reduced to 50 %. The intense combustion was delayed by 10 h, see Figure 6.16. However, when the opening was reduced further to 25 % there was no delay in the intense combustion period. On the other hand, the duration of the intense period increased.

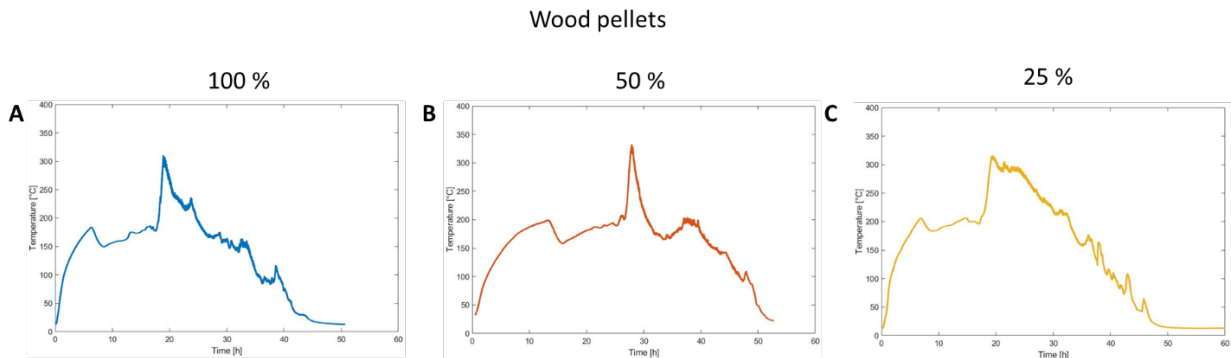


Figure 6.16: The average temperature in wood pellets samples of 10 cm with open pipe and the coverage of 50 % and 25 %. A) Fully open pipe had a short intense combustion period at approximately 20 h. B) Opening reduced to 50 %, resulted in a short intense combustion period at approximately 30 h, 10 h later than a fully open pipe. C) Opening reduced to 25 %. In this case the trend changes, the intense combustion lasted longer, but started at 20 h.

For oily pellets, the duration of the intense combustion period changed as the opening at top of the pipe was reduced, see Figure 6.17. A reduced opening of 50 % increased the duration of the intense combustion period, while an opening of 25 % resulted in an earlier intense combustion with a shorter peak. After the intense combustion period, a long period with stable temperature around 200 °C followed for the 25 % case. A reduced opening of 25 % resulted in lower temperature peak compared with fully open pipe and 50 % coverage. The average peak for 100 % and 50 % was 350 °C, while the temperature was reduced to 300 °C when the opening was only 25 %. Overall, the restrictions of the air supply affected the intense combustion: a faster occurrence, lower overall temperature, and increased duration of the intense combustion period.

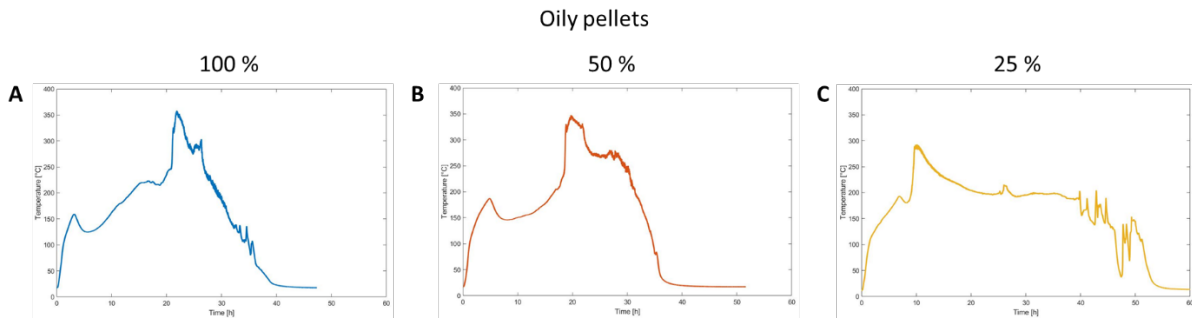


Figure 6.17: The average temperature of a 10 cm sample of oily pellets. A) Fully open pipe. B) Pipe opening reduced to 50 %, the intense combustion period started at around 20 h, and the duration is longer. C) The opening reduced to 25 %. There was a peak indicating intense combustion (at 10 h) before the temperature stabilized at a relatively high level (around 200 °C) for much of the remaining part of the experiment.

6.2.2 Effects of coverage of the opening for a sample height of 12 cm

Reduction of the pipe opening has an effect in a sample with a height of 12 cm. As the pipe was covered, the sample had to be heated longer before a self-sustained smoldering combustion was established. This could have been caused by the condensate dripping back to the top of the sample. Water to the pellets have previously shown to create a hard surface and therefore reducing the oxygen flow to the smoldering front, which could impact the establishment of a self-sustaining smoldering combustion. The average temperature of a 12 cm sample with wood pellets is shown in Figure 6.18. The maximum temperature peak decreased when the pipe opening was reduced. The number of smaller temperature peaks increased with reduced opening. A reduction to 25 % opening led to two intense combustion periods, where the second period had the highest temperature.

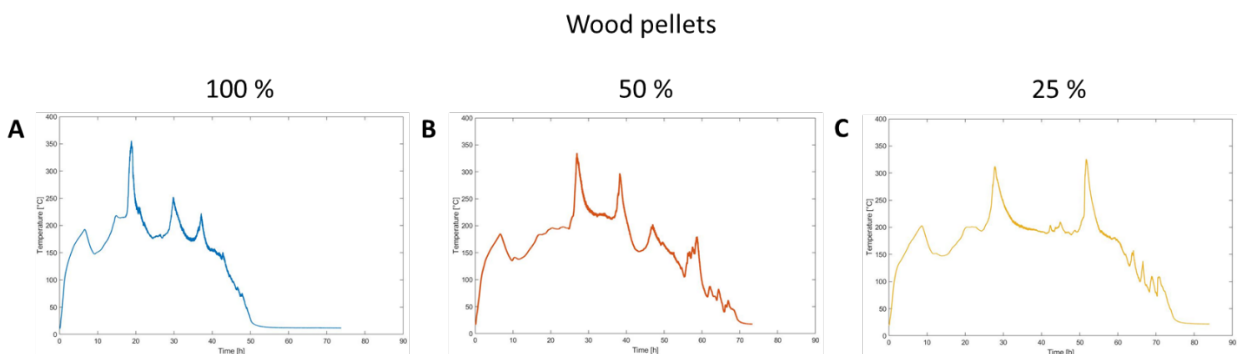


Figure 6.18: The average temperature in a 12 cm high sample with wood pellets. A) Temperature with 100 % opening of the pipe. There was one intense combustion period at 19 h and two secondary peaks with lower temperature at 30 h and 37 h. B) Opening of pipe reduced to 50 %. The intense combustion period was delayed by 8 h compared with open pipe. The number of smaller peaks increased from two to six (38 h, 47 h, 59 h, 62 h, 64 h, 67 h). C) Opening reduced to 25 %. The intense combustion period occurred around the same time as the 50 % coverage, however, there were two maximum temperature peaks (28 h, 52 h), where the second peak had higher temperature (326 °C). After the two intense period, there were four smaller peaks (62 h, 64 h, 69 h and 71 h).

The duration of the intense combustion period increased with decreasing opening of pipe for the oily pellets, see Figure 6.19. In addition, the temperature of the sample decreased during the intense combustion period. As shown in Figure 6.19B, when the opening was reduced to 50 %, the sample temperature was higher compared with a fully open pipe, when the external heating was switched off. The temperature of the hotplate was equal for all experiments.

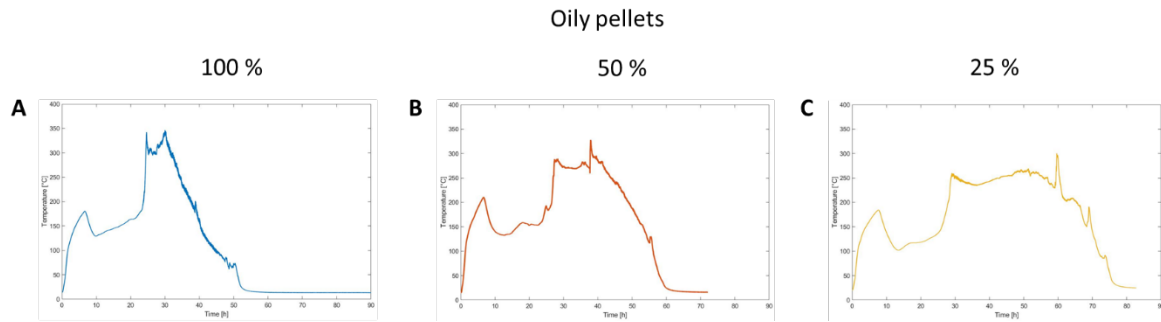


Figure 6.19: The average temperature oily pellets sample of 12 cm and different coverages of the steel pipe. A) 100 % open pipe, the intense combustion period had a longer duration than the wood pellets (compare with Figure 6.18A. B) Reduced opening by 50 %. The duration of the intense combustion increased. In addition, the average temperature was lower during the intense combustion period. C) Opening of pipe reduced to 25 %. The intense combustion period was longer. The average temperature was lower during the intense combustion period when the air flow was reduced to 25 %.

The main differences found for the two materials with reduced opening are: several small intense combustion periods in wood pellets, while oily pellets had a longer intense combustion period. In addition, wood pellets needed to be heated for longer when the opening was reduced. Oily pellets on the other hand only needed increased external heating time when the air supply was reduced to 25 %. This could be a result of the natural contents of oil in the oily pellets. Restriction of the pipe opening reduced the maximum temperature of the sample of both these biomass materials.

6.2.3 Air supply at the height 20 cm with coverage of pipe opening

Reduction of the pipe opening affected the locations of warm and cold air flows in the pipe at 20 cm. A reduced opening of 50 % divided the region at 20 cm into two sides, one warm and one cold, see Figure 6.20. The dark lines represent the opening at the top of the pipe, see Figure 3.8. The warm and cold areas are stable during the intense combustion. Before (Figure 6.20A), during (Figure 6.20B) and after (Figure 6.20C) intense combustion, the warm smoke exits in the top and to the left (in the figure), while the cold air enters in the middle and bottom right.

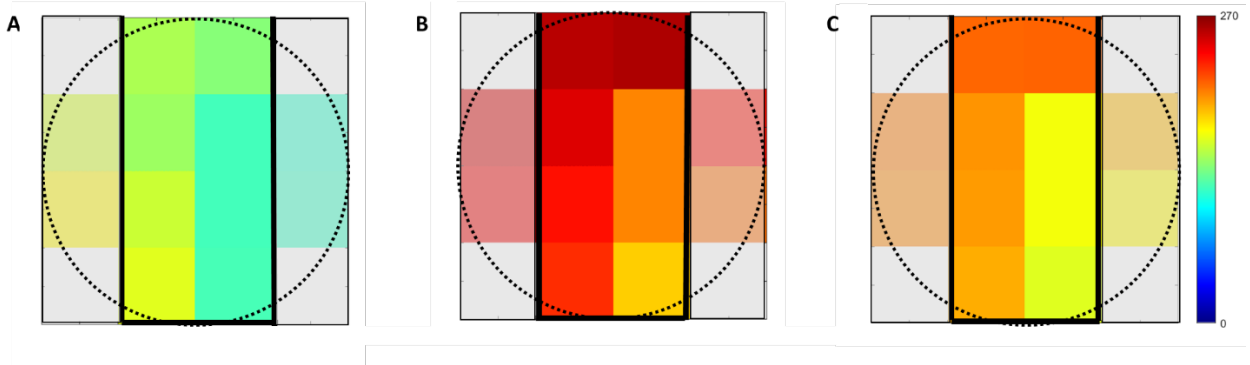


Figure 6.20: The temperature distribution at the height of 20 cm when the pipe was 50 % covered. There was a division between the cold and warm air flow at the center of the pipe. These illustrations are at the start (A), during (B) and at the end (C) of the intense combustion period in a 10 cm sample with wood pellets. The black lines indicate the opening of the pipe, while the light grey area represent the steel plate, and dotted circle is the pipe walls see Figure 3.8B.

6.2.4 Mass-loss rate during intense combustion: effect of coverage

Reduction of the air supply to the sample affected impacted the mass-loss rate for both types of pellets. As the air supply to the sample was reduced, the intense combustion period occurred later. The mass loss during intense combustion differed, caused by a lower combustion temperature. For sample height 12 cm, the mass-loss rate decreased as the coverage of the pipe increased, see Figure 6.21.

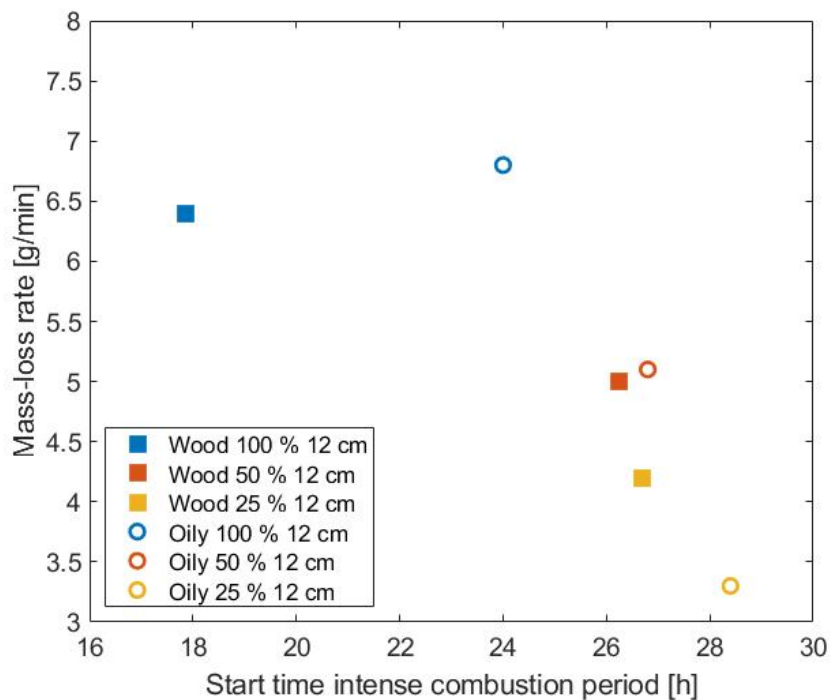


Figure 6.21: Mass-loss rate during intense combustion as a function of start time of the intense combustion period for 12 cm of wood pellets (filled squares) and oily pellets (circles). The opening of the pipe was reduced from 100 % to 50 % and the smallest the pipe opening was reduced to 25 %. As the air supply was reduced, the mass-loss rate decreased and the start time for intense combustion increased for both materials.

The mass-loss rate during intense smoldering combustion for wood and oily pellets show a decreasing trend as the coverage increased, see Figure 6.22. A correlation analysis confirmed that the reduced pipe opening influences the mass-loss rate during the intense combustion, see Table 6.1. When there was no restriction of the air flow, the mass-loss rate was higher, as expected since the temperature in the sample was higher. Mass loss and temperature are connected. A higher temperature results in a higher mass-loss rate, which is reasonable since a higher temperature leads to higher combustion efficiency.

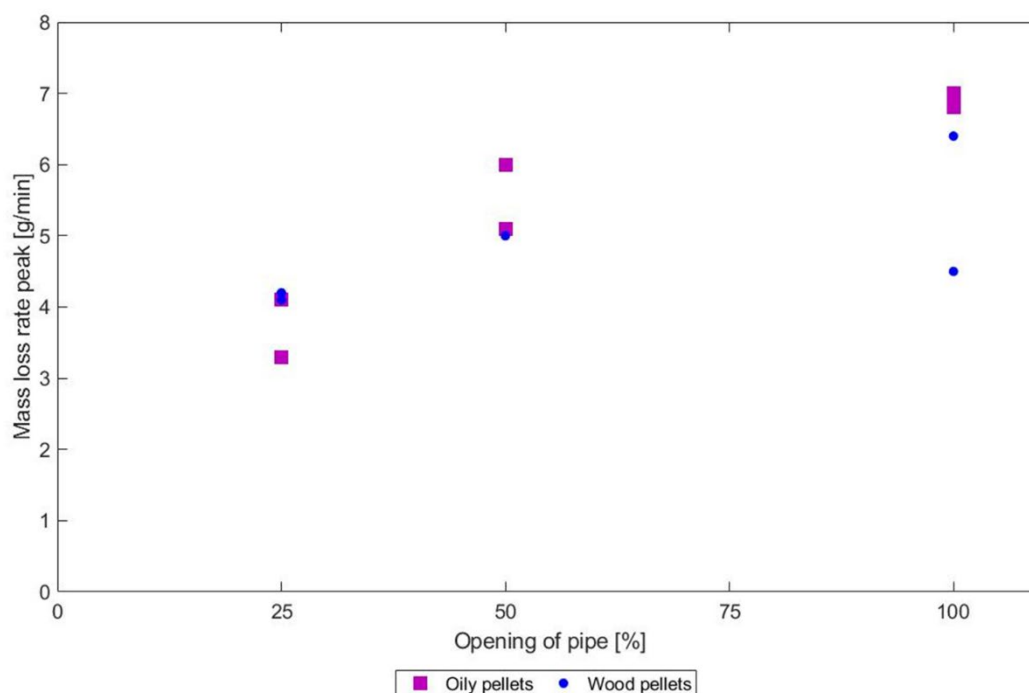


Figure 6.22: Mass-loss rate during maximum temperature peak as a function of pipe opening. The mass-loss rate decreased as the opening is reduced.

Table 6.1: Correlation analysis of the mass-loss rate during the intense combustion period with the pellet type, sample height and pipe opening.

	Pellet Type [W/O]	Sample height [cm]	Pipe opening [%]	Mass-loss rate peak [g/min]
Pellet Type [W/O]	1			
Sample Height [cm]	-0.1	1		
Pipe opening [%]	-0.0255655	-0.0255655	1	
Mass-loss rate peak [g/min]	0.22860903	-0.0028502	0.7785128	1

7. Long-run smoldering experiments with transition to flaming

The long-run experiments were a continuation of the initial experiments and were carried out to investigate how the smoldering fire behave when consumed pellets were replaced at certain intervals. The consumed mass was refilled at predetermined intervals to replace the combusted mass and continue the smoldering process, therefore these experiments are denoted as long-run experiments. The initial aim was to reproduce the intense combustion period with massive mass loss found in section 4.4. The smoldering combustion showed a large mass loss in the intense combustion period, where 15 % of the total mass was lost during a short time interval (section 4.4). By refilling the sample at given intervals of 8 h, the consumed mass was replaced with fresh material and the smoldering combustion was prolonged. There were two effects of refilling: cooling of the sample, which could lead to extinguishment, or a combustion that could last indefinitely. The experiments were conducted in the top-ventilated steel pipe, where the sample initially was heated from below, as described in section 3.2.2. Some findings from the long-run experiments will be presented in this chapter, as the long-run experiments is an ongoing project. The experimental work has been conducted in cooperation with Anita Meyer.

A reason for concern during smoldering combustion is the possibility of transition to flaming fire. In the experiments in section 4 (without refill), temperatures observed indicated only smoldering and no transition to flaming fire. The temperatures above the sample did not reach values indicating flaming (750 to 1000 °C). However, in the long-run experiments transition to flaming combustion was observed in several experiments. A total of 48 experiments were conducted in the long-run category, and more are planned in the future, however in this work the experiments of interest are the 12 experiment with a transition to flaming fire. The refilling of the pellets led to conditions suitable for a transition from smoldering to flaming fire. An understanding of these conditions could help understand the risk for a transition to flaming fire.

7.1 Typical smoldering behavior in the long-run experiments

Typical smoldering for wood pellets with refilling to initial sample mass displayed several periods with both low and high intensity combustion. Temperatures during smoldering of a 10 cm sample is shown in Figure 7.1A. The sample was heated for 14.5 h, during smoldering there were several intense combustion periods, with temperature peaks from 500 to 600 °C. However, at 80 h there is a peak with distinctly higher temperature, of 800 °C. At this point, the temperature increased rapidly in the upper parts of the pipe and above the sample (18 – 20 cm) and a transition to flaming was visually observed in the pipe. From 30 h to 60 h low-intensity combustion occurred, with temperatures below 200 °C in large parts of the sample.

A typical mass-loss curve with refills is showed in Figure 7.1B. The maximum mass-loss rate for this experiments was 12.4 g/min After intense combustion periods the refills are large, more than 400 g of fresh material is added, constituting 34 % of the initial sample mass, the larger refills can been seen by the large drops in the curve. The low-intensity combustion periods (30 – 60 h), had small refills. From 60 h to 120 h there were several intense combustion periods, where the mass loss exceeded 400 g. Transition to flaming fire occurred at 80 h and lasted for approximately 20 minutes. The sample had been refilled 2 hours before.

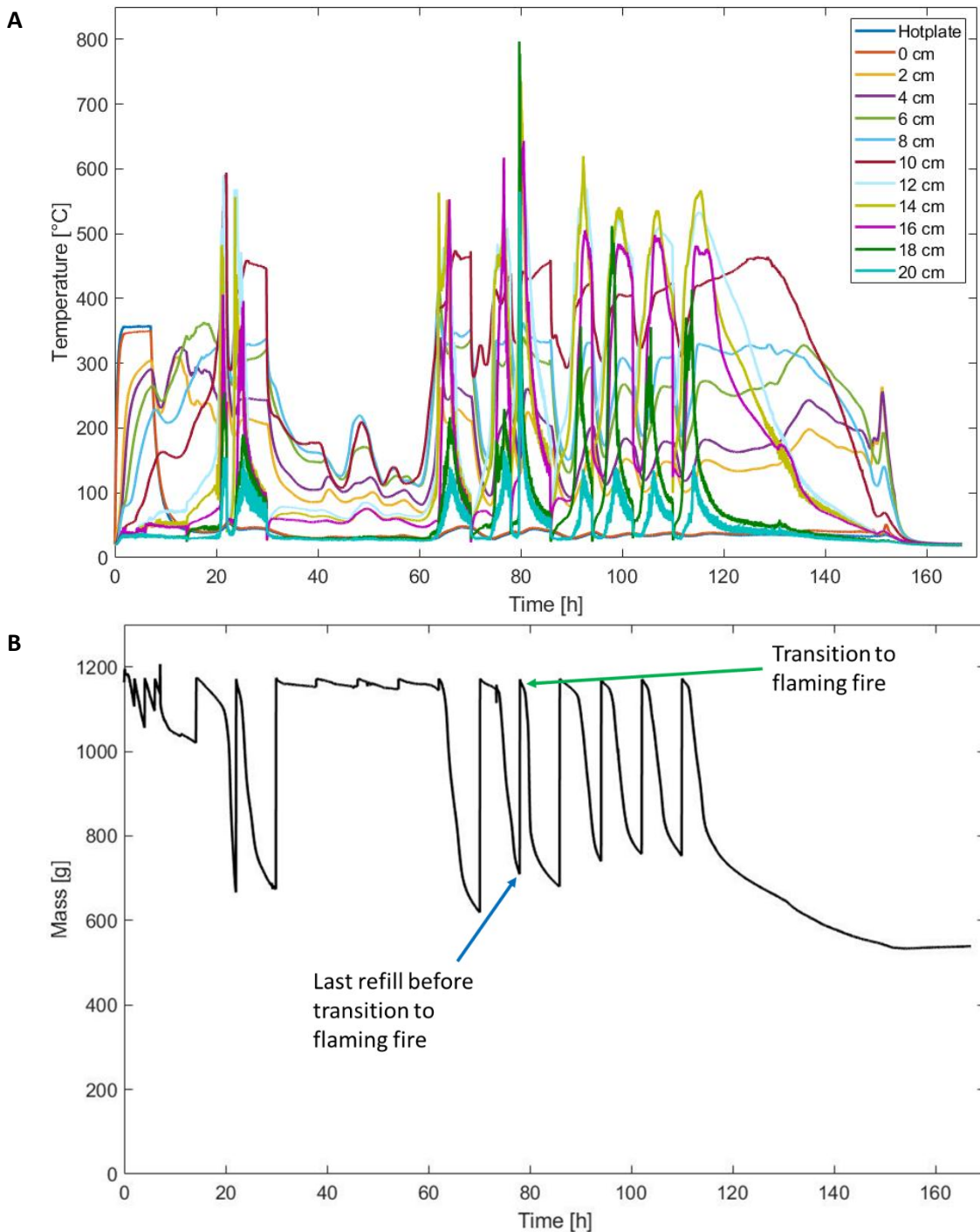


Figure 7.1: Typical temperature and mass-loss development during a long-run experiment. The experiment has an initial sample height of 10 cm, a duration for approximately 160 h, and was refilled 19 times. A) The temperature development, the sample endured several temperature peaks at times: 10. At approximately 80 h transition to flaming fire was observed. In the period between 30 – 70 h, there was a low-intensity combustion, large part of the sample had a temperature below 200 °C. B) mass loss during this experiment. There are larger refills in connection with the intense combustion periods, shown rapid increase in mass. Low-intensity combustion consumed smaller amounts of pellets, leading to an uneven wave shape.

7.2 Transition from smoldering to flaming fire

Transition from smoldering to flaming fire is difficult to obtain. Several factors are necessary, such as hot spots and sufficient pyrolysis gas, heat, and oxygen supply. Knowledge of the conditions in the pipe at the time of transition are of importance for extinguishing a smoldering fire and avoiding transition to flaming fire. Through understanding how conditions in the sample could affect the outcome, the hazards with storage of biomass pellets could be reduced.

Transition to flaming fire in these long-run experiments could be difficult to detect, since video recording of the experiment was not possible. A camera above the sample recording the top of the sample would rapidly be contaminated by tar. A recording from the side would not detect a fire if the flames were lower than the pipe height. In addition, the thermocouples were located at a vertical plane in the center, and the flame could occur at any position in the pipe. However, indicators of a transition had been found in the experimental data. The first indication of a transition to flaming was an especially high temperature above the surface of the sample, combined with high mass-loss rate. Direct visual observations photos of transition to flaming fire are shown in Figure 7.2A and B. The transition to flaming combustion occurred after approximately 51 h, for a 14 cm sample with wood pellets. The flame started at one side of the pipe (Figure 7.2A) and moved to the opposite side (Figure 7.2B), there were 8 min between the photos. Flaming combustion had a short duration, approximately 20 min.

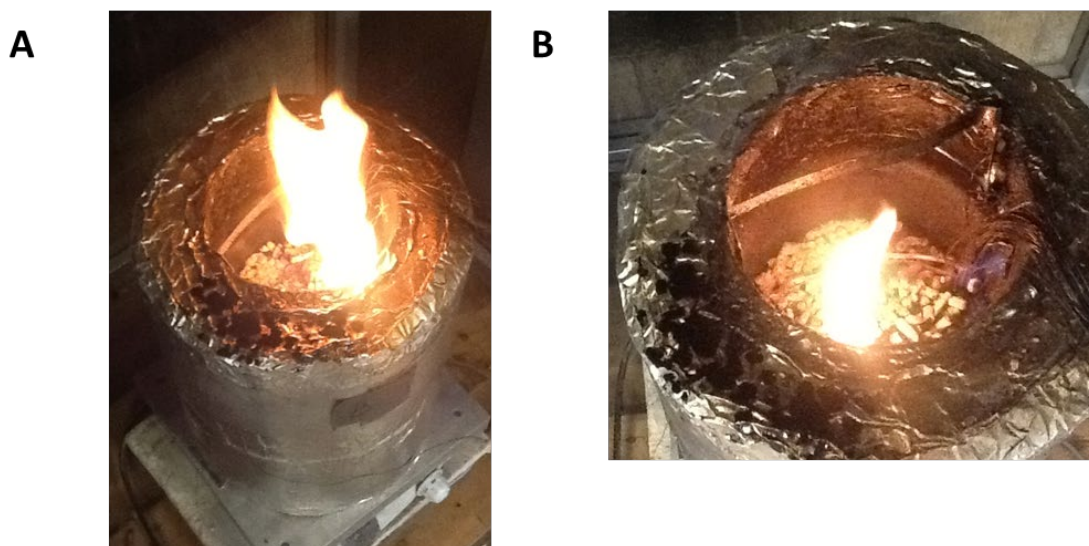


Figure 7.2: Flaming fire inside the steel pipe, visually observed and photographed by Anita Meyer. The sample height was 14 cm, and the transition from smoldering to flaming occurred at 50.8 h. The flame was initially observed at one side of the pipe (part A) and moved across the sample to the other side (part B).

The refilling of material to the sample increased the sample height. A charred layer of pellets was located at the bottom of the sample, with fresh pellets at the top. Since no material was removed from the pipe, the amount of charred pellets increased with increased duration of the experiment. As a result

of the refill on top and swelling of the pellets, the sample height increased. A transition to flaming fire occurred in the gas phase above the sample. Therefore, to establish occurrence of flaming combustion from high temperature readings above the sample, the increasing sample height needed to be determined using a combination of temperature and standard deviation (see section 4.4.3).

Flaming combustion in the wood pellets experiment as shown in Figure 7.2 was short, the duration was 20 min. The temperatures before, at and after the maximum peak are displayed in Figure 7.3. Before the transition to flaming fire (Figure 7.3A), the highest temperatures were located at 10 – 14 cm and estimated sample height was 18 cm. The temperatures were lower at heights 2 – 6 cm, caused by heat loss to the surroundings through the aluminum plate. At the temperature peak, Figure 7.3B, the highest temperatures were at the top of the sample, 18 cm to 20 cm, and exceeded 750 °C. There was a hot spot inside the sample at 12 – 14 cm (center to right). After the temperature peak (Figure 7.3C), the top part at 18 – 20 cm cooled, and a hot spot was located in the center at 12 – 14 cm. There was an increase in temperature lower in the sample (6 – 8 cm), which could have been a results from the higher temperatures of the sample caused by the flaming fire.

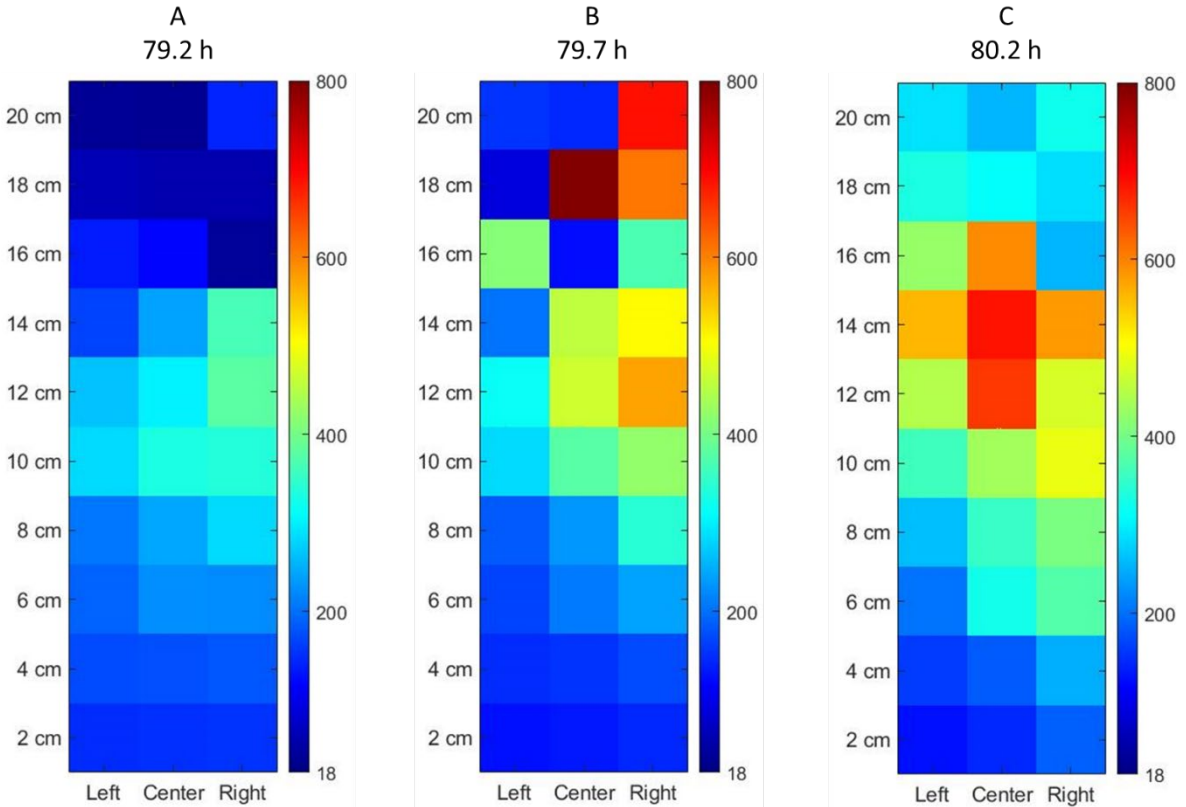


Figure 7.3: The temperature distribution inside a 10 cm sample (same experiment as Figure 7.2) with transition to flaming fire, 0.5 h before, at, and 0.5 h after the maximum temperature peak. At the transitioning to flaming, the estimated sample height was 18 cm. Part A) The temperature of the sample 0.5 h before observation of flames and maximum temperature. Part B) At maximum temperature peak, the warmest temperatures measure was above the sample, indicating a transition to flaming fire. Part C) 0.5 h after the maximum temperature.

7.3 Hot spots in sample before transition to flaming

Hot spots inside the sample at the start of intense combustion were found for the experiments analyzed in section 4.4. Similar hot spots were found in the long-run experiments. The temperature of these could indicate conditions needed for a transition from smoldering to flaming combustion. One of the criteria for an intense combustion period to occur was a hot spot in the sample as described in section 4.4.3. To determine the start of intense combustion period, the average temperature of the initial sample and above the sample are evaluated. The two temperature curves are shown in Figure 7.4, where the solid line shows the average temperature above the initial sample height and the dashed line shows the average sample temperature. Figure 7.4 shows how the temperature inside and above the sample varied from a refill at 78 h and towards an intense combustion period at 79 h. The trend of the two temperature curves differs, the temperature above the sample was increasing, while the temperature of the sample was decreasing as the sample approaches the intense combustion period, see Figure 7.4. The decrease in temperature was a result of refill of sample. At 78 h, a refill caused a rapid temperature decrease in the higher parts of the sample. Due to thermal inertia, the lower parts of the sample were not as affected by the refill as the top part and this led to a lower decrease in temperature in the lower parts of the sample. Generally, the temperature of the sample was dependent on the size of the refill and the time from refill and until the next intense combustion period. Close to the previous refill the temperature was decreasing, and close to the next refill the temperature was increasing, and in between the temperature was stable.

The method used to find the start time of the intense period is shown in Figure 7.4 and involves two time estimates, one from inside the sample and one for the region above the sample. These two time estimates were averaged and the temperatures at this estimated start time were found from the data set, at each position measured inside the pipe. To obtain an unambiguous criterion, the initial sample height was used to distinguish between sample and above-sample temperatures. The initial sample height was 10 cm, the temperature was therefore averaged from 2 – 10 cm, leading to the dashed line, and 12 – 20 cm, leading to the solid line, see Figure 7.4A. The start time of the intense combustion period was determined by a tangent (1) along the curve drawing of the rapid temperature increase above the sample. Likewise a tangent (2) was drawn along the slope during low-intensity combustion. The intersection between these two tangents gives an estimate for the time when the intense combustion above the sample started, see Figure 7.4B. The average temperature in the sample is lower than the average temperature above the sample during intense combustion, and therefore the hot spot was located above 10 cm. It is likely that the sample height was higher than 10 cm at this point due to refilling. The time when the intense combustion in the sample started was found using the same method. Two tangents (3) and (4) (Figure 7.4C) were drawn along the temperature curve for the sample. Thus, two start times for the intense combustion period were found, applying to the sample and the region above the sample respectively, based on the average temperatures.

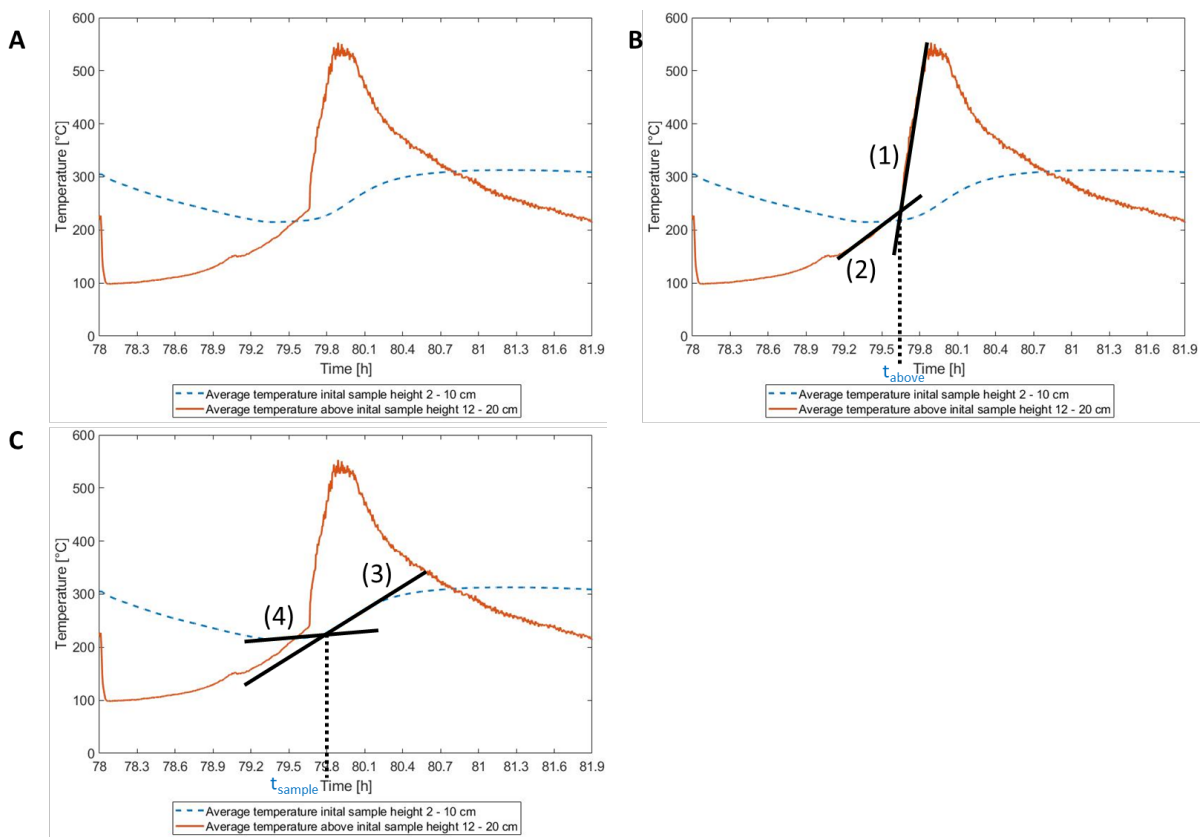


Figure 7.4: Method used to find the start time of an intense period for experiments with transition to smoldering. Part a) Average temperature of all up to initial sample height (dotted line) and average of all temperatures above (solid line). Part b) Tangents (1) and (2) were drawn along the temperature curve for the region above the sample height. The intersection between the two tangents gives the start time of the intense period above the sample. Part c) Similarly, tangents (3) and (4) were drawn for the temperatures inside the sample. The two start times were averaged, and the temperatures were extracted from the data set at the estimated start time.

A hot spot was observed during the intense combustion period. The definition of hot spot in this thesis is the four highest temperatures above 300 °C inside the sample. This is same criteria as in section 4.4.3. The hot spots were located in the upper part of the sample. However, to determine its position, the sample height needed to be estimated. The estimation was done from the temperature curve and the standard deviation. The basis for the analysis were 15 experiments with transition to flaming fire. The average temperature of hot spot ranged from 328 – 549 °C, with an average temperature of 418 °C. Figure 7.5 shows the temperature at the start of an intense combustion at approximately 80 h, in a 10 cm high sample. Due to the refilling of the sample, the sample height has at this point increased to 18 cm. A hot spot was located at 12 – 14 cm, with the highest temperature measured at 18 cm, above the hot spot at 12 – 14 cm. These four measurement points enclosed by black lines represent the hot spot in the sample. Their average temperature was 549 °C. There is an uncertainty in the height estimations, observations of the temperatures in Figure 7.5 indicate a height around 14 cm, because of the cooler area above the hot spot at 12 – 14 cm.

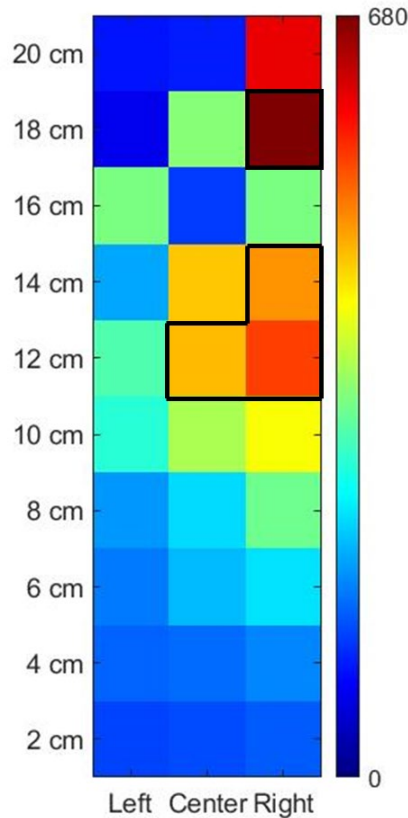


Figure 7.5: Hot spot of a sample with an initial sample height of 10 cm at 79.7 h the start of an intense combustion period (same experiment as Figure 7.4). The estimated sample height at the start of the intense combustion was 18 cm. The warmest area is found at 18 cm, and 12 – 14 cm to the right in the sample (indicated by black lines). It is reasonable to assume that 18 cm was close to the surface of the fuel, as the positions just below 18 cm were cooler. The four measurement points had an average temperature of 549 °C.

Hot spots were also found in the smoldering experiments in section 4.4. As the intense combustion period started, a warm core area was located inside the sample. The average temperature of the hot spots in those 26 experiments was 367 °C, 51 °C lower than the average for the 15 experiments with transition to flaming fire. The peak temperature and the average temperature of the hot spot for standard smoldering and for smoldering with transition to flaming fire are shown in Figure 7.6. Smoldering experiments had a peak temperatures between 490 and 650 °C (orange squares), while transition to flaming combustion had between 630 to 1010 °C (blue circles). The hot spots in smoldering are grouped together, while with transition to flaming fire the hot spots are spread. A reasonable assumption is that if the average temperature of the hot spot exceeds 450 °C, and the sample has a peak temperature above 700 °C, the sample would transition from standard smoldering to flaming combustion.

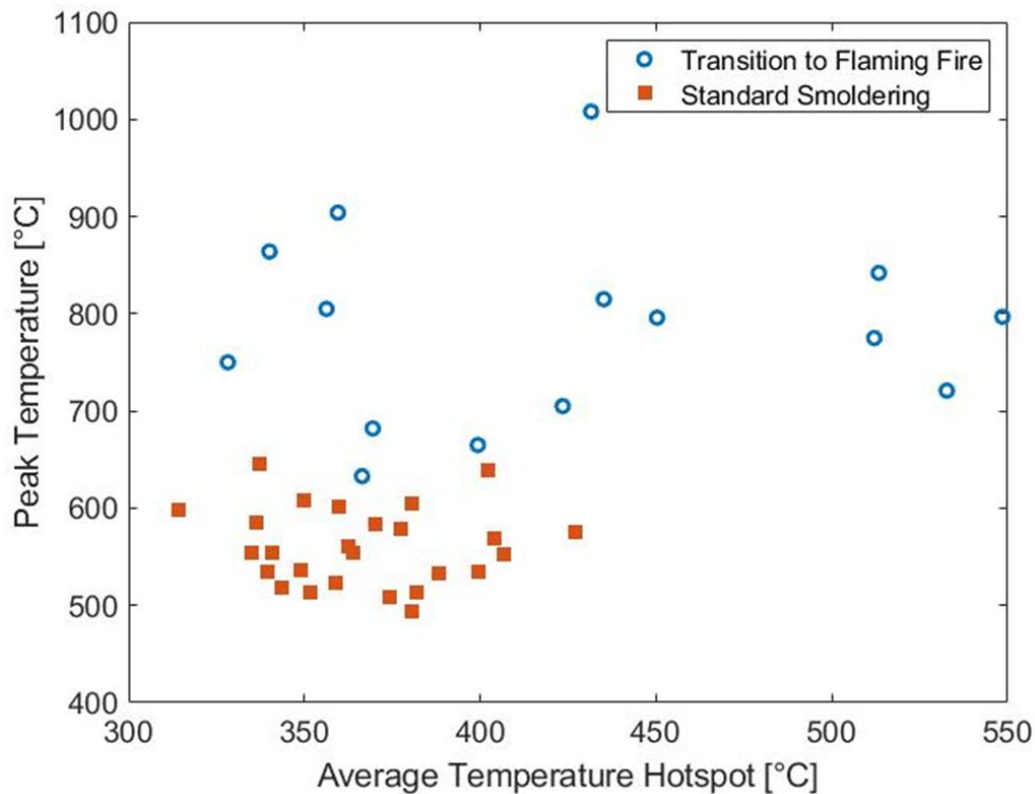


Figure 7.6: Standard smoldering and smoldering with transition to flaming fire hot spot temperature. The standard smoldering experiments are the experiments described in section 4.4. The transition to flaming fire are from the long-run experiments. Temperature of the hot spot in standard smoldering had a lower temperature peak and the points are group together. The peak temperature was between 500 and 600 °C. The temperatures for long-run experiments with transition to flaming fire showed a larger spread and a higher peak temperature.

7.4 Mass-loss rate during transition to flaming combustion

The maximum mass-loss rate during intense combustion was 6.2 g/min for standard smoldering. The long-run experiments with a transition to flaming combustion had a higher mass-loss rate, 8.4 – 14.7 g/min. To determine if a sample have transitioned from smoldering to flaming, the mass-loss rate may be used as an indicator because of the significantly higher mass-loss rate compared with smoldering fire. However, the mass-loss rate itself cannot predict transition to flaming alone. The combination of high temperatures above the sample and high mass-loss rate are indicators of a transition to flaming fire. The combination of high temperature and high mass-loss rate could be a way to validate a transition to flaming fire without visible observations. It is reasonable to assume, based on Figure 7.7, there is a correlation between the peak temperature and the maximum mass-loss rate. A temperature above 800 °C indicate a transition to flaming fire and mass-loss rate above 10 g/min.

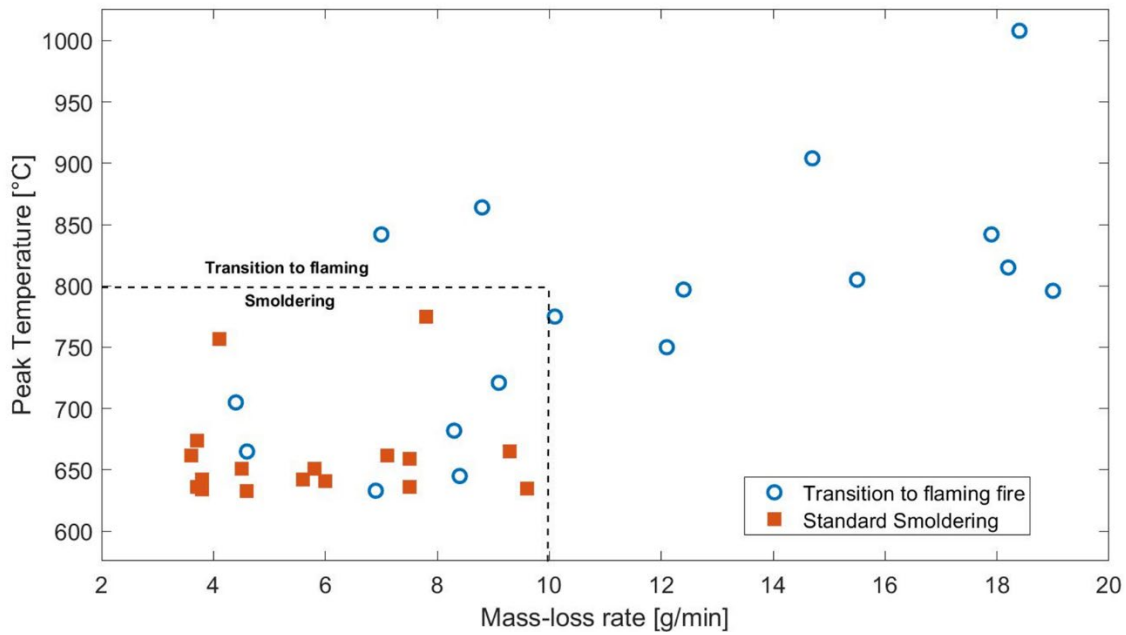


Figure 7.7: Mass-loss rate as a function of peak temperature. If the temperature is above 800 °C and the mass-loss rate is above 10 g/min it is reasonable to assume that there has been a transition from smoldering combustion to flaming combustion.

Similarities of the initial smoldering experiments and the long-run experiments are found, such as the hotspots and the rapid large mass loss. However, by refilling the same to its initial weight, one creates a condition inside the pipe that has a larger potential of transition to flaming fire. The charred pellets at the bottom of the pipe are the insulating layer which reduces heat loss to through the aluminum plate, causing a warmer center of the sample. The refill ensures fresh fuel and more combustible gases through the combustion process. The experiments without any refill showed a massive mass loss at the point when the smoldering combustion front has reached the surface of the fuel, all the sample temperatures had been over 200 degrees and a hot spot inside was established. Similar trends are found in the long-run experiments, expect due to the warmer hot core and more combustible gas, a transition to flaming fire was possible under the right conditions.

8. Discussion

Aspects of smoldering behavior in both wood pellets and oily pellets will be discussed in this chapter. Together with the effect of changes in external conditions on the smoldering process. In addition will the conditions needed for a transition from smoldering to flaming combustion be further discussed.

8.1 Onset of smoldering

The investigation of onset of smoldering in wood pellets shows the importance of ignition criterium duration of heating and sample size.

8.1.1 Cut-off temperature vs duration of heating

Onset of smoldering has been investigated (see section 4), with focus on temperature and duration of external heating. The cut-off temperature needed to obtain smoldering fires varied with sample height (6, 8, 10, and 12 cm) and wood pellet type (see Figure 4.6). The cut-off temperature for experiments in the low pipe increased with increasing sample height for pellet A, however an opposite trend was found for type B.

The criterion cut-off temperature resulted in a variation of external heating time. It was decided to investigate the duration of heating for the two pellet types. The result showed similarities between the two materials, as the sample height increased, the duration of external heating to achieve smoldering increased. Through a logistic regression analysis of the results, it was found that the duration of the heating and the cut-off temperature are both highly significant for the onset of smoldering in this experimental setup. As the heating period of the sample increased, the material became drier and the pyrolysis stronger and the likelihood of smoldering increased. The freshness of the fuel could impact the onset of smoldering. Pellet B had been stored for a longer time and could therefore be less reactive than pellet A. This resulted in longer duration of heating for Pellet B at lower cut-off temperatures, with a decreasing trend for cut-off temperature, as was observed for this pellet type. This confirms that the duration of external heating has the largest impact on the onset of smoldering combustion. As seen from the statistical analysis, as the sample height increased, the duration of heating increased, and the trend is similar for both pellet types. Pellets degradation have been discussed by Lehtikangas [41] and the storage effect on pellet reactivity Lönnemark et. al [57]. Pellet storage decreases the reactivity of the pellet and degrades the material. Similarly, Guo [58] showed the impact of aging on wood pellets and reactivity. Fresh pellets had higher heat-release rate than older pellets, this will impact the combustion and the hazards connected to the storage of pellets. Combining this previous research with the behavior of the current pellets show that, the focus on storage units and handling of materials needs to be increased.

8.1.2 Effect of prolonged external heating

With increased sample height, a longer duration of heating was necessary to initiate smoldering. The sample was heated from the bottom, the top layer acted as a heat sink, prolonging the heating time. As the heating duration increased, a larger part of the sample was dried, preheated and a larger part of the material was partially combusted. The effects of longer heating periods were confirmed by the residue after non-smoldering experiments, as described in section 4.2. The different layers of coloring shown in Figure 4.5 in section 4.2 show to what extent the heat affects the sample. Closest to the aluminum plate (at heights 0 - 2 cm), the pellet color was black. Analysis layer by layer showed black pellets closest to the heat source (aluminum plate), followed by a dark brown layer. Towards the top of the sample the color of the pellet was brighter, from brown to partially brown, and in the top layer pristine fuel (sample height 10 cm and 12 cm). This is consistent with the findings by Baileys and Blankenhorn [54]. Their analysis showed that wood changed color from beige/light brown to black when exposed to a temperature of 300 °C. A temperature of 250 °C, changed the color of wood to dark brown. A longer duration of external heating, increases the affected part of the pellets sample, ensuring a drier sample and a stronger pyrolysis, situated deeper inside the sample. The formation of a minimum depth of smoldering propagation and the temperature for self-sustained smoldering was influenced by the duration of external heating.

8.1.3 Minimum sample height

The present experiments show a correlation between the minimum sample height and ignition of smoldering combustion. There was observed a threshold for when the sample is too small for smoldering combustion. Lower samples (6 – 8 cm), had a volume to area ratio, which resulted in a larger heat loss relatively to the heat production from the smoldering front. A non-smoldering sample of 6 cm contained a residue completely affected by the external heating. This reflects the fact that the heat generated did not exceed the heat loss and thus self-sustained smoldering was not established [59]. However, the sample was still affected by the heating process. A sample height lower than 6 cm would most likely not smolder, due to the high free-surface-to-volume ratio. The heat loss would be greater than the heat generated. This indicated a sample height close to the layer for minimum thickness. Rosa et al. [32] studied the importance of the thickness of the charred layer for obtaining self-sustained smoldering combustion, see Figure 2.2. Palmer [21] and Rein [20], reported a minimum for the amount of fuel needed to obtain self-sustained smoldering combustion for both dust and polyurethane foam.

8.2 Mass loss during smoldering in a top-ventilated system

During all the experiments with wood pellets (without refill, section 4.4), the mass loss followed the same trend, independent of sample height. The most significant increase in mass-loss rate occurred when the three following conditions were present in the sample: the smoldering front had reached the top of the sample, temperatures were above 200 °C throughout the sample, and a hot core with temperatures exceeding 300 °C was located in the center/upper part of the sample. During this intense combustion, the temperature increased rapidly, and the mass-loss rate increased significantly. The rapid increase in mass loss started at the beginning of the intense combustion period, when the temperature was above 300 °C. The rapid mass loss ended as the temperature peaked around 490 – 650 °C. This is consistent with the findings of Baileys and Blankenhorn [54] who analyzed the evolution of carbonized wood, and found large mass loss in the temperature range from 200 °C to 400 °C, and with the largest mass loss occurring between 300 °C and 350 °C.

The smoldering front reaching the top of the fuel is one of the criteria for an intense combustion period. However, the physical change to the pellets affects the height of the sample during external heating and the low-intensity combustion. Visual observations of pellets during smoldering combustion continued a change in the material as the sample was heated, see Figure 4.17. The residue after both non-smoldering and smoldering experiments showed changed to the physical appearance of the pellets. In the current experiments the swelling was mainly observed in the top layer of the sample and could be caused by condensation of volatiles and moisture from the pyrolysis of the lower layers and shrinking of the pellets more affected by the heat development in the sample. Similarly Baileys and Blankenhorn [54] reported changes in physical appearance of wood. Shrinking of the material was found when wood was exposed to temperatures above 300 °C. The residue consisted of black charred pellets, with a smaller diameter than for the pristine fuel. Similar shrinking was also observed by Paulauskas et al. [60]. At lower temperatures, swelling of the pellets was also observed by Paulauskas.

The physical changes affect the sample height. Shrinking and swelling of the sample height was uneven because the smoldering process differed laterally, see Figure 4.18 (temperatures in the left column). There was therefore a variation in the sample height along the pipe wall. Early findings by Rein [20] show an elongated bell shape for the smoldering front, during reverse smoldering. This is consistent with the findings in this thesis, as the sample height vary laterally during combustion, see Figure 4.19, the height at middle of the sample decreased first, giving a temperature increased at the middle first, followed by left and right side. The shrinking of the sample is therefore important since it affects the time for the smoldering front to reach the surface of the sample.

As the smoldering front reached the surface of the sample, oxygen flowed more easily into the smoldering zone. This flow of oxygen increased the intensity of the combustion, causing higher

temperature and an increasing mass-loss rate. The smoldering direction changes from reverse smoldering (upwards in the pipe) to forward smoldering (downwards in the pipe) as the front reached the surface of the fuel. The change in the direction of the smoldering front causes the front to move through the sample again. Resulting in secondary char oxidation of the sample. Ohlemiller [61] stated that char oxidation rate increased with increasing air flow. An increased oxygen supply resulted in secondary charring intensified the combustion, causing a rapid increase in mass-loss rate.

The intense combustion period with high mass loss was a result of increased air supply to the upper layer. As the smoldering front reached the upper surface of the fuel, the smoldering fire intensified, and the temperatures increased rapidly resulting in a large mass loss. Similar observations were made by Krause and Schmidt [62, 63]. A glowing nest was used as an ignition source for smoldering in dust (cocoa, cork and beech). The glowing nest was inserted into the sample. A stable temperature was measured until the smoldering front reached the surface of the fuel. At this point, the mass-loss rate increased rapidly, and the front changed direction and burned back into the sample, through a secondary char oxidation. This correlates with the observations in the experiments with wood pellets, the intense combustion occurred through the char oxidation of the material, where the front shifted from reverse to forward smoldering.

Forward smoldering and secondary char oxidation will result in intense combustion with higher temperatures and mass-loss rate. Palmer [21] found a correlation between oxygen and smoldering direction in dusts. When oxygen flow and smoldering were in the opposite direction, the combustion rate was low. However, when smoldering and air flow had the same direction, the smoldering rate was higher. Similarly, in these wood pellets experiments, when the smoldering front reached the surface of the fuel, a char oxidation occurred in the opposite direction, shifting the process from reverse to forwards smoldering (Figure 5.4). The oxygen supply and combustion front have the same direction during the intense combustion period, increasing the combustion rate.

The mass loss showed a two-step trend: significant mass loss during external heating and the intense combustion period. In the initial phase with external heating mass was lost because of drying and pyrolysis. The STA/TGA analysis of the wood pellets showed a two-step mass loss, where the steps consisted of a release of volatiles and char oxidation, respectively. A similar trend has been observed for different biological materials such as cellulose [64], wood chips and sewage sludge [65]. Other materials show a three-step process or no steps at all, see by the review of smoldering combustion by Torero, Gerhard and Martins et al. [66]. Comparison of mass loss for different materials such as polyurethane foam, peat, and cotton with wood pellets show differences in the mass-loss behavior. Anderson et. al [67] found a three-step mass-loss rate for smoldering in polyurethane foam. The two first steps occurred during heating, the third step during self-sustained smoldering. For each of the three phases the mass-loss rate was increased. Huang et. al [68] found a correlation between heating

and mass-loss rate in peat. A peak in mass-loss rate occurred during heating, when the ignition source was removed, the mass-loss rate decreased. Hagen et. al [69] reported a steady decrease in mass with time for cotton. A period of intense smoldering combustion did not significantly increase the mass-loss rate. These findings indicate different behavior for different materials. Variations in chemical compositions could be the cause for the different behavior in mass loss. In addition, physical properties density and particle size differ. Wood pellets consists of larger particles, ensuring an easier access to air flow from the surroundings, as described in Villacorta et. al [18], while dust has smaller particles.

The mass lost during external heating of wood pellets for the different sample height (6, 8, 10, and 12 cm) could indicate which type of scenario that will occur in the experiment: smoldering or non-smoldering. The external heating had similar effect on the pellets for all experiments in terms of pyrolysis and drying of layers closest to the aluminum plate. The duration of the external heating was the critical factor. After the hotplate had been switched off, the mass loss continued until the temperatures had decreased sufficiently. The size of mass loss during heating was dependent on the duration of external heating, combined with cut-off temperature and external conditions of the lab. The longer the duration of heating, the more prone the wood pellets were to smolder. A longer duration of heating resulted in a drier sample, and a larger charred area, increasing the likelihood of smoldering combustion, as discussed previously in section 8.1.3. Furthermore, a minimum thickness of charred pellets was necessary to obtain self-sustained smoldering combustion. If the mass loss during the heating phase was below 200 g and external heating duration was less than 5 h no smoldering was observed. It is reasonable to assume that in the non-smoldering cases there was too much moisture left inside the sample and as a partial consequence, the heat loss was greater than the heat generated. Smoldering was observed when the external heating exceeded 5 h with mass loss higher than 250 g. When more mass was lost the sample was drier, and it could be assumed that the smoldering front had reached higher into the sample, ensuring a warmer core deeper inside the sample, which was less affected by the aluminum plate as a heat sink. The findings indicate importance of the volume fraction of dried and pyrolyzed material to obtain a self-sustained smoldering combustion. Mass loss behavior is therefore an important indicator of the different combustion phases in a smoldering fire in this top-ventilated system.

8.3 Air flow above sample and reduced opening of pipe

The impact of the restriction of airflow to the top of the top-ventilated system had an impact of the smoldering combustion. As the limitation of air supply down the pipe impacted the duration of heating to obtain self-sustained smoldering combustion. In addition, the behavior of the air flows shows a interesting phenomenon, as the warm core absorb the cold air from the surroundings to increase the smoldering combustion, while the warm smoke is pushed out through the colder parts of the pellet sample.

8.3.1 Air flow in the cross-section

In this top-ventilated system, it was initially assumed that cold air would enter the sample along the pipe wall and warm smoke would exit in the middle of the pipe, see section 6. The temperature of the air was used as an indication of warm and cold zones above the sample, corresponding to smoke exiting, and surrounding air entered the sample, respectively. The results showed cold surrounding air entering the middle of the pipe, while warm smoke exited along the pipe wall, opposite of the assumption, see Figure 6.4, and will be discussed below.

The smoldering process inside the sample and the air flow seems to be connected. The results showed cold surrounding air entering the warmest part of the sample, and warm smoke exiting through the cold part of the sample. Oxygen plays a crucial role in the intense combustion period, as discussed in section 8.2. Krause and Schmidt [63] showed an increase in combustion rate and temperature as the smoldering front reached the surface of the fuel. Similarly, for these experiments, as the front reached the surface of the fuel, oxygen supply increased, and an intense combustion period occurred. Leach et al [70] states that the heat generated during oxidation of the fuel is controlled by the oxygen supply to the sample. Moussa et al. [29] reported a correlation between the maximum temperature of the smoldering front and the ambient oxygen concentration in cellulose materials. All these previous observations are consistent with the current experiments, where the intense combustion occurred as the smoldering front reached the surface of the fuel, and the secondary char oxidation started. The temperatures increase rapidly during this oxidation. Smoldering combustion is an oxygen deprived process, and the smoldering intensity seems to be linked with the air available. One way to look at this is that the smoldering hot spots requires the air for the secondary char oxidation to occur in the sample. A hot spot consumes the inflowing cold air, the hot smoke is pushed outwards the colder side of the sample.

Velocity measurements could help determining the direction of the flow. However, initial measurements by hand-held anemometers did not give useful results. The velocity of the smoke from smoldering combustion was too low to be measured with this measurement techniques. Other options were considered, however, smoke from the wood pellets contains tar, which could condense and affect

the equipment. Hotwire probes were considered however, contamination of the equipment was a concern, as the hotwire probe should be free from contamination for accurate results. In addition, the high temperature of the smoke could damage part of the equipment. Another option was bi-directional probe that could record both velocity and the direction of the air flow. However, the diameter of the pipe itself is small, and to obtain a good understanding of the air movement, more than one probe would be necessary, and the size of the probes compared to the diameter of the pipe is large. The use of several probes could influence the air flow inside the pipe, thereby, disturbing the experiment. Bi-directional probes could be suitable for experimental set-up using pipes / silos with significant larger diameter than the pipe in the current experiments. Further work on air velocities is needed to understand air flow due to smoldering fire behavior.

8.3.2 Reduced pipe opening to pellets sample

The reduction of the pipe opening affected both wood pellets and oily pellets (see chapter 6). Samples of height 12 cm had a delayed intense combustion period as the coverage of the pipe increased. Easier access to air could result in a smoldering front propagating at higher velocities. This is consistent with the findings of Palmer [21], the smoldering rate for dust samples increased with an imposed air flow. Marlow and Krause [44] found that an increased volume fraction of oxygen increased the combustion rate. In addition, their results showed decreasing temperature, with decreasing oxygen supply. In these experiments, as the top of the steel pipe was covered the temperature of the intense combustion period decreased. The findings indicates that oxygen is a major controlling mechanism for smoldering combustion.

Reduced opening of the pipe increased the duration of external heating necessary to obtain self-sustained smoldering, especially for wood pellets, where the duration increased with each reduction in the pipe opening cover. Visual observations revealed condensation on the underside of the cover. The physical effect of water drops from the underside of the cover, dripping onto the wood pellets was observed in the non-smoldering experiments. During cleaning of the pipe, it was found that tar and water drops had created a hard shield in the top layer of the pellets residue, and it was difficult to remove the sample from the pipe. The hard shield could restrict the oxygen supply downwards the sample, causing the need of a stronger pyrolysis front, therefore increasing the duration of external heating necessary to establish self-sustained smoldering combustion. Koppejan et. al [27] reported similar findings, pellets glued together above the ignition source, caused by heat and moisture. The combustion products from wood pellets are char and ash, in addition to moisture and volatiles (gases and tar) [71]. Extinguishing smoldering fire in wood pellets have proven to be difficult. Water as an extinguishing agent is not suitable. Wood pellets in contact with water swell and break apart, in addition to forming a hard shield [27]. By covering part of the opening of the pipe, oxygen transport in

the pipe was reduced. At the same time water drops from condensation would hit wood pellets forming a hard shield, which also would affect oxygen transport. The reduced oxygen transport would reduce the temperature in the sample and delay the intense combustion period.

8.4 Transition from smoldering to flaming fire

Transition from smoldering to flaming combustion occur when the following conditions are present: oxygen supply, pyrolysis gases, and heat. These three conditions will be discussed in relation to the long-run experiments.

In the long-run experiments, the large number of refills and periods of semi-constant smoldering caused a build-up of char and black pellets in the lower parts of the pipe. The insulating char layer reduced heat loss through the aluminum plate and could be a factor for build-up of higher temperatures in the sample and increased production of combustible pyrolysis gases. A higher temperature in the sample increased the temperature of the smoke, as shown in the measurements of smoke and air flow above the sample in section 6. In these experiments, a combination of higher sample temperature and smoke temperature may have increased the likelihood of transition to flaming fire. Atreya [72] determined that a spontaneous ignition of the pyrolysis gases occurred when the temperatures was high enough to ensure a thermal runaway in the gas phase. Tse et. al [73] demonstrated a transition to flaming fire inside the char region in polyurethane foam. Starting with a high temperature of the hot spot within sample of 600 °C and localized temperatures up to 1200 °C indicating transition to flaming combustion in the long-run experiments.

Before an intense combustion period, there is a build-up of a hot spot in the pellet sample. The hot spots before transition to flaming fire (avg. 549 °C) show higher temperatures compared with the intense combustion period for smoldering (avg 418 °C). Hot spots with sufficient temperature is a criteria to obtain a transition to flaming fire. An average hot spot temperature above 450 °C increased the likelihood of transition. The hot spots are local, with increased production of flammable gases, similar findings were reported by Ohlemiller [61], who found higher temperatures than average in local areas of the char when a transition to flaming occurred.

A warmer hot spot result in higher temperatures for the pyrolysis gases, increasing the probability of transition to flaming fire. This is consistent with the findings of Kuo and Hsi [74], who showed that the temperature of an air stream can determine the time for flaming ignition, when igniting wooden spheres in a hot air stream.

It is difficult to determine the exact ignition position in this experimental setup from visual observations. However, glowing particles have been observed, for both semi-constant smoldering and smoldering with transition to flaming, which indicates that there is a need for warmer pyrolysis gases

in addition to the glowing particles to have a transition to flaming fire. However, it is reasonable to assume that the transition to flaming occur when there is char oxidation at the top of the sample as the transition to flaming combustion also needs a sufficient air supply for the flaming combustion. This is supported by the findings of Tse et al. [73], who found a transition from smoldering to flaming fires in polyurethane foam, governed by the flow of volatiles and oxidizer to the char region. A transition to flaming fire occurred in the gas-phase of the char after the smoldering reaction, and not through an increase in smoldering velocity. For polyurethane foam, Putzeys et al. [75] found that a transition to flaming combustion occurred behind the pyrolysis front, in the char. Char oxidation affects the transition to flaming fire. Large pores, sufficient fuel and heat promote a gas-phase reaction. Hagen et al [33] also found a correlation between smoldering and the char oxidation of cotton to obtain a transition to flaming combustion.

The long-run experiments display several intense combustion periods, where char oxidation and smoldering combustion must occur simultaneously. It is reasonable to assume that in the freshly added fuel, pyrolysis occurred together with, drying of the material and the beginning burning process. Pellets in lower parts of the sample, on the other hand endured char oxidation. This could cause a build-up of char oxidation zone, which meets the pyrolysis process of the fuel. Combined with an increase in oxygen supply, a transition from smoldering to flaming combustion could occur in the long-run experiments. The mixture of charred pellets and fresh pellets added to the top of the sample could enhance the creation of cavities in the charred pellets, with the intense combustion causing regions with larger amount of pyrolysis gases. Ohlemiller [76] found that cavities in the material could causes local areas with enough flammable gases and high enough temperature for transition to flaming fire.

A higher temperature, with increased production of pyrolysis gases, combined with supply of fresh material, contributed to a transition to flaming fire. However, the area for a transition is limited [35]. The different conditions need to be present simultaneously. A transition to smoldering fire could be triggered by a sudden increase in oxygen supply. Therefore, the location of the smoldering front could affect the transition to flaming fire. An intense combustion period occurred as the front reached the surface of the fuel, as previously described in section 4.4. Similar assumptions are reasonable for these long-run experiments. A large refill with fresh material at the start of a rapid temperature increase (see Figure 7.1B, approximately at 80 h) caused the sample to cool and stop the process. The oxygen supply was reduced by the added fresh fuel, and therefore the condition needed for an intense combustion was no longer present in the pipe. The smoldering front reaching the surface of the fuel is crucial for the intense combustion period, it is at this point the oxygen supply to the secondary char oxidation is sufficient to intensify the combustion process. If the amount of pyrolysis gases is sufficient when the front reaches the surface of the fuel, and the char combustion has sufficient

temperature, transition from smoldering to flaming can occur. Krause and Schmidt [77] also found that a transition to flaming fire could occur when the reaction front had reached the surface of the fuel.

Refill of the sample to its initial mass without removing the charred material in the lower layers of the sample, lead to an increase in sample height. The height of the sample could affect the possibility of transition. The significant duration of these experiments leads to an increasing insulating layer of char and a hot spot located higher in the sample. It is likely that the heat loss from the hot spot is reduced, as the insulating layer increases, which ensures a higher temperature of the hot spot. In the experiments without refill there was no transition to flaming fires, this could be connected to the height of the sample. Similar to the minimum sample height for onset of smoldering, there could also be a limitation on the sample size for transition to flaming fire. Initial sample heights above 14 cm has proven to be difficult for obtaining smoldering combustion with intense periods in the long-run experiments. However, for an initial sample height, 14 cm or lower, with systematic refill, starting 6 h after starting external heating, the material in the pipe is drier and more prone to smolder when the refills start and is not as affected by the refills as higher samples. The sample height slowly increased for a longer experiment duration, this slowly increased the char layer and decreasing the heat loss from the hot spot. The results was an increased probability of transition to flaming fire. Chang et.al [78] also found a correlation with the size of the sample. In the experiments with polyurethane, the width of the sample and transition from smoldering to flaming fire were correlated. A sufficiently wide sample was necessary to obtain a transition to flaming fire. Similar relations were found by Hagen et. al [33] on the density of cotton sample and the transition to flaming, a higher density resulted in flaming fire. In addition, increasing the cotton sample height increased the possibility for transition to flaming fire. Both a more compact sample combined with a higher sample could result in a larger hot spot inside the sample, which was needed for the transition to flaming combustion.

The sample height is essential in the analysis of the transition from smoldering to flaming fire and was also used to determine if the smoldering front had reached the surface of the fuel at the intense combustion period. When smoldering fire transitioned to flaming fire, the flames were located above the sample. An estimation of sample height was of importance to determine the locations of measurement points with temperatures above 700 °C. The sample height was estimated from the temperature curve and standard deviation (see section 4.4.3). The method used noise as an indicator of a thermocouple being located inside the sample, or freely. This method also included the possible variation in sample height laterally.

In the wood pellet experiments, an intense combustion lead to an increased mass-loss rate, even higher mass-loss rates were found in experiments with a transition to flaming fire, 8.4 – 14.7 g/min. The mass-loss rate was one of the criteria used to determine if transition from smoldering to flaming combustion had occurred for cases where direct observations were not made. The increase in mass-

loss rate is a result of the radiation from the flaming fire to the top of the fuel surface. The duration of the flaming fire is short, around 30 min, and the radiation from the flame will contribute to a higher mass-loss rate compared with the intense period during smoldering combustion. A correlation between mass-loss rate and transition to flaming fire was also found in cotton in the work by Hagen et al. [33]. However, the mass-loss rate alone cannot establish that a transition to flaming fire had occurred, the temperature above the sample also needs to be in the temperature range of flaming fire.

A refill close to the intense combustion cooled the sample could therefore affect the production of pyrolysis gases, which could influence the possible transition to flaming fire. A pretreated refill, where the pellets were heated for 15 min before added, resulted in easier transition to flaming fire. Pretreated fuel did not cool the sample to the same extent as room-temperature fuel, the hot spots stayed intact, and generation of heat was not disturbed. In the preheated fuel, moisture had evaporated, and the material was more prone to pyrolysis. During production of pellets, the pellets are heated, and warm pellets are then added into the silo storage unit. Warm pellets could lead to flaming fire with catastrophic consequences. Even though it is difficult to rescale the small-scale experiments described above to real life, the adding of warm/dry fuel could have severe consequences for an industry.

8.5 Wood pellets and oily pellets

The fundamental behavior of biomass pellets under external conditions that replicate actual storage conditions have been investigated in this thesis (see chapter 5). The increased demand for biomass fuel has led to development of biomass products other than wood. The two pellet types tested here, wood and oily, differ during smoldering combustion. Material differences found for wood and oily pellets, may have large consequences, and knowledge about material differences should be incorporated into routines for the handling and storage of pelletized materials. Reduced pipe opening increased the external heating time necessary to obtain self-sustained smoldering for wood pellets. Oily pellets on the other hand, did not experience any increase in the necessary external heating until the opening was reduced to 25 %. This indicated that less energy is needed to obtain a smoldering fire in oily pellets.

Smoldering fires in different pelletized materials have shown difference in combustion behavior. Knowledge about different biomass materials have been a concern, there is not enough information on the behavior and consequences of an unwanted event for different biomass materials. Simpson et. al [38] raised concern for smaller private consumers of biomass products. Not only large consumers need increased knowledge and experience transfer. Hedlund et.al [1] questions the transparency from accidents, how to learn from the different incidents. This research shows how small changes to the external conditions can change the smoldering process. To avoid fatal accidents, the basic knowledge of the smoldering combustion is important.

Both wood pellets and oily pellets are biomass materials, produced to replace fossil fuels as energy sources and reduce pollution from greenhouse gases. In addition, pellets from sunflower production reduces waste. Both types of pellets are used for the heating of public or domestic buildings, and the demand for such products is increasing [1, 4-6, 79]. Their physical properties are similar, and there are only slight differences in the calorific values (Table 3.1 and Table 3.2) of the two material used in these experiments. Both types of pellets are stored and handled in the same way, and there are hazards in connection with these handling processes. Compared with wood pellets, oily pellets are a naturally oil-rich material. The impact of oil could affect the smoldering combustion, but also the behavior of the pellet itself. Martinka et. al [80] investigated the influence of heat treatment of spruce wood, and found an increase in residue. One of the reasons for the increased residue in the treated material was the build-up of a charred layer on the surface of the fuel. This surface layer slowed down the heating of the wood. Preliminary experiments with single wood and oily pellets where pellets were placed directly on a hotplate, showed a difference in combustion behavior [81]. Oily pellets increased in temperature more rapidly than the wood pellet, and the whole pellet endured glowing combustion. For the wood pellet on the other hand, the glowing combustion occurred inside the pellet, while the outer layer was observed to consist of ash/charred material, consistent with the findings of Martinka et. al [80]. Thus, the smoldering combustion process differ for the two materials. Martinka et al. [82] found a higher peak heat-release rate for sunflower seed pellets compared with solid wood. This could be the reason for the longer duration of intense combustion for oily pellets compared with wood pellets observed for the current experiments.

To further compare equalize the two types of pellet, it was discussed to add oil to wood pellets. The impact of oil could affect the burning of the pellet, however, previous research has demonstrated some negative effects of oil usage in wood pellets. Mišljenović et. al [5] produced wood pellets where the wood was blended with vegetable oil before pressed into a cylindrical pellet form. For the pellet, the oil had a negative effect, the binding abilities was poorer when the material contained oil, and the surface of the pellet had a more porous structure, lacking the smooth surface of a regular wood pellet. The introduction of vegetable oil led to a less compressible material and reduced the strength of the pellet. Ståhl et al. [79] mixed rapeseed cake with sawdust to produce wood pellets. They also found undesirable changes to the pellets. On the other hand, a producer of pellets have saturated the pellets with oil, this reduced the dust created by the pellet during transport and handling [83]. This reduces the hazards during transport and handling, but the effect on combustion is unclear and should be further studied.

The development of new biomass products is fast, and biomass materials will replace fossil fuels within a short period of time. To be able to exploit this resource it is important to understand the material properties for the different biomass materials, such as seen for the wood and oily pellets. Small differences in material properties can have large impact. Smoldering combustion of biomass

materials are affected by storage and how new materials (pellets) are introduced to the storage, oxygen supply and heating of the materials. The current work has shown how detailed understanding of material properties for different materials is important to avoid smoldering and other hazards related to storage of biomass materials.

9. Conclusion

The onset of smoldering combustion in this top-ventilated system is dependent on the duration of heating. A large enough portion of the sample needs to be heated to a sufficient high temperature for self-sustained smoldering combustion to occur.

In an otherwise chaotic event in terms of temperature development, the mass loss follows a distinct trend, independent of the sample height. The mass loss at the initial phase of these experiments could indicate the probability of a self-sustained smoldering combustion. Furthermore, for an ongoing smoldering process may be an indication of a transition to flaming fire. A large mass-loss rate can indicate a strong intense combustion process, while a slow combustion would be reflected in a low mass-loss rate. By combining temperature and mass loss measurements one could increase the understanding of the smoldering phenomena, and how the mechanisms are controlled.

In this thesis, it has been investigated how different external conditions affect the smoldering processes. Experiments on the air flow inside the top-ventilated pipe resulted in unexpected results. The surrounding air enters the sample in the middle and to one side and enters the sample in the region of the hottest part of the sample. The smoke from the intense combustion is forced to exit on the opposite side, close to the pipe wall. When the pipe is covered, sample temperatures are lower, and the conditions mimics those inside a silo, where oxygen supply is limited. Reducing the opening of the pipe even more would decrease the smoldering temperature, and at one point the air supply would be insufficient to sustain smoldering combustion. The reduction of the air supply affects the two fuel types differently. The oily pellets endure a lower temperature during the slow smoldering combustion phase. Since these two materials are stored in similar silos, it is necessary to be aware of the difference in behavior and monitor of the temperatures.

After transition to flaming fire there are intense combustion and high temperatures in the sample. The refill of fresh fuel into a storage unit could be crucial if there is a smoldering combustion lower in the sample. The warm fuel added could contribute to an increased amount of combustible gases, sufficient heat and oxygen, triggering a transition to flaming fire.

Handling and storage of biomass material are similar, however, findings in this thesis indicate that each biomass material should have specific regulations during storage. Critical conditions change, and control systems should be adjusted to the specific material stored to avoid accidents. Overall, mass loss could be an indicator of smoldering combustion. Further analysis of the mass loss, and impact of mass-loss rate should be carried out for several biomass materials.

10. Further work

Smoldering fires are controlled by several mechanisms. Some of these are investigated in this thesis. However, more research is needed to understand the smoldering combustion phenomena to the full. Below are some further research ideas.

The velocity of the air flow above the sample, including the direction of the flow, is of interest for the understanding of the smoldering phenomena. Due to the small diameter of the pipe, a larger scale setup to avoid probes to cause disruption to the natural flow of smoke and air should be considered. Several biomass materials should be studied, to see if there are similarities in the air flow pattern, or if the different smoldering types are also reflected in the air flow.

Smoldering experiments with wood pellets infused with oil could be a next step. The pellets could be made directly, ensuring oil distributed throughout the material before pressed into a cylindrical shape. By doing so one could determine the influence of oil on smoldering combustion in biomass materials.

A further analysis of the coverage of the pipe could indicate when the pipe opening is too narrow for the sample to sustain self-sustained smoldering combustion. One possibility could be to reduce the opening of the pipe further to only 5 % of original opening. Another approach to coverage is a plate with small holes evenly distributed instead of forcing the air flow through the center of the sample.

The effect of the pipe opening could be tested by reducing the adding the cover to the pipe after external heating, where the steel plate with cut-out is placed on the pipe after an external heating of 6.5 h. Another approach is to increase remove the cover of the pipe when the intense combustion occurs. The question is then if the sample would be warm enough that the fresh oxygen would trigger a transition to flaming fire, or if the result would merely be higher temperatures and higher combustion rates in the smoldering zone. An increase in pipe opening would result when opening of silo during extinguishment of a smoldering fire.

The long-run experiments show interesting preliminary results. Transition to flaming combustion has occurred in the long-run experiments, and the effects of hot spots should be investigated further, as the hot spots could be indicators of the likelihood of a transition to flaming fire. Experiments where the sample is refilled with preheated pellets should be carried out and repeated to see if it is possible to obtain more than one transition to flaming fire. Preheated pellets are like fresh pellets and if the highly active pellets that could contribute to a transition to flaming fires. In the large picture, this could reduce the hazards during storage of biomass materials.

11. Bibliography

- [1] F. H. Hedlund and J. Astad, "Safety-A neglected issue when introducing solid biomass fuel in thermal power plants? Some evidence of an emerging risk," *Intelligent systems and decision making for risk analysis and crisis response*, pp. 263-68, 2013.
- [2] L. Shang *et al.*, "Lab and bench-scale pelletization of torrefied wood chips—process optimization and pellet quality," *BioEnergy Research*, vol. 7, no. 1, pp. 87-94, 2014.
- [3] F. Yazdanpanah *et al.*, "Permeability of wood pellets in the presence of fines," *Bioresource technology*, vol. 101, no. 14, pp. 5565-5570, 2010.
- [4] U. Svedberg, J. Samuelsson, and S. Melin, "Hazardous off-gassing of carbon monoxide and oxygen depletion during ocean transportation of wood pellets," *Annals of occupational hygiene*, vol. 52, no. 4, pp. 259-266, 2008.
- [5] N. Mišljenović, J. Mosbye, R. B. Schüller, O.-I. Lekang, and C. Salas-Bringas, "Physical quality and surface hydration properties of wood based pellets blended with waste vegetable oil," *Fuel Processing Technology*, vol. 134, pp. 214-222, 2015.
- [6] P. Pradhan, S. M. Mahajani, and A. Arora, "Production and utilization of fuel pellets from biomass: A review," *Fuel Processing Technology*, vol. 181, pp. 215-232, 2018.
- [7] P. Pradhan, A. Arora, and S. M. Mahajani, "Pilot scale evaluation of fuel pellets production from garden waste biomass," *Energy for Sustainable Development*, vol. 43, pp. 1-14, 2018.
- [8] U. S. E. I. Administration. U.S Energy Information Administration.
<https://www.eia.gov/energyexplained/biomass/> (accessed 29.04, 2020).
- [9] R. Saidur, E. Abdelaziz, A. Demirbas, M. Hossain, and S. Mekhilef, "A review on biomass as a fuel for boilers," *Renewable and sustainable energy reviews*, vol. 15, no. 5, pp. 2262-2289, 2011.
- [10] W. Stelte, J. K. Holm, A. R. Sanadi, S. Barsberg, J. Ahrenfeldt, and U. B. Henriksen, "A study of bonding and failure mechanisms in fuel pellets from different biomass resources," *Biomass and bioenergy*, vol. 35, no. 2, pp. 910-918, 2011.
- [11] W. Stelte, "Guideline: storage and handling of wood pellets," *Danish Technological institute, Denmark*, 2012.
- [12] P. Janzé. "Biomass storage pile basics." <http://www.advancedbiomass.com/2011/11/biomass-storage-pile-basics/> (accessed).
- [13] G. Rein, "Smouldering Combustion Phenomena in Science and Technology," *International Review of Chemical Engineering*, vol. 1, pp. 3-18, 2009.
- [14] D. Drysdale, *An Introduction to Fire Dynamics*. Wiley, 2011.
- [15] G. Rein and C. Belcher, "Smouldering fires and natural fuels," *Fire phenomena and the Earth system: an interdisciplinary guide to fire science*, no. 1984, pp. 15-33, 2013.
- [16] U. Krause, *Fires in Silos: Hazards, Prevention, and Fire Fighting*. Wiley, 2009.
- [17] F. H. Hedlund and J. Nichols, "Fighting pellet silo fires," *Pellet Mill Magazine*, vol. 8, no. 1, p. 9, 2018.
- [18] E. Villacorta *et al.*, "Onset of smoldering fires in storage silos: Susceptibility to design, scenario, and material parameters," *Fuel*, vol. 284, p. 118964, 2021/01/15/ 2021, doi: <https://doi.org/10.1016/j.fuel.2020.118964>.
- [19] R. F. Mikalsen, "Fighting flameless fires: initiating and extinguishing self-sustained smoldering fires in wood pellets," 2018.
- [20] G. Rein, "Smoldering Combustion," in *SFPE Handbook of Fire Protection Engineering*, M. J. Hurley Ed., 5 ed. New York: Springer, 2016, pp. 581-603.
- [21] K. Palmer, "Smouldering combustion in dusts and fibrous materials," *Combustion and Flame*, vol. 1, no. 2, pp. 129-154, 1957.
- [22] J. F. Griffiths and J. A. Barnard, *Flame and combustion*. CRC Press, 1995.
- [23] T. J. Ohlemiller, "Modeling of smoldering combustion propagation," *Progress in Energy and Combustion Science*, vol. 11, no. 4, pp. 277-310, 1985/01/01/ 1985, doi: [https://doi.org/10.1016/0360-1285\(85\)90004-8](https://doi.org/10.1016/0360-1285(85)90004-8).
- [24] J. F. Griffiths and J. A. Barnard, *Flame and Combustion, 3rd Edition*. Taylor & Francis, 1995.
- [25] V. Babrauskas, *Smoldering fires*. New York: Fire Science Publishers, 2021.

- [26] T. G. Prather, "Silo Fires: Prevention and Control Conventional and Sealed Silos," 1988.
- [27] J. Koppejan *et al.*, "Health and safety aspects of solid biomass storage, transportation and feeding," *IEA Bioenergy*, vol. 1, pp. 3-23, 2013.
- [28] N. Moussa, T. Toong, and C. Garris, "Mechanism of smoldering of cellulosic materials," in *Symposium (International) on Combustion*, 1977, vol. 16, no. 1: Elsevier, pp. 1447-1457.
- [29] N. A. Moussa, T. Y. Toong, and C. A. Garris, "Mechanism of smoldering of cellulosic materials," *Symposium (International) on Combustion*, vol. 16, no. 1, pp. 1447-1457, 1977/01/01/ 1977, doi: [https://doi.org/10.1016/S0082-0784\(77\)80427-X](https://doi.org/10.1016/S0082-0784(77)80427-X).
- [30] V. Babrauskas, "Ignition handbook: principles and applications to fire safety engineering, fire investigation, risk management and forensic science," 2003.
- [31] J. Torero, A. Fernandez-Pello, and M. Kitano, "Opposed forced flow smoldering of polyurethane foam," *Combustion Science and Technology*, vol. 91, no. 1-3, pp. 95-117, 1993.
- [32] A. Rosa, A. W. Hammad, E. Qualharini, E. Vazquez, and A. Haddad, "Smoldering fire propagation in corn grain: an experimental study," *Results in Engineering*, p. 100151, 2020.
- [33] B. C. Hagen, V. Frette, G. Kleppe, and B. J. Arntzen, "Transition from smoldering to flaming fire in short cotton samples with asymmetrical boundary conditions," *Fire Safety Journal*, vol. 71, pp. 69-78, 2015.
- [34] O. M. Putzeys, A. C. Fernandez-Pello, G. Rein, and D. L. Urban, "The piloted transition to flaming in smoldering fire retarded and non-fire retarded polyurethane foam," *Fire and Materials: An International Journal*, vol. 32, no. 8, pp. 485-499, 2008.
- [35] V. Babrauskas, "Engineering guidance for smoldering fires (Unpublished report)," 2016.
- [36] B. C. Hagen and A. K. Meyer, "From smoldering to flaming fire: Different modes of transition," *Fire Safety Journal*, vol. 121, p. 103292, 2021.
- [37] J. Heinimö and M. Junginger, "Production and trading of biomass for energy—an overview of the global status," *Biomass and Bioenergy*, vol. 33, no. 9, pp. 1310-1320, 2009.
- [38] A. T. Simpson, M. A. Hemingway, and C. Seymour, "Dangerous (toxic) atmospheres in UK wood pellet and wood chip fuel storage," *Journal of occupational and environmental hygiene*, vol. 13, no. 9, pp. 699-707, 2016.
- [39] A. Pa and X. T. Bi, "Modeling of off-gas emissions from wood pellets during marine transportation," *Annals of occupational hygiene*, vol. 54, no. 7, pp. 833-841, 2010.
- [40] U. R. Svedberg, H.-E. Högberg, J. Högberg, and B. Galle, "Emission of hexanal and carbon monoxide from storage of wood pellets, a potential occupational and domestic health hazard," *Annals of Occupational Hygiene*, vol. 48, no. 4, pp. 339-349, 2004.
- [41] P. Lehtikangas, "Storage effects on pelletised sawdust, logging residues and bark," *Biomass and Bioenergy*, vol. 19, no. 5, pp. 287-293, 2000.
- [42] R. Hadden, A. Alkatib, G. Rein, and J. L. Torero, "Radiant ignition of polyurethane foam: the effect of sample size," *Fire Technology*, vol. 50, no. 3, pp. 673-691, 2014.
- [43] B. C. Hagen, V. Frette, G. Kleppe, and B. J. Arntzen, "Onset of smoldering in cotton: Effects of density," *Fire Safety Journal*, vol. 46, no. 3, pp. 73-80, 2011.
- [44] M. Malow and U. Krause, "Smoldering combustion of solid bulk materials at different volume fractions of oxygen in the surrounding gas," *Fire Safety Science*, vol. 9, pp. 303-314, 2008.
- [45] D. Botnen, "Hallingdal trepellets 5. juli 2010 (in Norwegian)[Hallingdal wood pellets]," *Hallingdal Fire Service, Torpomoen, Norway*, nd.
- [46] R. K. Eckhoff, *Dust Explosions in the Process Industries: Identification, Assessment and Control of Dust Hazards*. Elsevier Science, 2003.
- [47] P. Russo, A. De Rosa, and M. Mazzaro, "Silo explosion from smoldering combustion: A case study," *The Canadian Journal of Chemical Engineering*, vol. 95, no. 9, pp. 1721-1729, 2017.
- [48] R. A. Ogle, S. E. Dillon, and M. Fecke, "Explosion from a smoldering silo fire," *Process Safety Progress*, vol. 33, no. 1, pp. 94-103, 2014.
- [49] *Biofuel Cylindrical pellets of pure wood Classification and requirements*, S. Norge, 1999.
- [50] *SS 18 71 20:1998 Biofuels and peat - Fuel pellets*, S. S. Institute, 1998.
- [51] D. Madsen *et al.*, "Emerging risks in smoldering fires: initial results from the EMRIS project," in *Conference proceedings*, 2016, vol. 2, pp. 1346-1356.
- [52] F. Rogers and T. Ohlemiller, "Smolder characteristics of flexible polyurethane foams," *Journal of Fire and Flammability*, vol. 11, no. 1, pp. 32-44, 1980.

- [53] R. E. Walpole, R. H. Myers, S. Myers, and K. Ye, "Probability and Statistics for Engineers and Scientists , 9th," ed: Pearson, January, 2011.
- [54] R. T. Baileys and P. R. Blankenhorn, "Calorific and porosity development in carbonized wood," *Wood Science*, vol. 15, no. 1, pp. 19-28, 1982.
- [55] A. Savitzky and M. J. Golay, "Smoothing and differentiation of data by simplified least squares procedures," *Analytical chemistry*, vol. 36, no. 8, pp. 1627-1639, 1964.
- [56] R. W. Schafer, "What is a Savitzky-Golay filter? [lecture notes]," *IEEE Signal processing magazine*, vol. 28, no. 4, pp. 111-117, 2011.
- [57] A. Lönnermark, P. Blomqvist, H. Persson, and M. Rahm, "Use of small scale methods for assessments of risk for self-heating of biomass pellets," ed, 2012.
- [58] W. Guo, "Self-heating and spontaneous combustion of wood pellets during storage," University of British Columbia, 2013.
- [59] B. F. Gray, "Spontaneous combustion and self-heating," in *SFPE handbook of fire protection engineering*: Springer, 2016, pp. 604-632.
- [60] R. Paulauskas, A. Džiugys, and N. Striūgas, "Experimental investigation of wood pellet swelling and shrinking during pyrolysis," *Fuel*, vol. 142, pp. 145-151, 2015.
- [61] T. Ohlemiller, "Smoldering combustion propagation on solid wood," *Fire Safety Science*, vol. 3, pp. 565-574, 1991.
- [62] U. Krause and M. Schmid, "Initiation of smouldering fires in combustible bulk materials by glowing nests and embedded hot bodies," *Journal of loss prevention in the process industries*, vol. 10, no. 4, pp. 237-242, 1997.
- [63] U. Krause and M. Schmidt, "Propagation of smouldering in dust deposits caused by glowing nests or embedded hot bodies," *Journal of Loss Prevention in the Process industries*, vol. 13, no. 3-5, pp. 319-326, 2000.
- [64] T. J. Ohlemiller, "Smoldering combustion propagation through a permeable horizontal fuel layer," *Combustion and Flame*, vol. 81, no. 3-4, pp. 341-353, 1990.
- [65] N. F. Anez, J. G. Torrent, L. M. Pejic, and C. G. Olmedo, "Detection of incipient self-ignition process in solid fuels through gas emissions methodology," *Journal of Loss Prevention in the Process Industries*, vol. 36, pp. 343-351, 2015.
- [66] J. L. Torero, J. I. Gerhard, M. F. Martins, M. A. Zanoni, T. L. Rashwan, and J. K. Brown, "Processes defining smouldering combustion: Integrated review and synthesis," *Progress in Energy and Combustion Science*, vol. 81, p. 100869, 2020.
- [67] M. K. Anderson, R. T. Sleight, and J. L. Torero, "Downward smolder of polyurethane foam: ignition signatures," *Fire Safety Journal*, vol. 35, no. 2, pp. 131-147, 2000.
- [68] X. Huang, G. Rein, and H. Chen, "Computational smoldering combustion: predicting the roles of moisture and inert contents in peat wildfires," *Proceedings of the Combustion Institute*, vol. 35, no. 3, pp. 2673-2681, 2015.
- [69] B. C. Hagen, V. Frette, G. Kleppe, and B. J. Arntzen, "Effects of heat flux scenarios on smoldering in cotton," *Fire safety journal*, vol. 61, pp. 144-159, 2013.
- [70] S. Leach, J. Ellzey, and O. Ezekoye, "A numerical study of reverse smoldering," *Combustion science and technology*, vol. 130, no. 1-6, pp. 247-267, 1997.
- [71] K. Ragland, D. Aerts, and A. Baker, "Properties of wood for combustion analysis," *Bioresource technology*, vol. 37, no. 2, pp. 161-168, 1991.
- [72] A. Atreya, "Ignition of fires," *Philosophical Transactions of the Royal Society of London. Series A: Mathematical, Physical and Engineering Sciences*, vol. 356, no. 1748, pp. 2787-2813, 1998.
- [73] S. D. Tse, A. Carlo, F. Nde-Pello, and K. Miyasaka, "Controlling mechanisms in the transition from smoldering to flaming of flexible polyurethane foam," *Symposium (International) on Combustion*, vol. 26, no. 1, pp. 1505-1513, 1996/01/01/ 1996, doi: [https://doi.org/10.1016/S0082-0784\(96\)80372-9](https://doi.org/10.1016/S0082-0784(96)80372-9).
- [74] J. T. Kuo and C.-L. Hsi, "Pyrolysis and ignition of single wooden spheres heated in high-temperature streams of air," *Combustion and Flame*, vol. 142, no. 4, pp. 401-412, 2005.
- [75] O. Putzeys, A. Bar-Ilan, G. Rein, A. C. Fernandez-Pello, and D. L. Urban, "The role of secondary char oxidation in the transition from smoldering to flaming," *Proceedings of the Combustion Institute*, vol. 31, no. 2, pp. 2669-2676, 2007.

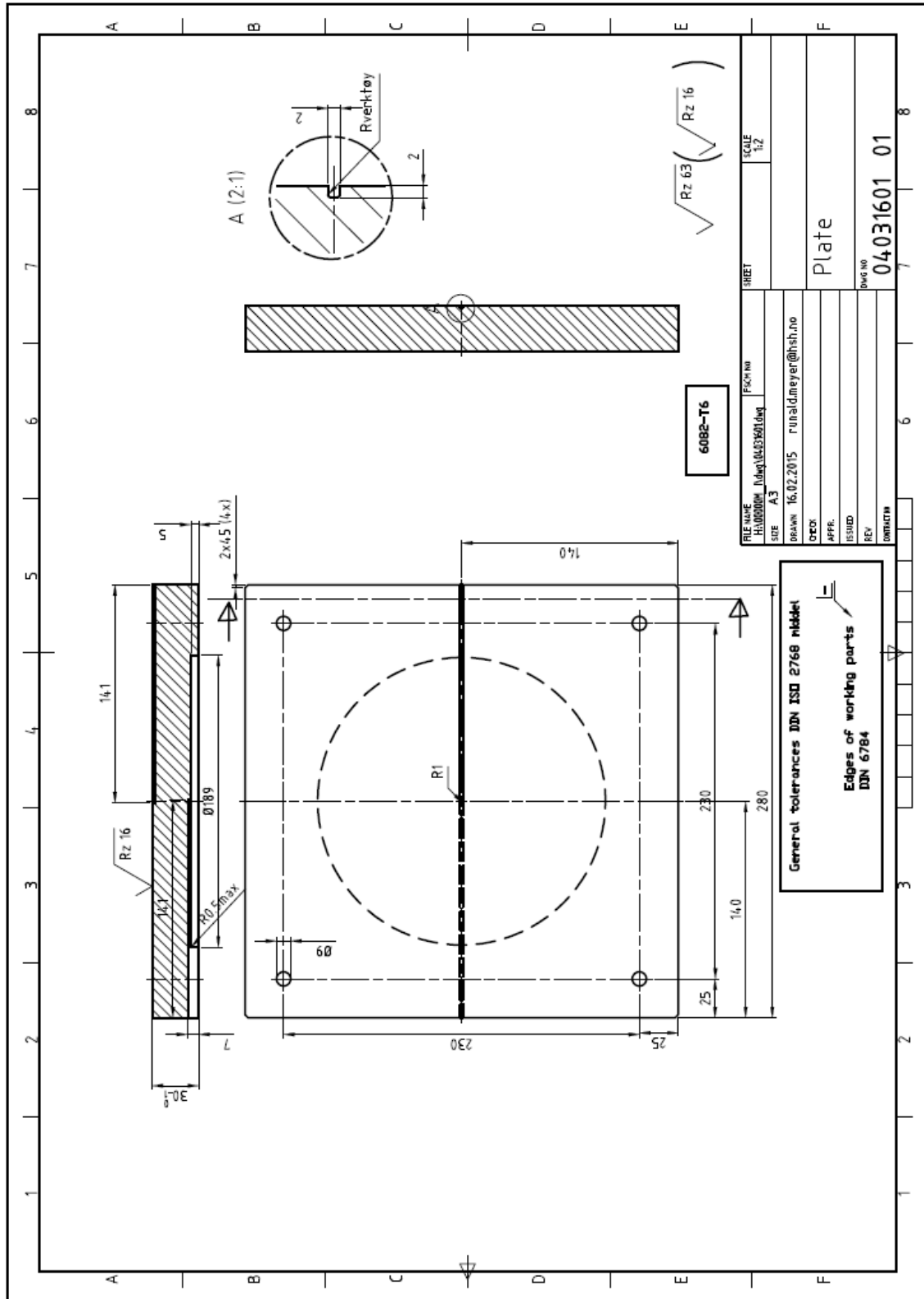
- [76] T. J. Ohlemiller, "Forced smolder propagation and the transition to flaming in cellulosic insulation," *Combustion and Flame*, vol. 81, no. 3-4, pp. 354-365, 1990.
- [77] U. Krause and M. Schmidt, "The influence of initial conditions on the propagation of smoldering fires in dust accumulations," *Journal of Loss Prevention in the Process Industries*, vol. 14, no. 6, pp. 527-532, 2001.
- [78] L. Chang, M. Die, P. Rongkun, P. Bei, and Y. Minggao, "The effect of sample size on smoldering and the transition to flaming combustion," in *2011 Third International Conference on Measuring Technology and Mechatronics Automation*, 2011, vol. 3: IEEE, pp. 793-797.
- [79] M. Ståhl and J. Berghel, "Energy efficient pilot-scale production of wood fuel pellets made from a raw material mix including sawdust and rapeseed cake," *Biomass and Bioenergy*, vol. 35, no. 12, pp. 4849-4854, 2011.
- [80] J. Martinka, E. Hroncová, T. Chrebet, and K. Balog, "The influence of spruce wood heat treatment on its thermal stability and burning process," *European journal of wood and wood products*, vol. 72, no. 4, pp. 477-486, 2014.
- [81] I. Haraldseid *et al.* Smoldering in wood and oily pellets: the effect of reduced air supply (Manuscript).
- [82] J. Martinka, P. Rantuch, and K. Balog, "Fire hazard and heat of combustion of sunflower seed hull pellets," *Journal of Thermal Analysis and Calorimetry*, vol. 130, no. 3, pp. 1531-1540, 2017.
- [83] G. pellets. <https://www.german-pellets.dk/gp-dk/powerplus/> (accessed 2020).

Attachments

I. Technical drawings

I. Technical drawings

Aluminum plate



Steel plates used for coverage of pipe opening, 50 % opening

